

NASA Conference Publication 10099

Ongoing Progress in Spacecraft Controls

(NASA-CP-10099) ONGOING PROGRESS IN
SPACECRAFT CONTROLS (NASA) 143 p

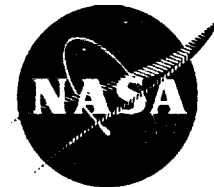
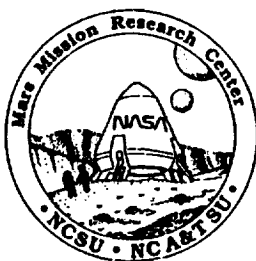
N92-28730
--THRU--
N92-28738
Unclass

G3/18 0106542

Edited by
D. Ghosh
Lockheed Engineering & Sciences Company
Hampton, Virginia

Proceedings of a workshop sponsored by
the NASA Langley Research Center and the
Mars Mission Research Center and held at
Langley Research Center
Hampton, Virginia
January 13, 1992

JULY 1992



National Aeronautics and
Space Administration
Langley Research Center
Hampton, Virginia 23665-5225

PREFACE

The Mars Mission Research Center is a cooperative program shared by North Carolina State University and North Carolina A&T State University to broaden the nation's engineering capability to meet the critical needs of the civilian space program. Its funding is shared by the National Aeronautics and Space Administration and participating industries. The first workshop, held October 1990, was devoted to "Technology for Lunar/Mars Aerobrakes". The second workshop, held 13 January 1992 at Langley Research Center, focused on "Ongoing Progress in Spacecraft Controls". It was jointly sponsored by the NASA Langley Research Center Guidance, Navigation and Control Technical Committee and the Mars Mission Research Center. This publication is a compilation of the papers presented at that workshop. The technical program addressed additional Mars mission control problems that currently exist in robotic missions in addition to human missions. The topics included control system design in the presence of large time delays, fuel-optimal propulsive control, and adaptive control to handle a variety of unknown conditions.

Dave Ghosh, Editor

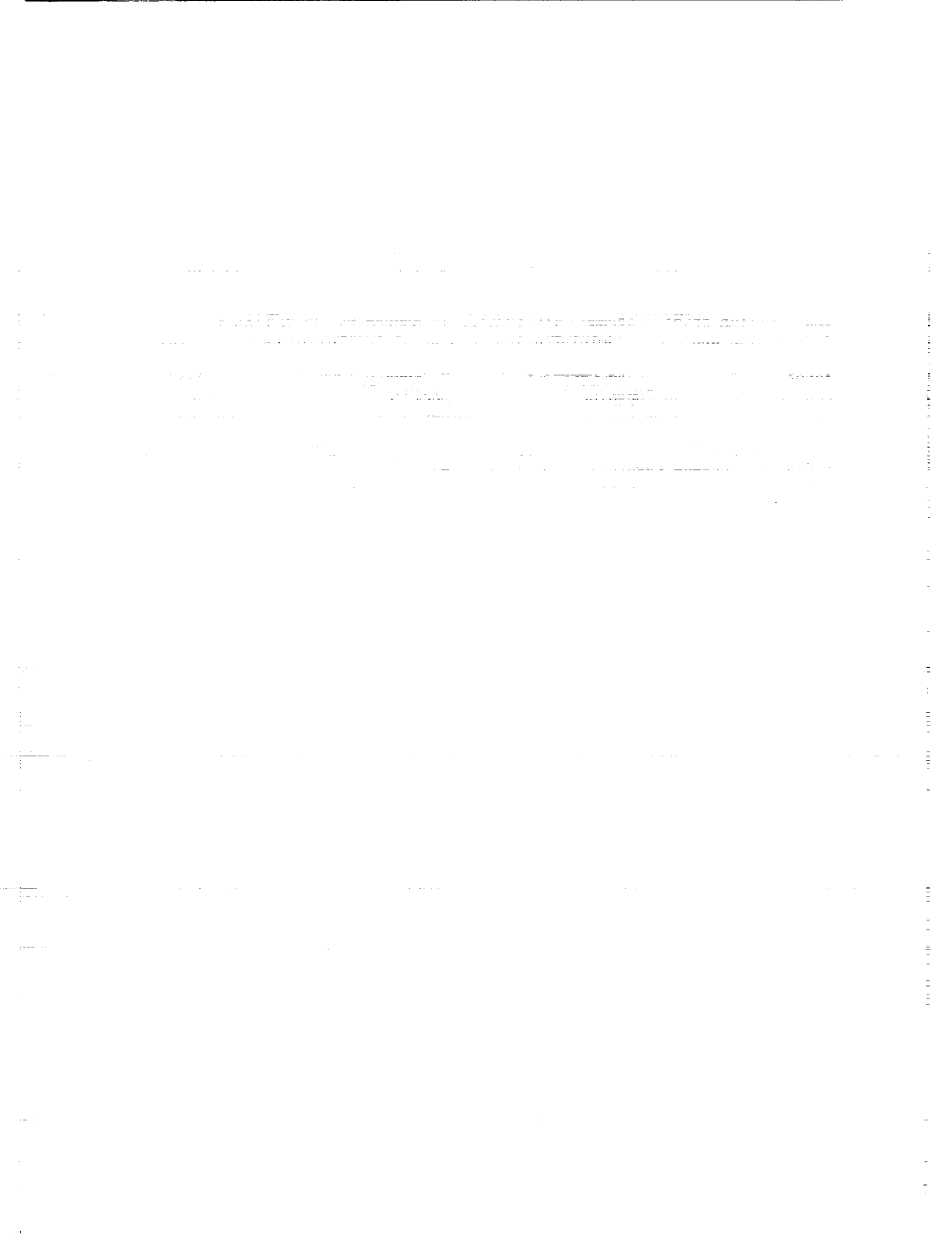
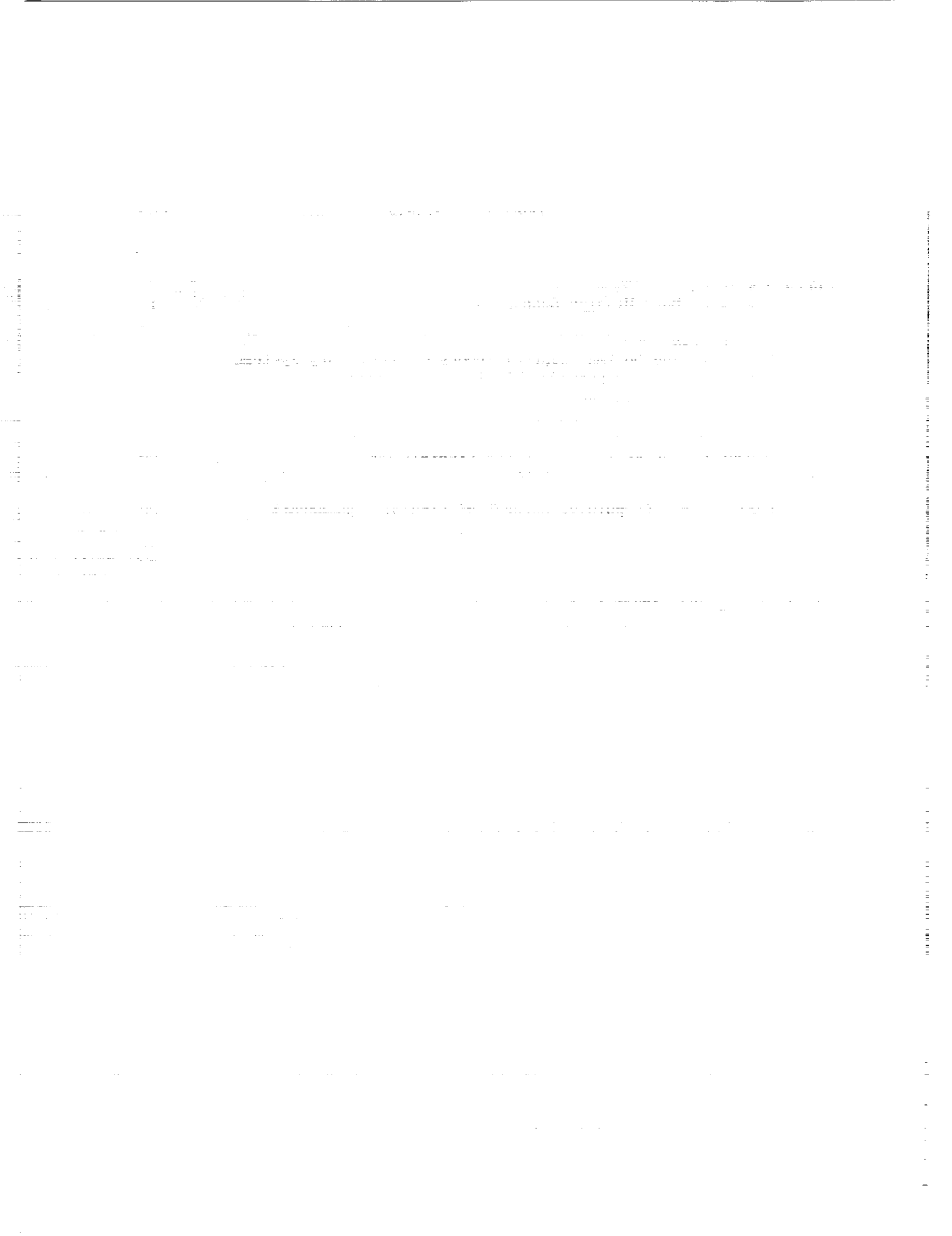


TABLE OF CONTENTS

	page
<i>Gerald Walberg</i> Review of Mars Mission Scenarios	1
<i>Ethelbert Chukwu</i> Stability and Optimal Control Theory of Hereditary Systems with Applications from Oscillating Flying Vehicles, Mechanical Systems and Robotics.	13
<i>Nancy A. Nimmo</i> Sensor Filter Designs for Large Flexible Spacecraft	25
<i>Jim Redmond</i> Fuel Optimal Propulsive Reboost of Flexible Spacecraft	39
<i>John L. Meyer</i> Fuel Optimal Maneuver: Experimental Testbeds	55
<i>S. S. Giang and Gordon K. F. Lee</i> Initial Investigation of an Adaptive Discrete-Time Controller for Non-Linear Time-Varying Models	77
<i>Chung-Wen Chen</i> Identification of Linear System Models and State Estimators for Controls	107
<i>R. J. Stanley II and H. Roberts</i> Fuzzy Logic Controllers for Manipulator Systems: Preliminary Results	123
Editor's Summary of the Panel Discussion	149

PRECEDING PAGE BLANK NOT FILMED



N92-28731

Review of Mars Mission Scenarios

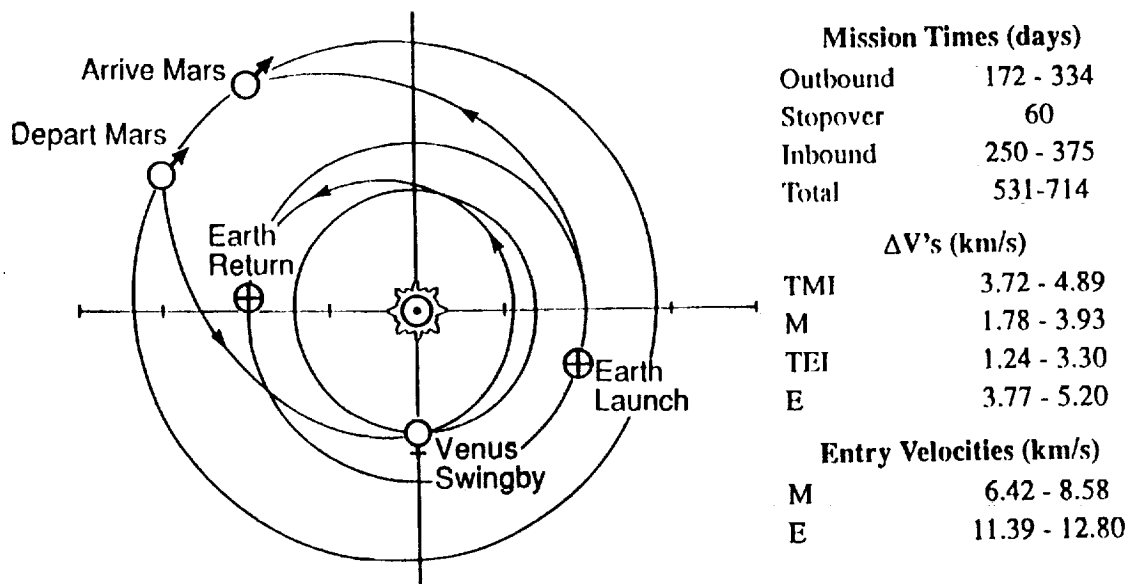
Dr. Gerald Walberg

North Carolina State University

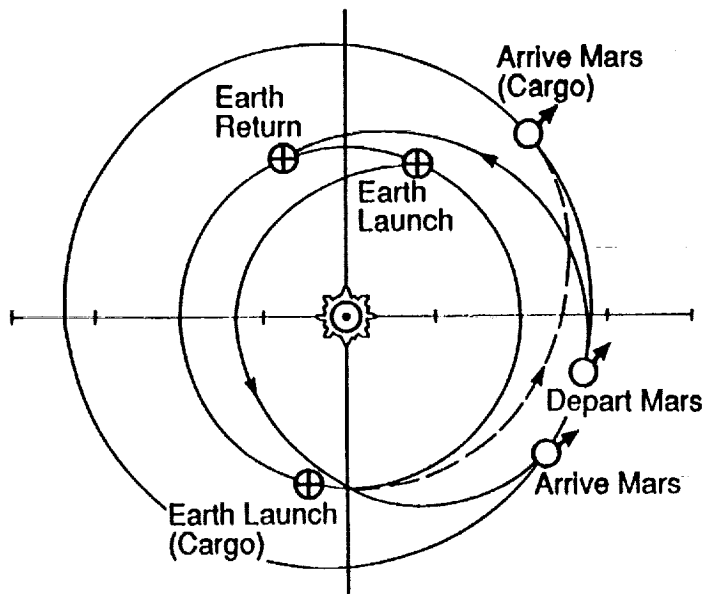
HOW SHALL WE GO TO MARS?

- Mission Scenarios
 - Far Term Missions
 - Initial Missions
- Exposure to Reduced Gravity
- Exposure to Space Radiation
- Initial Mass in Low Earth Orbit

Opposition-Class Missions 2002-2015



Split Sprint Missions 2002-2015

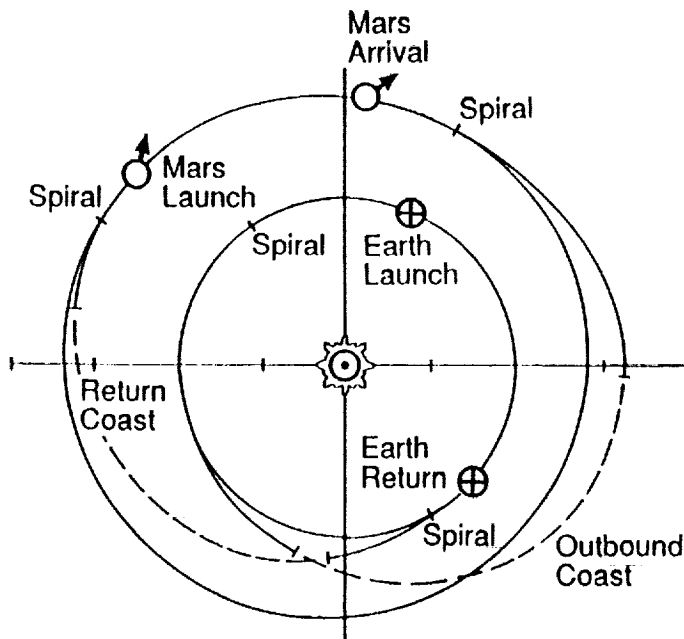


Mission Times (days)	
Outbound	238 - 287
Stopover	30
Inbound	145 - 172
Total	440 - 470

ΔV 's (km/s)	
TMI	4.01 - 6.04
Midcourse	VSB - 3.47
M	3.93
TEI	1.99 - 4.21
E	3.71 - 4.26

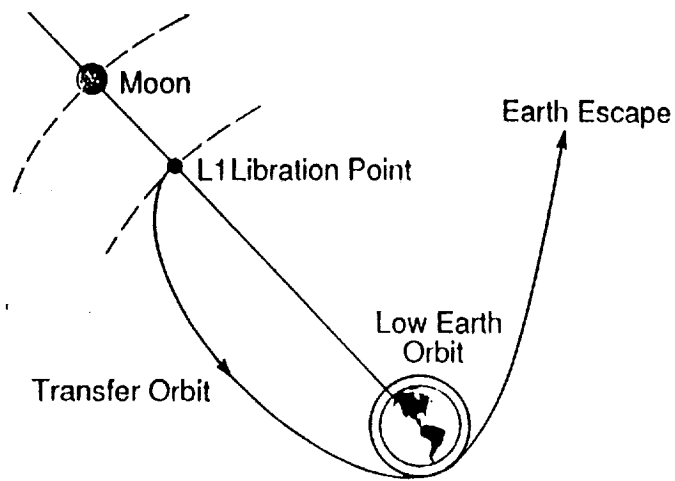
Entry Velocities (km/s)	
M	8.57
E	11.32 - 11.87

Low Thrust Mission

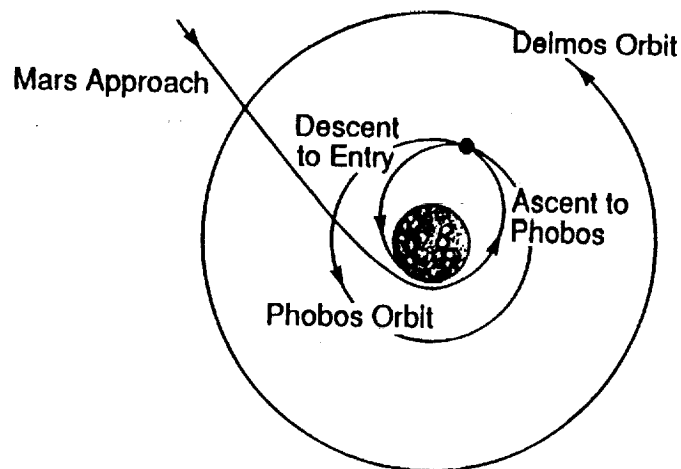


Mission Times (days)	
Earth Spiral	52
Outbound	510
Mars Spiral	39
Stopover	100
Mars Spiral	23
Inbound	229
Earth Spiral	16
Total	969

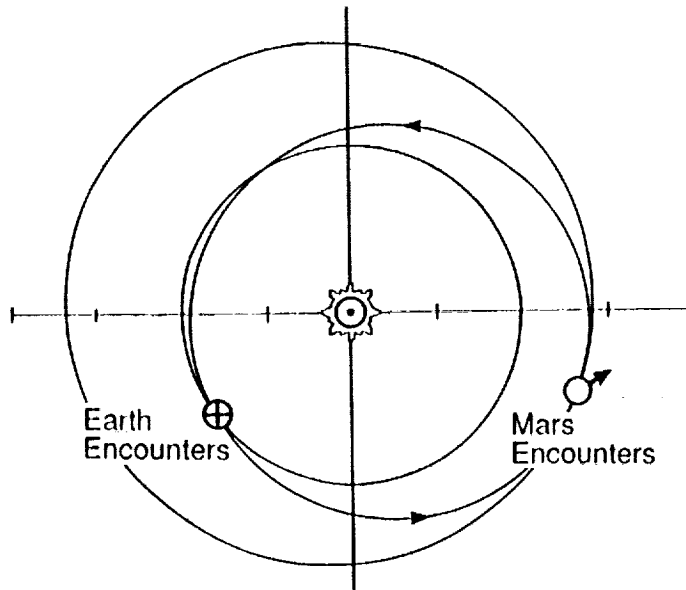
Staging From Earth-Moon Libration Point



Mars Staging From Phobos



Visit 1 Trajectory One Cycling Spacecraft 2001-2016

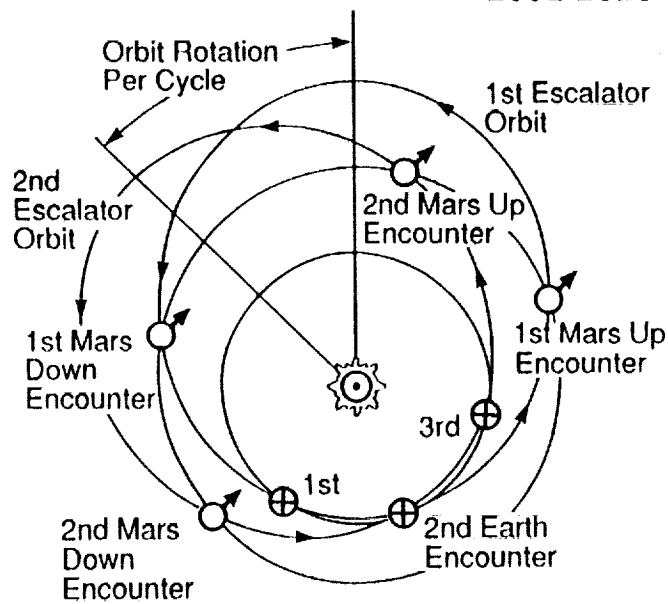


Mission Times (days)	
Outbound	221 - 1101
Stopover	1331 - 1352
Inbound	197 - 1193
Total	1849 - 2545

ΔV 's (km/s)	
TMI	3.94 - 4.04
M	1.50 - 1.69
TEI	1.50 - 1.69
E	3.94 - 4.04

Entry Velocities (km/s)	
M	6.14 - 6.33
E	11.56 - 11.65

Up-Escalator, Down-Escalator Scenario Two Cycling Spacecraft 2001-2016



Mission Times (days)	
Outbound	148 - 169
Stopover	~ 730
Inbound	146 - 170
Round Trip	1020 - 1069

ΔV 's (km/s)	
TMI	4.47 - 4.72
M	3.11 - 8.06
TEI	3.55 - 7.92
E	4.43 - 4.72

Entry Velocities (km/s)	
M	7.75 - 12.70
E	12.04 - 12.33

GROUND RULES

• REDUCED GRAVITY EXPOSURE

3 Criteria Considered:

Cumulative Reduced g Exposure
Cumulative Zero g Exposure
Continuous Zero g Exposure

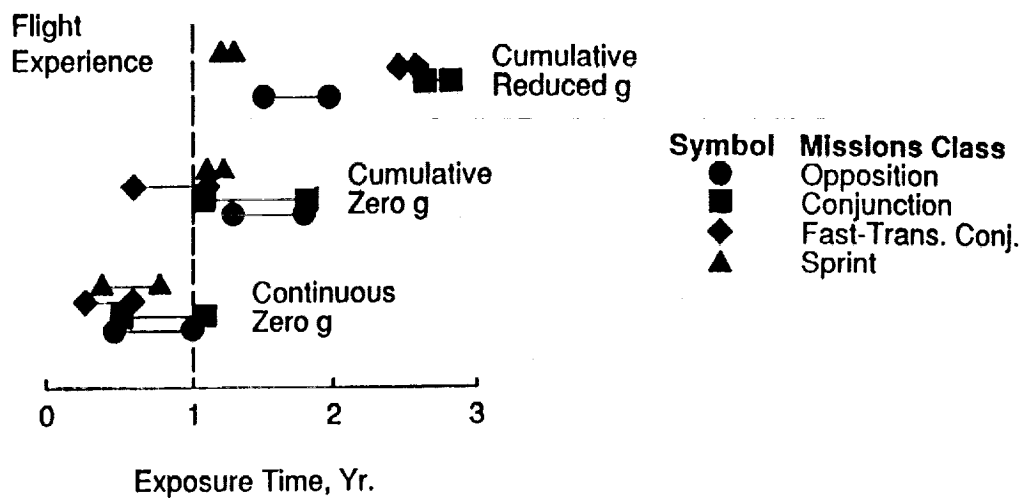
• RADIATION DOSE

- **Ignore Van Allen Belts and Nuclear Rocket**
- **Consider Galactic Cosmic Rays and Solar Flares**
- **GCR's Vary with Solar Cycle**
- **Solar Flare Dose Varies Inversely with Distance from Sun**
- **One Giant Solar Flare each Year at Worst Time and Place**
- **Charged Particle Transport Analyses of Simonsen, Nealy, Townsend and Wilson**
- **25 cm H₂O Storm Shelter**
- **Shielding by Martian Atmosphere and Terrain**

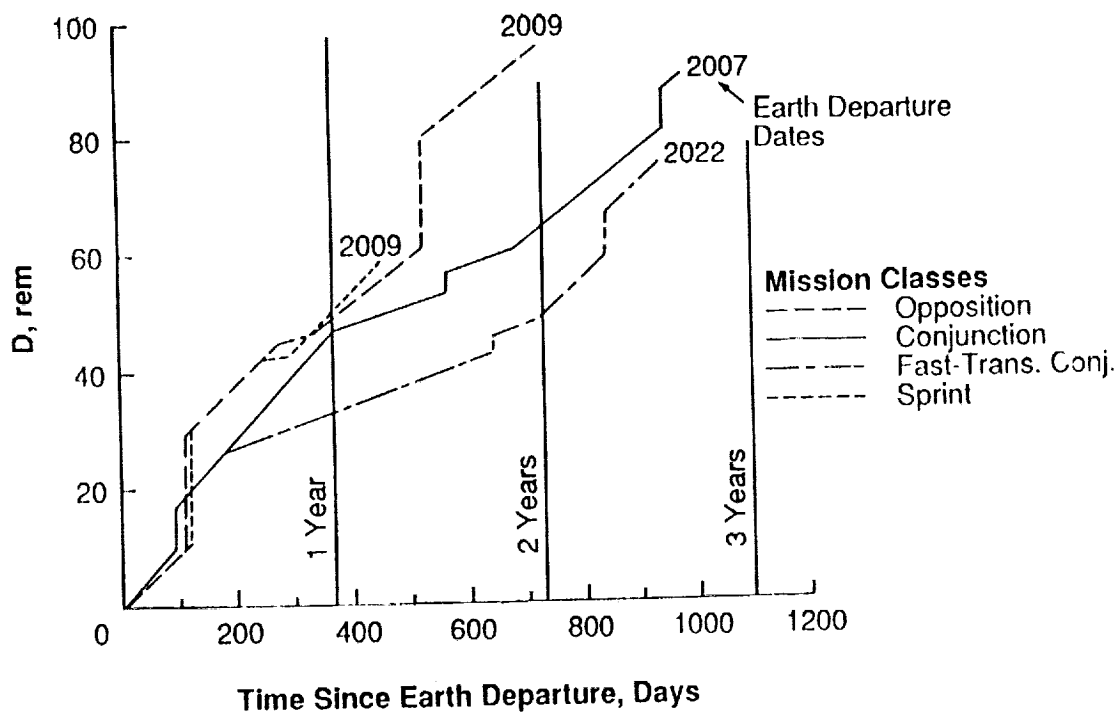
• IMLEO

- **Rocket Equation Analysis**
- **$(m_s + m_p)/m_p = 1.1$**
- **$(m_{AB} + m_{p/L})/m_{p/L} = 1.15$**
- **$I_{sp} = 480 \text{ sec and } 960 \text{ sec}$**

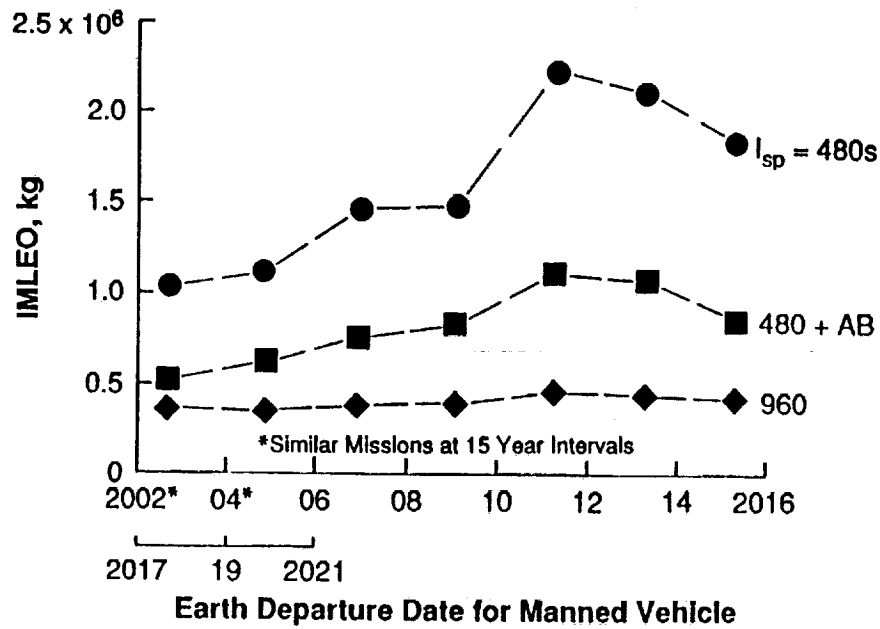
Crew Exposure to Reduced Gravity



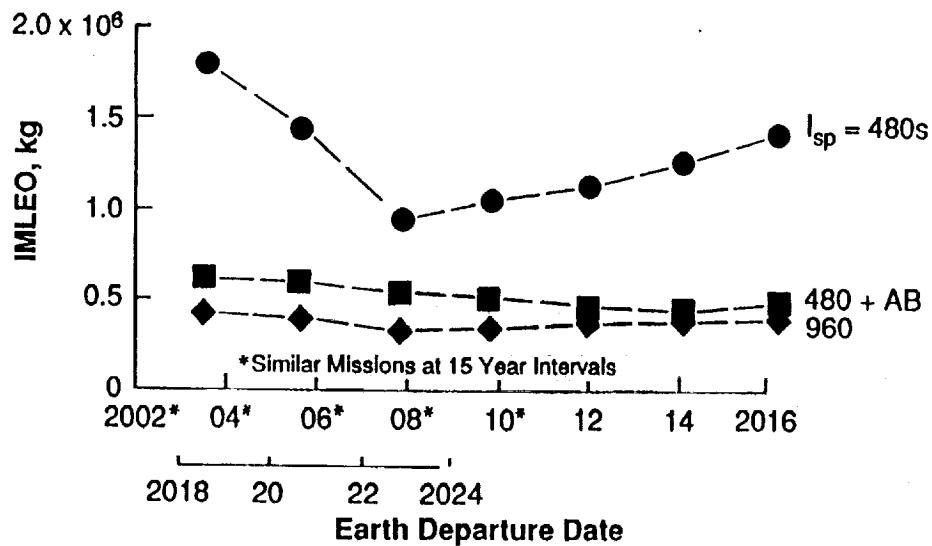
Blood Forming Organ Radiation Doses



Earth Departure Masses Split Sprint Missions



Earth Departure Masses Fast Transfer Conjunction Missions



SUMMARY

- **MANY VARIED SCENARIOS PROPOSED**
 - **Far Term Mission Candidates:**
 - Extraterrestrial Resources
 - Complex Space Infrastructures
 - Advanced Technologies
 - **Initial Mission Candidates:**

<ul style="list-style-type: none">• Simple Infrastructure• Near Term Technology• Low Cost	}	<ul style="list-style-type: none">• Conjunction Class• Opposition Class• Split Sprint• Fast Trans. Conj.
---	---	---
- **SCENARIO CHOICE DEPENDS ON REDUCED GRAVITY EXPOSURE CRITERIA, IMLEO AND OTHER COST FACTORS**
 - Radiation Dose Important But Not a Mission Discriminator
 - IMLEO is Useful (But Incomplete) Mission Cost Indicator
 - Criterion = Cumulative Reduced g:
→ Sprint → Nuclear Thermal Propulsion
 - Criterion = Cumulative Zero g:
→ Sprint or Fast Trans. Conj. → Nuclear Thermal or Chemical/AB
 - When Cost Factors Other Than IMLEO are Considered, Chemical/AB and Nuclear Thermal Propulsion are Competitive

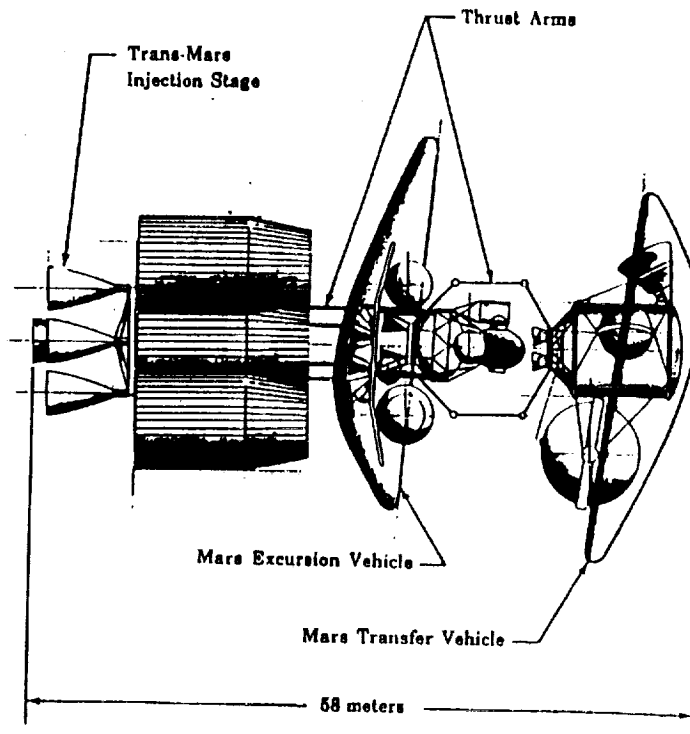
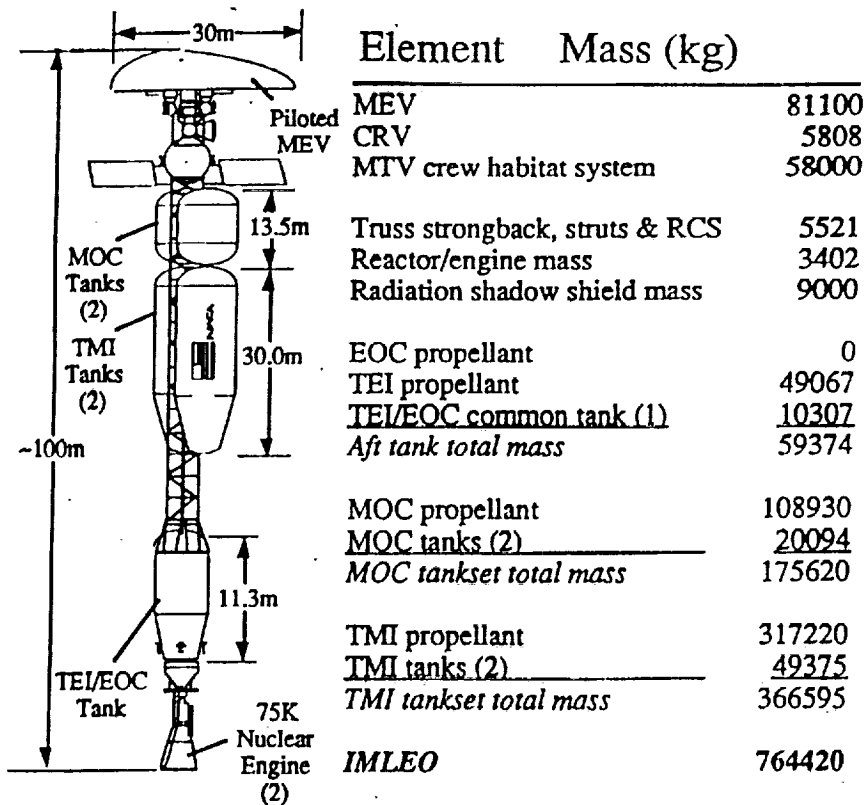


Figure 3-16 Mars Transportation System



N 9 2 - 2 8 7 3 2

**STABILITY AND OPTIMAL CONTROL THEORY OF HEREDITARY
SYSTEMS WITH APPLICATIONS FROM OSCILLATING FLYING
VEHICLES, MECHANICAL SYSTEMS AND ROBOTICS**

Ethelbert Nwakuche Chukwu

**Mathematics Department
North Carolina State University
Raleigh, NC 27695-8205**

PRECEDING PAGE BLANK NOT FILMED

§0. Motivation.

Consider an n -dimensional system

$$\dot{x}(t) = Ax(t), \quad (0.1)$$

where $x(t)$ belongs to E^n , the Euclidean n -space. The aim is to stabilize the rest position $x = 0$ by adding a damping term $A_1x(t)$. In practice the damping term which is added has a time delay because it does not react instantaneously but only after a time lag $h > 0$. Thus it is more accurately modelled by adding $A_1x(t-h)$ instead of $A_1x(t)$. The equation considered is

$$\dot{x}(t) = Ax(t) + A_1x(t-h). \quad (0.2)$$

The problem then is to stabilize the rest position: find a necessary and sufficient condition for the damped system (2) to be asymptotically stable. This problem is natural in systems where servomechanisms are used to improve performance and efficiency, in ship and aircraft stabilization and automatic steering.

As reported by Minorsky in [7], [8], for ships exposed to turbulent waters the problem encountered is undesirable self-excited oscillations. Here the engineers aim to eliminate the oscillations. An automatic control servomechanism introduces the delayed damping term $A_1x(t-h)$ to (0.1) to reduce the oscillations. In a similar situation the flap of an airplane wing is regulated by an automatic control. In such systems, controls u are introduced via a control matrix B to yield a system whose dynamics is governed by

$$\dot{x}(t) = Ax(t) + A_1x(t-h) + Bu(t) \quad (0.3)$$

The aim of the control device is to 'steer' the system (0.3) to an equilibrium position as fast as possible.

The system (0.3) is a special case of the dynamics of the deterministic model of a flying vehicle, which is derived in Kolmanovskii and Nosov [4, pp 120-123]. The equations have the form

$$\begin{aligned} \ddot{q}(t) - \int_0^t B_{-1}(s)\ddot{q}(t-s)ds + B_0\dot{q}(t) + B_1q(t) \\ = \int_0^t B_2(s)\dot{q}(t-s)ds + Du(t). \end{aligned}$$

This can be recast in the form

$$\begin{aligned} \dot{x}(t) - \int_0^t A_{-1} \dot{x}(t-s) ds &= A_0 x(t) \\ + \int_0^t A_1(s) x(t-s) ds &+ B u(t). \end{aligned} \quad (0.4)$$

The drives of control surfaces are described by Bu , where u is the control signal that drives the signals. In the above equation q is a vector of generalized coordinates.

In the scalar case we have the one-dimensional oscillation of the control surface, the so called control surface buzz [4]. If a rigid wing moves in a gas flow and turns with respect to an axis, the angular wing displacement are restricted by an elastic spring of rigidity k . The equation of motion is

$$\begin{aligned} \ddot{q}(t) + a\dot{q}(t) + bq(t) &= k_1 \int_0^\infty J_0(s) \dot{q}(t-s) ds \\ + k_1 \int_0^t J_1(s) \ddot{q}(t-s) ds &+ q u(t) \end{aligned}$$

for some constraints a, b . In both cases u is a control signal that helps to stabilize the wing.

The problem of interest which is proposed for investigation for (0.4) can be stated as follows: Find an optimal control subject to its constraints such that the solution of (0.4) with this control and with an initial state $x(t) = \phi(t), t \in [-h, 0]$ will hit the zero target in minimum time T and remain there for every after. Another problem we propose to solve is that of minimizing some effort or energy function $E(u) = \int_0^T G(u(t))$ when u is constrained, for the system (0.4) whose dynamics transfers an initial data ϕ to a final point Φ . For physical applications particularly in aerospace where one is interested in the deployment in space of large assemblies of flexible structures, the performance $E(u)$ may be fuel consumption, the maximum thrust available for the control system or the energy. We propose also to explore the problem of time optimality which minimizes fuel consumption.

For the linear (0.3) or (0.4) the classical approach would be solve

(i) the related initial problem of determining conditions for asymptotic stability of

$$\dot{x}(t) = A_0 x(t) + A_1 x(t-h),$$

or

$$\dot{x}(t) - A_1 \dot{x}(t-h) = A_0 x(t) + A_1 x(t-h);$$

- (ii) the constrained controllability problem of (0.3) and (0.4), that is, the conditions needed to transfer any initial function to another using controls subject to its constraints

and finally to construct an optimal feedback control

$$f : C \rightarrow U$$

where U is the constraint set and $C = ([-h, 0], E^n)$ is the space of continuous functions into the n -dimensional Euclidean space E^n . Instead of C we can use the space $W_2^{(1)}$, the Sobolev space of absolutely continuous functions $x : [-h, 0] \rightarrow E^n$ whose derivated $\dot{x}(t) \in L_2([-h, 0], E^n)$.

Though a lot has now been achieved for (0.3) (see the forth coming book, E. N. Chukwu [1], "Stability and Time Optimal Control of Hereditary Systems"), the time optimal, minimum fuel problem of (0.4) has not yet been fully investigated. We propose to tackle the following problems:

I: The stability problem for (0.4) and its generalization

II: The controllability problem for nonlinear generalization of (0.4).

which can form the base of technological knowledge necessary for the expected deployment of large flexible structures in space.

We now motivate the equations which we propose to study in problems I and II.

§1. Mechanical Systems

We now examine some simplified mechanical problems whose optimal feedback control strategy will be investigated. The linearized equation of motion of a single degree of freedom mechanical subject to a retarded follower force and control is given by

$$ml^2 \ddot{q}(t) + (s - Fl)q(t) = -F(q(t-h) + u(t)) \quad (1.1)$$

The scalar q is the general coordinate, s is the torsional stiffness at the pin, m is the mass at the end of the light beam, l denotes the length of the beam, and F stands for the constant magnitude of the applied force. The measurable control u is introduced to restore the system to its equilibrium position in infinite time. The constant delay at the angle of the force is h .

ed.

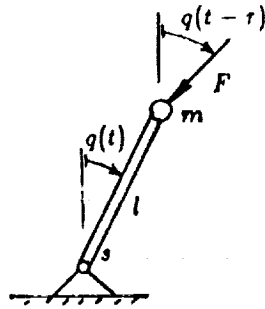


Figure 1.1

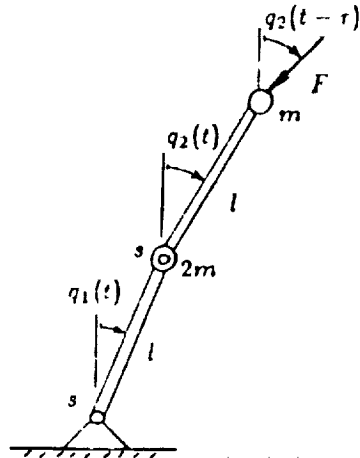


Figure 1.2

If the model has two degrees of freedom the mechanical system has the following dynamics

$$\begin{pmatrix} 3ml^2 & ml^2 \\ ml^2 & ml^2 \end{pmatrix} \begin{pmatrix} \dot{q}_1(t) \\ \dot{q}_2(t) \end{pmatrix} + \begin{pmatrix} 2s - Fl - s & \\ -s & s - Fl \end{pmatrix} \begin{pmatrix} q_1(t) \\ q_2(t) \end{pmatrix} + \begin{pmatrix} 0 & Fl \\ 0 & Fl \end{pmatrix} \begin{pmatrix} q_1(t-h) \\ q_2(t-h) \end{pmatrix} = \begin{pmatrix} u_1(t) \\ u_2(t) \end{pmatrix} \quad (1.2)$$

The two systems have nonlinear versions.

§2. Robotics

Problems of the dynamics of Robotics must incorporate delays [9, p. 30]. These can occur in the control system of the robot, in the transmission of information and in the mechanical part of the robot. Delays which occur in the information transmission are crucial in undersea and space teleoperations in [9, p. 131].

Mechanical model of an elastic robot is described by the systems

$$\begin{bmatrix} \dot{q}_1(t) \\ \dot{q}_2(t) \\ \dot{v}(t) \end{bmatrix} = \begin{bmatrix} 0 & 0 & 0 \\ 0 & 0 & 1 \\ \alpha^2 & -\alpha^2 & -2k\alpha \end{bmatrix} \begin{bmatrix} q_1(t) \\ q_2(t) \\ v(t) \end{bmatrix} + \begin{bmatrix} 0 & -k & 0 \\ 0 & 0 & 0 \\ 0 & -2Kk\alpha & 0 \end{bmatrix} \begin{bmatrix} q_1(t-h) \\ q_2(t-h) \\ v(t-h) \end{bmatrix} \quad (2.1)$$

where $\alpha = \sqrt{\frac{s}{m_2}}$ is the natural frequency of the undamped, uncontrolled system and

$$k = f/(2m_2)$$

the relative damping factor. One can of course introduce control variables on the right hand of the equation, and go beyond stability to study optimal control of the dynamics.

§3. Controllability Theory

Definition 3.1. The linear control process (4.1.1) is Euclidean controllable on the interval $[\sigma, t_1]$ if for each $\phi \in C$ and $x_1 \in E^n$ there is a square integrable controller u such that $x_\sigma(\sigma, \phi, u) = \phi$ and $x(t_1, \sigma, \phi, u) = x_1$. It is Euclidean null-controllable if in the definition $x_1 = 0$. It is Euclidean controllable if it is Euclidean controllable on every interval $[\sigma, t_1]$ $t_1 > \sigma$.

The conditions for Euclidean controllability have been well studied: See Kirillova and Churakova [5], [2], Weiss [11], Manitius and Olbrot [6]. They are all conditions on matrices representing the system.

Characterization of Euclidean controllability in terms of the systems coefficients is available for the autonomous system,

$$\dot{x}(t) = A_0 x(t) + A_1 x(t-h) + Bu(t), \quad (3.1)$$

where A_0, A_1, B are constant matrices. First introduce the so-called "determining equations",

$$\begin{aligned} Q_k(s) &= A_0 Q_{k-1}(s) + A_1 Q_{k-1}(s-h), \quad k = 1, 2, 3, \dots, \quad s \in (-\infty, \infty). \\ Q_0(s) &= \begin{cases} B & s = 0 \\ 0 & s \neq 0 \end{cases} \end{aligned} \quad (3.2)$$

and define

$$\bar{Q}_n(t_1) = [Q_0(s), Q_1(s) \dots Q_{n-1}(s) \mid s \in [0, t_1]]$$

We have:

Theorem 3.1. The system (3.1) is Euclidean controllable on $[0, t_1]$ if and only if

$$\text{rank } \bar{Q}_n(t_1) = n.$$

Remarks. Note that the non-zero elements of $Q_k(s)$ form the sequence:

$s = 0$	h	$2h$
$Q_0(s) = B_0$		
$Q_1(s) = A_0 B$	$A_1 B_0$	
$Q_2(s) = A_0^2 B$	$(A_0 A_1 + A_1 A_0) B_0$	$A_1^2 B_0$

Note that if $t_1 \leq h$, the only elements in the sequence are the terms $[B, A_0 B, \dots, A_0^{n-1} B]$, so that E^n -controllability on an interval less than h implies the full rank of $[B, \dots, A_0^{n-1} B]$.

If this has less than full rank and $t_1 > h$, other terms can be added to $\bar{Q}_n(t_1)$

§4 Constrained Controllability of Linear Delay Systems

In the last section the controls are big. In this section we consider controllability of

$$\dot{x}(t) = L(t, x_t) + B(t)u(t), \quad (4.1)$$

when the controls are required to lie on a bounded convex set U with non-empty interior. For ease of treatment U will be assumed to be the unit cube

$$C^m = \{u \in E^m : |u_j| \leq 1, j = 1, \dots, m\}. \quad (4.2)$$

Here u_j denotes the j th component of $u \in E^m$. Consistent with our earlier treatment the class of admissible controls is defined by

$$U_{ad} = \{u \in L_\infty([0, t_1]) : u(t) \in C^m \text{ a.e. on } [0, t_1]\}$$

Definition 4.1. The system (4.1) is null controllable with constraints if for each $\phi \in C$ there is a $t_1 < \infty$ and a control $u \in U_{ad}$ such that the solution $x()$ of (4.1) satisfies

$$x_\sigma(\sigma, \phi, u) = \phi, \quad x_{t_1}(\sigma, \phi, u) = 0.$$

It is locally null controllable with constraints if there exists an open ball O of the origin in C with the following property: For each $\phi \in O$ there exists a $t_1 < \infty$ and a $u \in U_{ad}$ such that the solution $x()$ of (4.1) satisfies

$$x_\sigma(\sigma, \phi, u) = \phi, \quad x_{t_1}(\sigma, \phi, u) = 0.$$

Theorem 4.1. Assume that

- (i) the system (4.1) is null controllable;
- (ii) the system

$$\dot{x}(t) = L(t, x_t) \quad (4.3)$$

is uniformly asymptotically stable, so that there are constants $k > 0$, $\alpha > 0$ such that for each $\sigma \in E$ the solution x of (4.3) satisfies

$$\|x_t(\sigma, \phi)\| \leq k\|\phi\|e^{-\alpha(t-\sigma)}.$$

Then (4.1) is null controllable with constraints.

§5. Optimal Feedback Control

We now consider the problem of the construction of an optimal feedback control needed to reach the Euclidean space origin in minimum time for the linear systems,

$$\dot{x}(t) = A_0 x(t) + \sum_{j=1}^N A_j x(t - \tau_j) + Bu(t). \quad (5.1)$$

Here $0 < \tau < 2\tau < \dots < \tau N = h$; A_i are $n \times n$ and B is an $n \times m$ constant matrices. The controls are L_∞ functions whose values on any compact interval lie in the m -dimensional unit cube

$$C^m = \{u \in E^m : |u_j| \leq 1, j = 1, \dots, m\}.$$

We shall show that the time optimal feedback system

$$\dot{x}(t) = \sum_{j=0}^N A_j x(t - \tau_j) + Bf(x(t)) \quad (5.2)$$

executes the time-optimal regime for (5.1) in the spirit of Hájek [3] and Yeung[12]. The construction of f provides a basis for direct design, and it is done for strictly normal systems which we now define.

Definition 5.1. Let

$$J_0 = \{t = j\tau, j = 0, 1, 2, \dots\},$$

and assume J_0 is finite. Suppose $U(\varepsilon, t)$ is the fundamental matrix solution of

$$\dot{x}(t) = A_0 x(t) + \sum_{j=1}^N A_j x(t - \tau_j) \quad (5.3)$$

on some interval $[0, \varepsilon]$, $\varepsilon > 0$. Note that $U(\varepsilon, t)$ is piecewise analytic, and its analyticity may break down only at points of J_0 , (see Tadmor [10]). The system (5.1) is strictly normal on some interval $[0, \varepsilon]$ if for any integers

$$r_j \geq 0, \text{ satisfying } \sum_{j=1}^M r_j = n$$

the vectors

$$Q_{kj}(s) = \sum_{j=0}^N A_j Q_{k-1,j}(s - \tau_j) \quad k = 1, 2, \quad s \in (-\infty, \infty),$$

$$Q_{0j}(s) = \begin{cases} b_j & s = 0 \\ 0 & s \neq 0 \end{cases},$$

$$j = 1, \dots, m;$$

are linearly independent;

$$\text{and } B = (b_1 \dots b_m).$$

It follows from Theorem 7.1.4 in [1] that a complete, strictly normal system is normal, and has rank $B = \min[m, n]$. Indeed, choose any column b_j of B and set $r_j = n$, $r_i = 0$ for $i \neq j$ in the definition.

Theorem 5.1. Consider the system

$$\dot{x}(t) = \sum_{j=0}^N A_j x(t - \tau_j) + Bu(t), \quad (5.1)$$

and assume

- (i) The system (5.1) is Euclidean controllable
- (ii) The system

$$\dot{x}(t) = \sum_{j=1}^N A_j x(t - \tau_j), \quad (5.3)$$

is uniformly asymptotically stable.

- (iii) The (5.1) is strictly normal.

then there exists an $\varepsilon > 0$ and a function $f : \text{Int } \mathbf{R}(\varepsilon) \rightarrow E^m$ which is an optimal feedback control of (5.1) in the following sense: If

$$\dot{z}(t) = \sum_{j=0}^N A_j z(t - \tau_j) + Bf(z(t)), \quad z \in \text{Int } \mathbf{R}(\varepsilon) \quad (5.2)$$

then the set of solutions of (5.3) coincides with the set of optimal solutions of (5.1) in $\text{Int } \mathbb{R}(\varepsilon)$. Also $f(0) = 0$ for $x \neq 0$, $f(x)$ is among the vertices of the unit cube U . Furthermore $f(x) = f(x) = -f(-x)$. If $m \leq n$ f is uniquely determined by the condition that optimal solutions of (5.1) solve (5.3).

REFERENCES

1. E. N. Chukwu, *"Stability and Time Optimal Control of Hereditary Systems"*, Academic Press (1992).
2. R. Gabasov and F. Kirillova, *The Qualitative Theory of Optimal Processes* Marcel Dekker, New York, New York (1976).
3. O. Hájek, *Terminal Manifold and Switching Locus*, Mathematical Systems Theory **6** (1973), 289-301.
4. V. B. Kolmanovskii and V. R. Nosov, *Stability of Functional Differential Equations*, Academic Press (1986).
5. F. M. Kirillova and S. V. Churakova, *On the Problem of Controllability of Linear Systems with After Effect*, Differential Equations **3** (1967), 436-445.
6. A. Manituis and A. W. Olbnot, *Controllability Conditions for Linear Hereditary Systems*.
7. N. Minorsky, *Nonlinear Oscillations*, D. Van Nostrand, Co., Inc., Princeton (1962).
8. N. Minorsky, *Self-Excited Oscillations in Dynamical Systems Possessing Retarded Actions*, J. Appl. Mech. **9** (1942), 65-71.
9. G. Stépán, *Retarded Dynamical Systems: Stability and Characteristic Functions*, Springer Verlag (1990).
10. G. Tadmor, *Functional Differential Equations of Retarded and Neutral Type; Analytic Solutions and Piecewise Continuous Controls*, J. Differential Equations **51** (1984), 151-181.
11. L. Weiss, *An Algebraic Criterion for Controllability of Linear Systems with Time-Delay*, IEEE. Trans. on Aut. Control AC-15 (1970), 443.
12. D. S. Yeung, *Time Optimal Feedback Control*, Journal of Optimization Theory and Applications **21** (1977), 71-82.

N 9 2 - 2 8 7 3 3

**SENSOR FILTER DESIGNS FOR LARGE
FLEXIBLE SPACECRAFT**

by

NANCY A. NIMMO

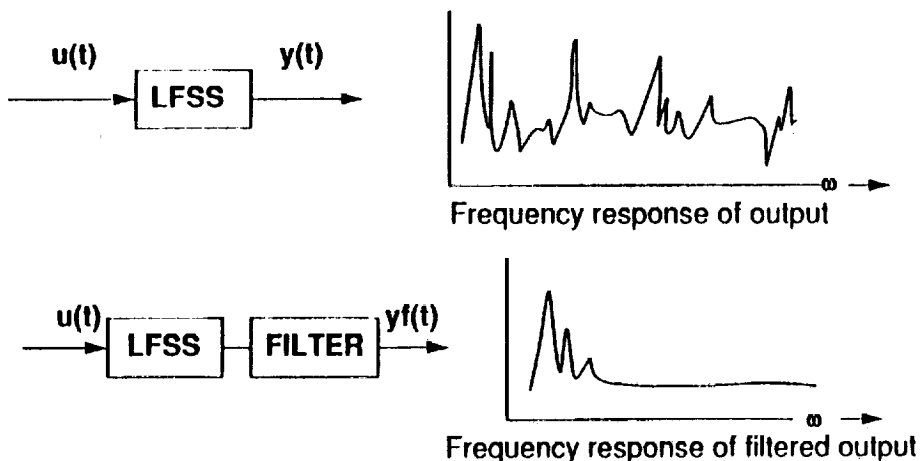
**ONGOING PROGRESS IN SPACECRAFT CONTROLS
JANUARY 13, 1992**

1. INTRODUCTION
2. LOW-PASS FILTER DESIGNS
3. CSI TEST ARTICLE
4. CONTROL STRATEGY
7. CLOSED-LOOP SIMULATION
8. CLOSED-LOOP LABORATORY EXPERIMENTS
9. CONCLUSION AND FUTURE WORK

1. INTRODUCTION

Problem

Traditional control methods may excite flexible modes causing degraded performance or instability of large flexible space structures (LFSS). Control techniques developed for control of LFSS require a numerical model of the structure and some knowledge of model error. This will be increasingly difficult with the complex space structures planned for the future. If filters could be used to condition the sensor output, control design would be less demanding.



2. CONVENTIONAL LOW-PASS ANALOG FILTER DESIGNS

Objective of low-pass filter design

Preserve desired frequency components and attenuate undesired frequency components

Conventional low-pass filter designs

Filter approximations with frequency response characteristics which satisfy the following specifications:

passband frequency, stopband frequency,
passband attenuation, stopband attenuation.

TERMINOLOGY

Filter transfer function:
$$T(j\omega) = \frac{Y(j\omega)}{U(j\omega)} = |T(j\omega)| \angle \theta(j\omega)$$

Attenuation:
$$\alpha = -20 \log |T(j\omega)| \text{ dB}$$

Filter Specifications

Passband frequency	$\omega_p = 1 \text{ rad / sec}$
Stopband frequency	$\omega_s = 2 \text{ rad / sec}$
Maximum attenuation	$\alpha_{\max} = 3 \text{ dB}$
Minimum attenuation	$\alpha_{\min} = 20 \text{ dB}$

Filters satisfying specifications

Butterworth: fourth-order
Chebyshev: third-order
Cauer: second-order
Bessel: none (Bessel filter transition band too wide)

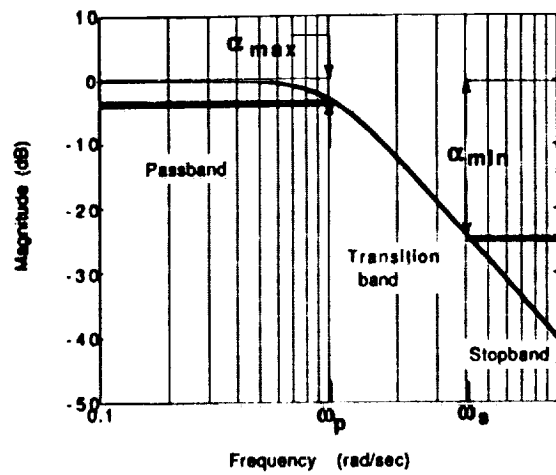


Figure 2.3 Low-pass filter specifications

21

Comparison of Filters

Frequency Response Characteristics

Butterworth: maximally flat magnitude response in passband

Bessel: maximally flat delay characteristics in passband,
largest transition band

Chebyshev: ripple in passband, sharp rolloff,
nonlinear phase response

Cauer: ripple in stopband and passband, sharpest rolloff
nonlinear phase response

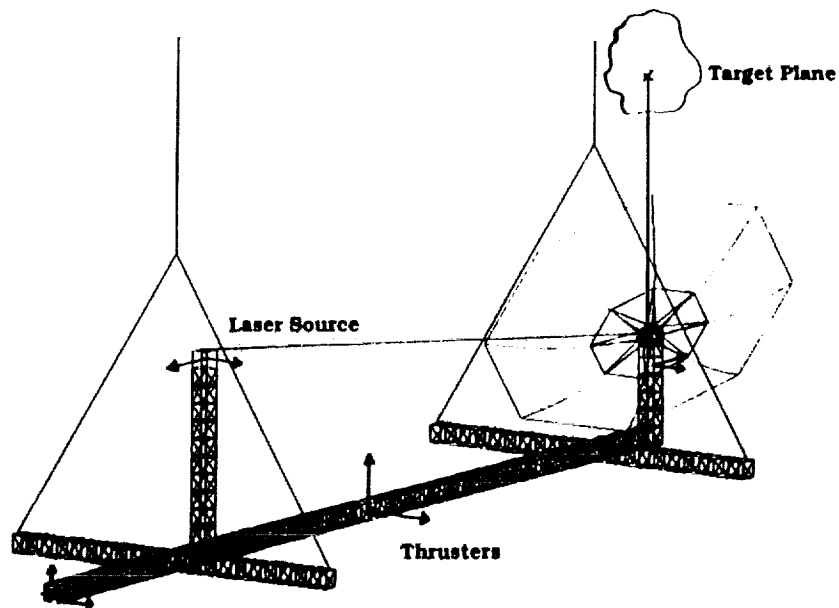
3. Controls Structures Interaction (CSI) Test Article

Some objectives of the NASA CSI Program is to develop and validate the technology needed to design, verify, and operate spacecraft in which the structure and control system interact beneficially to meet the requirements of future spacecraft.

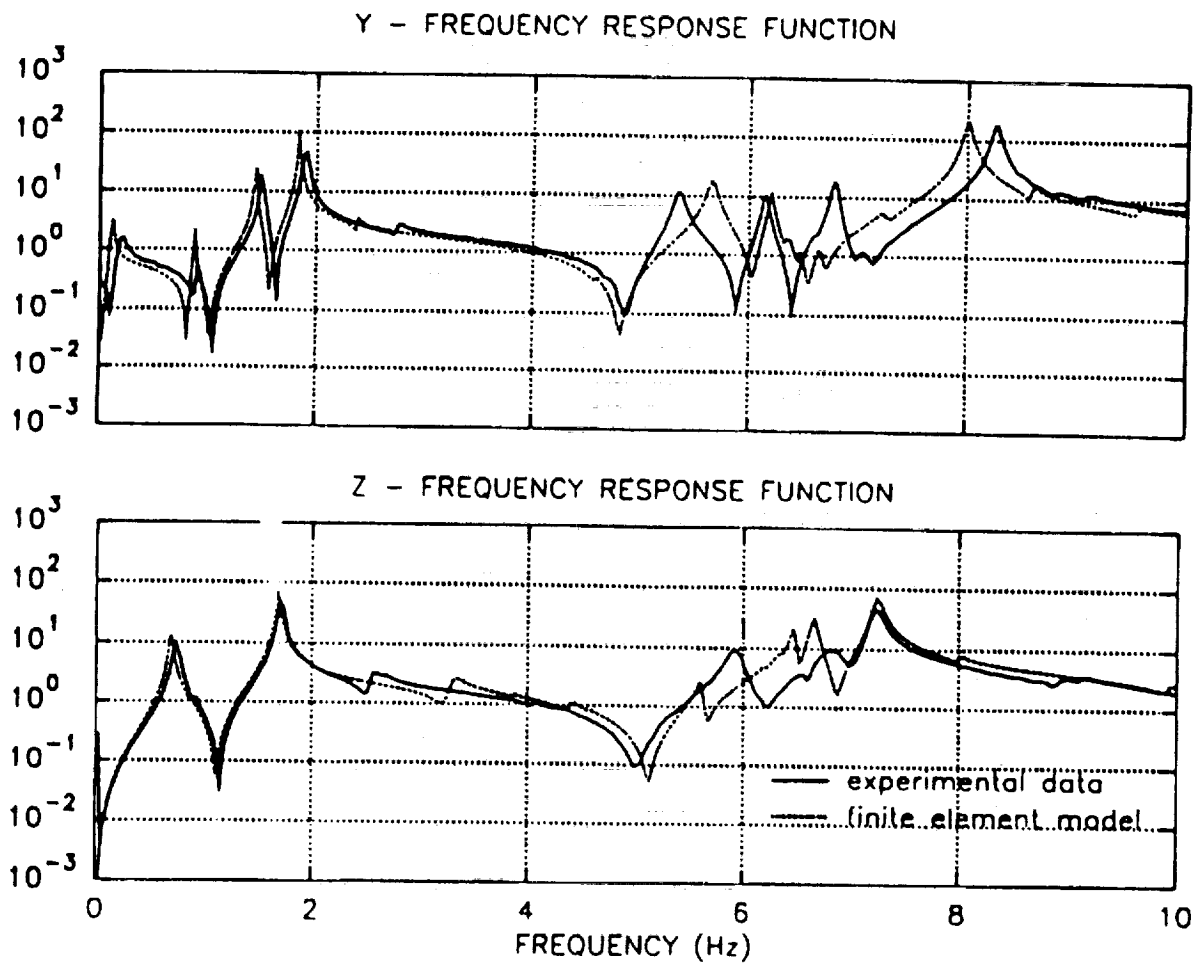
A CSI testbed has been developed to validate CSI design methodology, to implement practical sensors and actuators for LFSS control, and to evaluate controller designs.

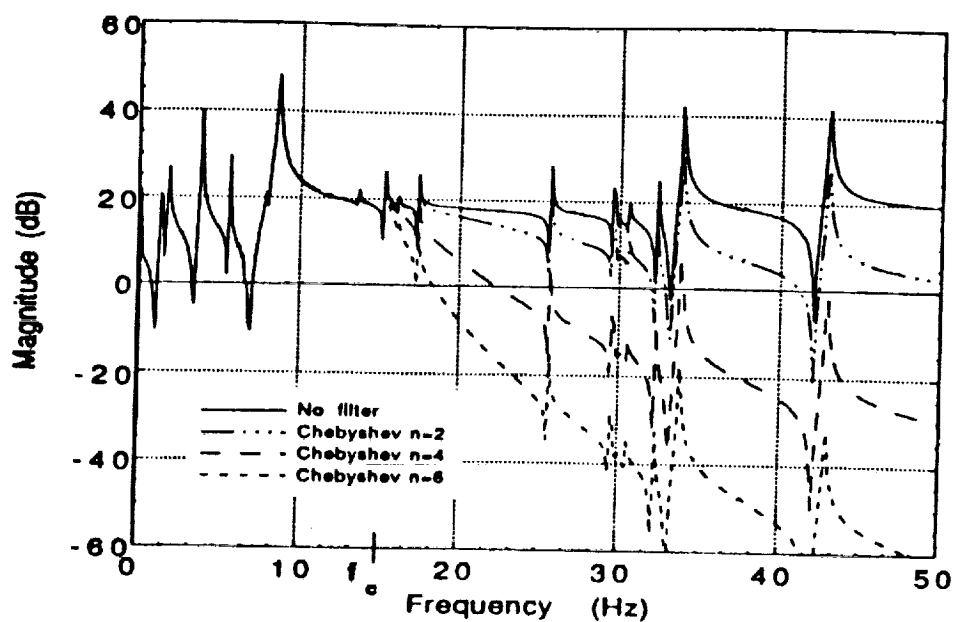
The Phase-0 CSI Evolutionary Model (CEM) was the test article used for this study

CSI Evolutionary Model Phase-Zero

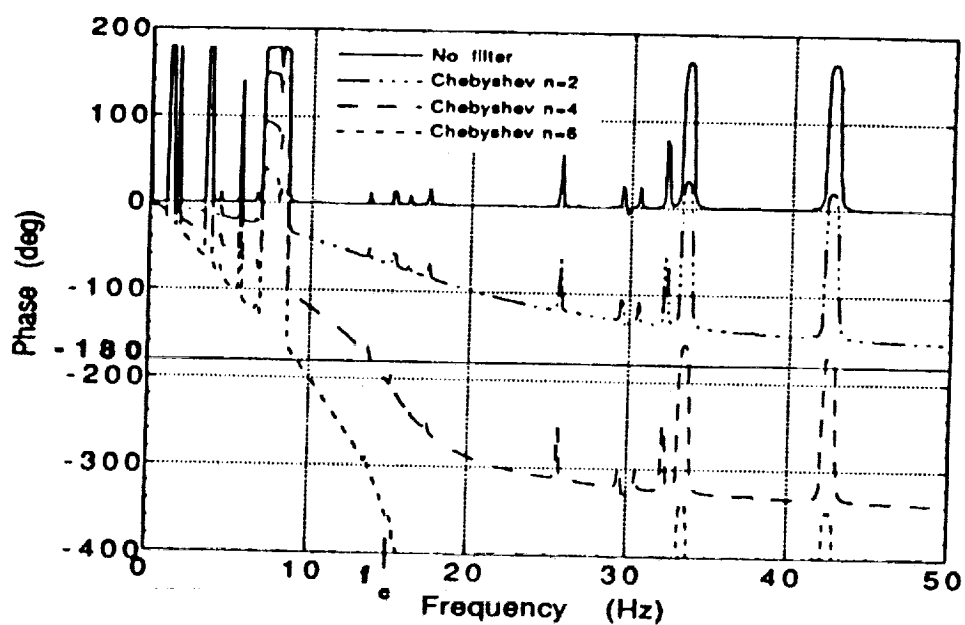


System ID Frequency Response Functions





(a) Magnitude Response



(b) Phase Response

Figure 5.4 Frequency Response of CSI Evolutionary Model with Chebyshev filters

4. CONTROL STRATEGY

Objectives for control of large flexible space structures (LFSS)

Accurate line-of-sight (LOS) pointing
Vibration suppression

Challenges for control design

Model parameter errors
Incomplete model (unmodeled modes)

Robust control methods

Static dissipative control (local velocity control)
Virtual passive control (2nd-order formulation)

5. Closed-Loop Simulation

Objective: Investigate the effect of sensor filtering on performance of feedback controllers

- A. Controllers developed without filter dynamics in the design model
 - i. Static dissipative control (SD-0)
 - ii. Virtual passive control (AVA)
- B. Controllers developed WITH filter dynamics in the design model (static dissipative control)

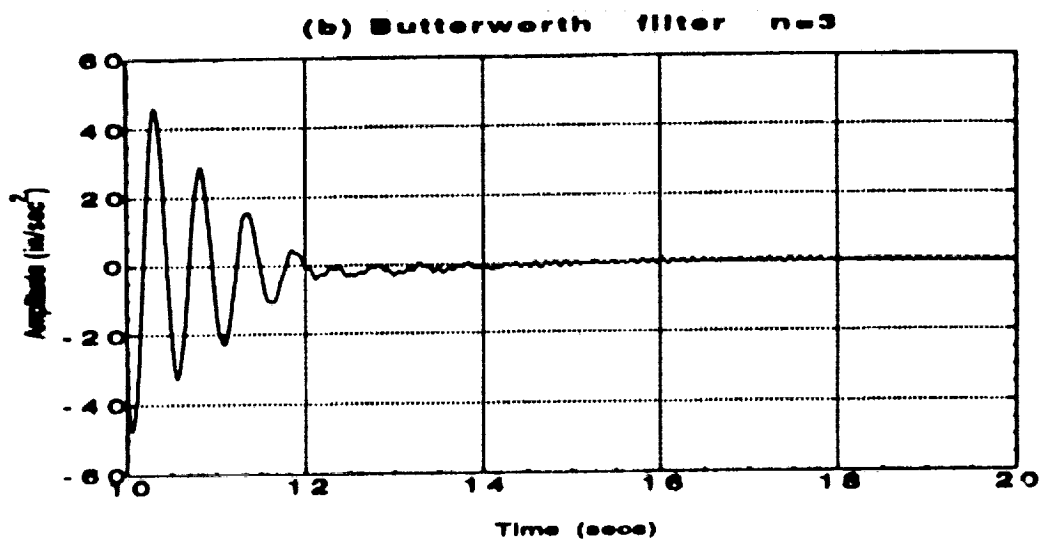
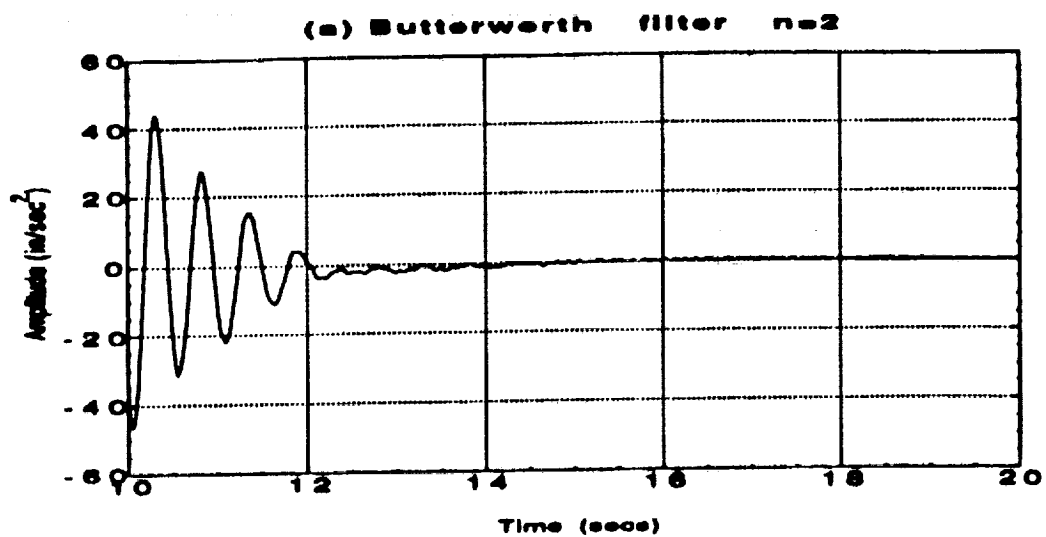


Figure 7.9 Acceleration response of closed-loop system with controller AVA and Butterworth filters (sensor location 1)

6. Closed-Loop Laboratory Experiments

7 Hz mode unstable when sensor filters used in system

**Discrepancies between experiment and
simulation due to**

MODELING ERRORS

- inaccurate parameters**
- unmodeled modes**

DISCRETIZATION ERRORS

**closed-loop system is not a continuous-time
system but a hybrid system**

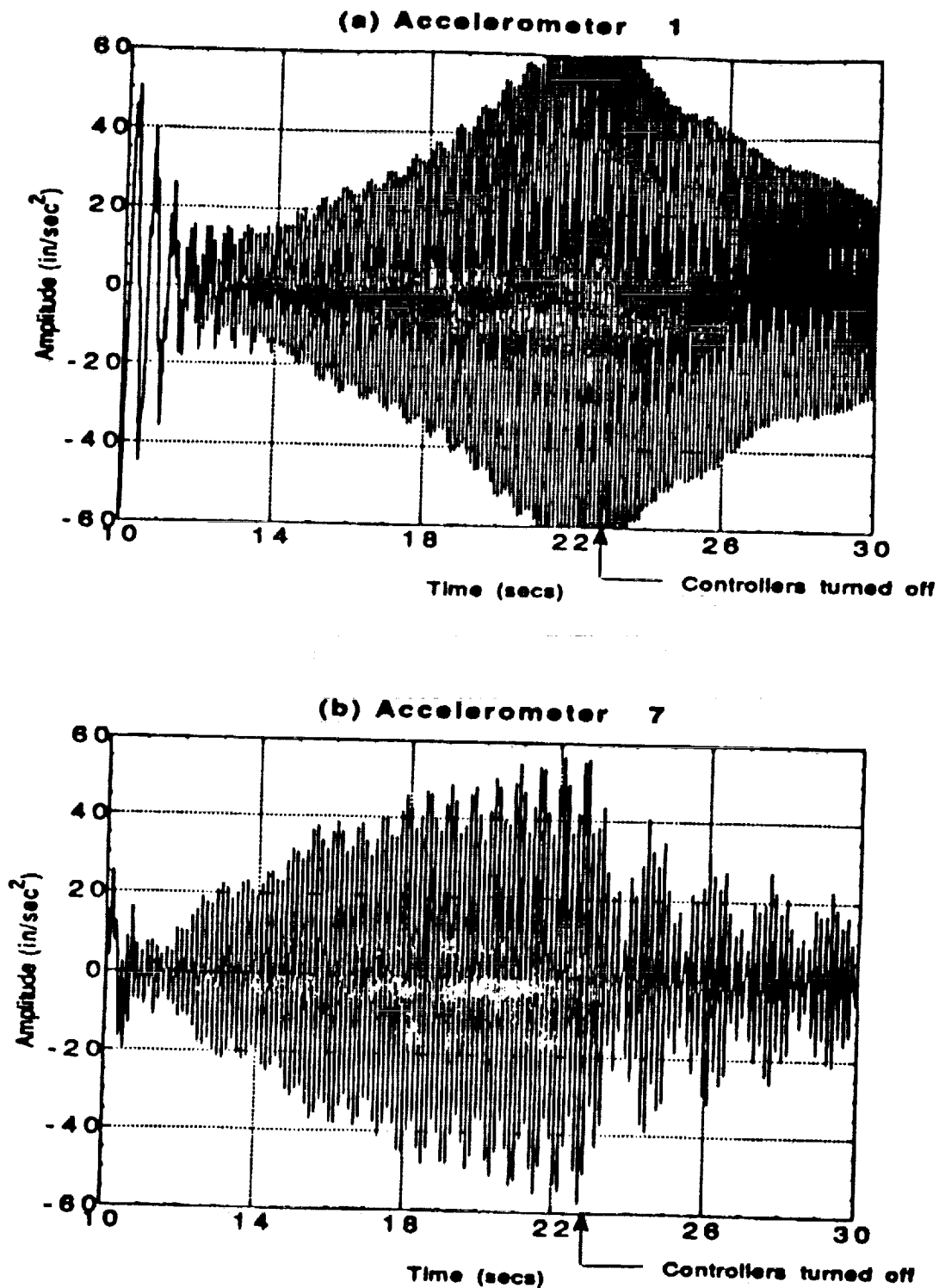


Figure 8.7 Experimental acceleration response of a closed-loop system with second-order Butterworth filters and controller AVA

Future Work

Modify filter design: Add zeros to numerator to compensate for phase lag

Formulate filter as a second-order system (corresponding to virtual passive control design)

Stability conditions for hybrid systems

Discretization issues: Method of implementing of digital filters

7. Conclusions and Future Work

Conclusions

- Sensor filters used successfully in closed-loop simulations
- Dynamics of higher-order filters must be considered in control law design
- Instability occurred in closed-loop experiments due to design model inaccuracies and discretization errors
- More accurate models of CSI test articles needed
- Stability conditions for continuous-time systems not valid for hybrid systems

N 9 2 - 2 8 7 3 4

**FUEL OPTIMAL PROPULSIVE REBOOST
OF FLEXIBLE SPACECRAFT**

by

Jim Redmond

*Building 1192C, Room 124
NASA Langley Research Center
Hampton, Virginia
January 13, 1992*

Motivation

Unbounded Fuel Optimal Control Problems

- Exact solutions are difficult to obtain for higher order systems.
- Impulsive forces cannot be implemented directly.
- Exact solutions provide basis for judging the optimality of approximate techniques.
- Properties of the exact solution can be used to develop improved approximations.

Floating Harmonic Oscillator

- Model possesses both rigid and flexible body motion characteristic of proposed spacecraft.

Overview

I. Fuel Optimal Propulsive Control

II. Numerical Solution by Adaptive Grid Bisection

III. The Floating Harmonic Oscillator

- a. System Definition
- b. Rigid Body Reboost Class
- c. Vibration Suppression Class
- d. General Reboost Class

IV. Concluding Remarks

Fuel Optimal Control

System Equation:

$$\dot{\underline{x}}(t) = A\underline{x}(t) + \sum_{j=1}^m \underline{b}_j u_j(t)$$

Control Objective:

Transfer the system from \underline{x}_0 to \underline{x}_1
in maneuver time T_f while
minimizing fuel consumption

Fuel Function:

$$\text{Fuel} = \sum_{j=1}^m \int_0^{T_f} |u_j(t)| dt$$

Fuel Optimal Control

General Solution:

$$\underline{x}(t) = e^{At} (\underline{x}_0 + \sum_{j=1}^m \int_0^t e^{-As} \underline{b}_j u_j(s) ds)$$

Reachable State:

$$\underline{y} = \sum_{j=1}^m \int_0^{T_f} e^{-At} \underline{b}_j u_j(t) dt = e^{-AT_f} \underline{x}_1 - \underline{x}_0$$

Control Index:

$$g_j(\underline{\eta}, t) = \underline{\eta}^T e^{-At} \underline{b}_j \quad j=1, 2, \dots, m$$

Hyperplane Constraint:

$$H = \{ \underline{\eta} : \underline{\eta}^T \underline{y} = 1 \}$$

Index Extremum:

$$\alpha^* = \min_{\underline{\eta} \in H} \max_{1 \leq j \leq m} \sup_{0 \leq t \leq T_f} |g_j(\underline{\eta}, t)|$$

Fuel Optimal Control

Optimal Control:
$$u_j^*(t) = \frac{\underline{\underline{g}}_j^T \underline{\underline{c}}_j}{\alpha^*} \quad (j=1,2,\dots,m)$$

Impulse Vector:
$$\underline{\underline{g}}_j = [\text{sgn}(\underline{\underline{g}}_j(\underline{\underline{\eta}}_j^*, \tau_{1j}))\delta(t-\tau_{1j}) \dots \text{sgn}(\underline{\underline{g}}_j(\underline{\underline{\eta}}_j^*, \tau_{N_{ij}}))\delta(t-\tau_{N_{ij}})]^T$$

Impulse Coefficient Vector:
$$\underline{\underline{c}}_j = [c_{1j} \ c_{2j} \ \dots c_{N_{ij}}]^T$$

Coefficient Constraint:
$$\underline{\underline{1}} = \underline{\underline{1}}^T \underline{\underline{c}}_j$$

$$\underline{\underline{1}} = [1 \ 1 \ \dots \ 1]^T \quad \underline{\underline{c}} = [\underline{\underline{c}}_1^T \ \underline{\underline{c}}_2^T \ \dots \ \underline{\underline{c}}_m^T]^T$$

Optimum Fuel:
$$\text{Fuel}^* = \frac{1}{\alpha^*}$$

Adaptive Grid Bisection

- (1) Generate a square grid G of normal vectors $\underline{\underline{\eta}}_1, \underline{\underline{\eta}}_2, \dots, \underline{\underline{\eta}}_p$ that form a subset of the hyperplane H .

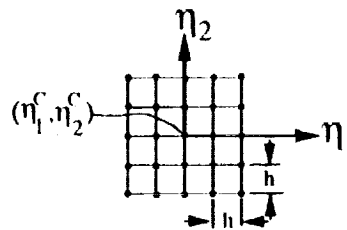


Figure 1 - Square Grid Generated in Step (1) in Which $n=3$ and $L=2$

Adaptive Grid Bisection

- (2) Determine $\alpha_{ij} = \sup_{0 \leq t \leq T_f} |g_j(\eta_i, t)|$ for each η_i ($i=1,2,\dots,p$) and for each ($j=1,2,\dots,m$). The suprema α_{ij} are computed to within the error margin ε_1 .

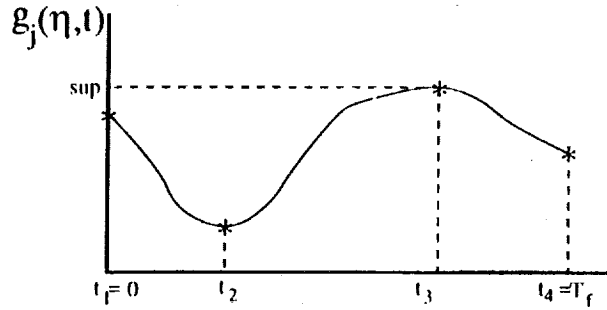


Figure 2 - Sample Function for Step (2)
Supremum Computation

Adaptive Grid Bisection

- (3) Determine the grid-optimal normal vector η_i^* for which $\alpha = \min_{1 \leq i \leq p} \max_{1 \leq j \leq m} \alpha_{ij}$.
- (4) Select an updated grid G of normal vectors η_2, \dots, η_p centered about the grid-optimal normal vector η_i^* based on the following:
- (a) If η_i^* is an interior grid point, decrease the grid spacing by 50% (bisection).
 - (b) If η_i^* is a boundary grid point, increase the spacing by 50%.

Adaptive Grid Bisection

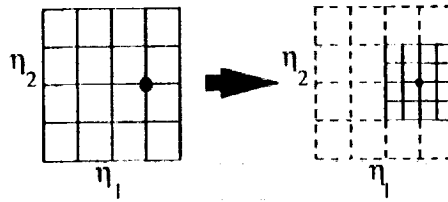


Figure 3 - $\tilde{\eta}_i^*$ in the Interior Leads to Grid Spacing Decreased by 50% in Step (4)

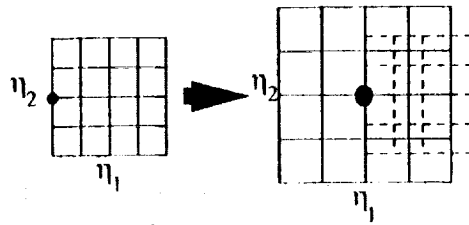


Figure 4 - $\tilde{\eta}_i^*$ on the Boundary Leads to Grid Spacing Increased by 50% in Step (4)

Adaptive Grid Bisection

- (5) Repeat steps (2)-(4) until the grid spacing is within the error margin ε_2 . The converged grid-optimal normal vector represents the optimal normal vector $\tilde{\eta}^*$.
- (6) Determine the number of impulses N_j associated with $u_j^*(t)$ ($j=1,2,\dots,m$), the corresponding impulse times τ_{ij} ($i=1,2,\dots,N_j$; $j=1,2,\dots,m$) and the sign functions $\text{sgn}(g_j(\tilde{\eta}^*, \tau_{ij}))$.

Adaptive Grid Bisection

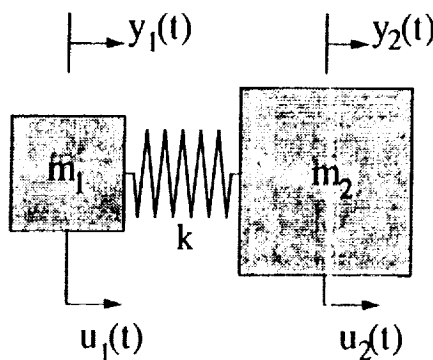
- (7) Compute the impulse coefficients c_{ij}
 ($i=1,2,\dots N_j$; $j=1,2,\dots m$).

$$\underline{P} \underline{c} = \underline{Q}, \quad c \geq 0$$

$$P = \begin{bmatrix} \frac{1}{\alpha^*} \int_0^{T_f} e^{-\Lambda t} \underline{b}_1 \underline{g}_1^T dt & \dots & \frac{1}{\alpha^*} \int_0^{T_f} e^{-\Lambda t} \underline{b}_m \underline{g}_m^T dt \\ \hline \underline{1}^T \end{bmatrix} \quad Q = \begin{bmatrix} y \\ \hline 1 \end{bmatrix}$$

Floating Harmonic Oscillator

System Definition



Equations of Motion:

$$m_1 \ddot{y}_1(t) + k(y_1(t) - y_2(t)) = u_1(t)$$

$$m_2 \ddot{y}_2(t) + k(y_2(t) - y_1(t)) = u_2(t)$$

State Definition:

$$x_1(t) = \frac{m_1 y_1(t) + m_2 y_2(t)}{m_1 + m_2} \quad x_2(t) = y_2(t) - y_1(t)$$

$$x_3(t) = \dot{x}_1(t) \quad x_4(t) = \dot{x}_2(t)$$

Floating Harmonic Oscillator

System Definition

State Space Representation:

$$\dot{\underline{x}}(t) = A\underline{x}(t) + \sum_{j=1}^m \underline{b}_j u_j(t)$$

System Matrices:

$$A = \begin{bmatrix} 0 & 0 & 1 & 0 \\ 0 & 0 & 0 & 1 \\ 0 & 0 & 0 & 0 \\ 0 & -\omega^2 & 0 & 0 \end{bmatrix} \quad \underline{b}_1 = \begin{bmatrix} 0 \\ 0 \\ \frac{1}{m_1+m_2} \\ -\frac{1}{m_1} \end{bmatrix} \quad \underline{b}_2 = \begin{bmatrix} 0 \\ 0 \\ \frac{1}{m_1+m_2} \\ \frac{1}{m_2} \end{bmatrix}$$

Natural Frequency of Oscillation:

$$\omega = \sqrt{\frac{k(m_1+m_2)}{m_1 m_2}}$$

Floating Harmonic Oscillator

System Definition

Matrix Exponential:

$$e^{At} = \begin{bmatrix} 1 & 0 & t & 0 \\ 0 & \cos \omega t & 0 & \frac{\sin \omega t}{\omega} \\ 0 & 0 & 1 & 0 \\ 0 & -\omega \sin \omega t & 0 & \cos \omega t \end{bmatrix}$$

Control Index Functions:

$$g_1 = \frac{-t}{m_1+m_2} \eta_1 + \frac{\sin \omega t}{\omega m_1} \eta_2 + \frac{1}{m_1+m_2} \eta_3 - \frac{\cos \omega t}{m_1} \eta_4$$

$$g_2 = \frac{-t}{m_1+m_2} \eta_1 - \frac{\sin \omega t}{\omega m_2} \eta_2 + \frac{1}{m_1+m_2} \eta_3 + \frac{\cos \omega t}{m_2} \eta_4$$

Reachable State:

$$\underline{y} = [-x_{10} \ -x_{20} \ 0 \ 0]^T$$

Hyperplane Constraint:

$$-\eta_1 x_{10} - \eta_2 x_{20} = 1$$

Initial Conditions:

$$y_{10} = y_{20} = 1$$

$$x_{10} = 1$$

$$x_{20} = 0$$

Optimal Normal Vector:

$$\tilde{\eta}^* = [-1 \quad 0 \quad -T_f/2 \quad 0]^T$$

Optimal Control:

$$u_j^*(t) = \frac{m_j}{T_f} [-\delta(t) + \delta(t - T_f)], \quad (j=1,2)$$

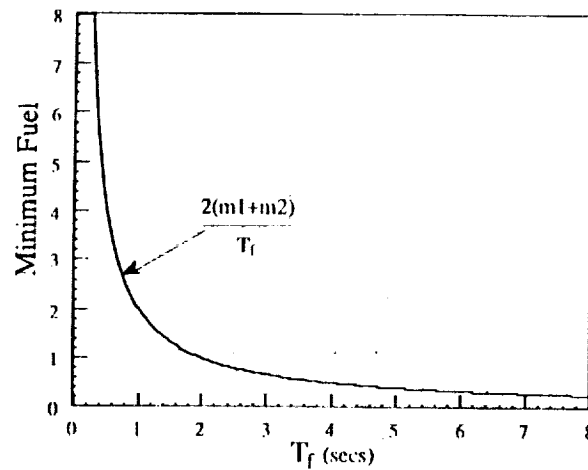


**Figure 5 - Rigid-Body Reboost Class:
Minimum Fuel versus Maneuver Time**

Floating Harmonic Oscillator Vibration Suppression Class

Initial Conditions: $y_{10} = \frac{-m_2}{m_1+m_2}$ $y_{20} = \frac{m_1}{m_1+m_2}$
 $x_{10} = 0$ $x_{20} = 1$

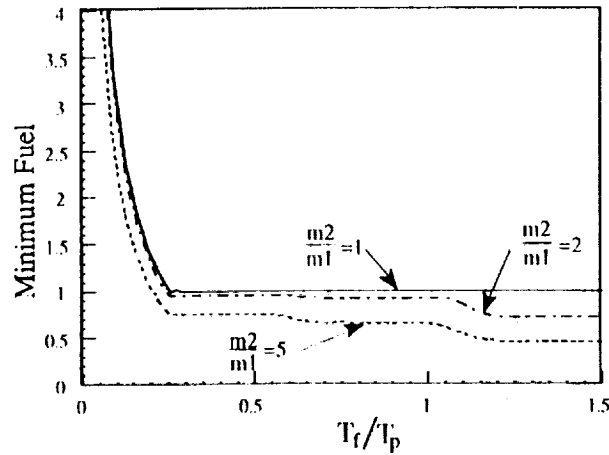


Figure 6 - Vibration Suppression Class:
Minimum Fuel versus Maneuver Time

Floating Harmonic Oscillator Vibration Suppression Class

Table 1 - Convergence Example: Vibration Suppression Class,
 $m_2=2m_1$ Case, $T_f=2.0s$

iteration	η_1	η_3	η_4	step-size	min max sup $lg_j(\eta_i)$
1	0.00000000	0.00000000	0.00000000	1.00000000	1.4142135623731
2	0.50000000	0.50000000	0.00000000	0.50000000	1.3041415131743
3	0.50000000	0.75000000	0.00000000	0.25000000	1.1265267495443
4	0.50000000	0.75000000	0.00000000	0.12500000	1.1265267495443
5	0.50000000	0.68750000	0.06250000	0.06250000	1.1009325628443
10	0.410156250	0.656250000	-0.013671875	0.0019531250	1.0811093227742
20	0.408424377	0.655029297	-0.013526916	0.000171661	1.0808406732402
35	0.408419866	0.655029163	-0.013533452	0.000000141	1.0808403397486
45	0.408419879	0.655029163	-0.013533430	0.000000001	1.0808403395831

Floating Harmonic Oscillator Vibration Suppression Class

Table 2 - Control Parameters:
Vibration Suppression Class, $m_2 = 2m_1$ Case

$T_f(\text{secs})$	$u_1(t)$ impulses			$u_2(t)$ impulses		
	$t_{1j}(\text{secs})$	$\text{sgn}(g_1)$	c_{1j}	$t_{2j}(\text{secs})$	$\text{sgn}(g_2)$	c_{2j}
0.5	0.000000	+	0.164045	0.000000	-	0.164045
	0.500000	-	0.335955	0.500000	+	0.335955
2.0	0.817892	-	0.498827	0.623410	+	0.436626
	2.000000	+	0.067895			
4.0	0.740480	-	0.250000			
	2.221441	+	0.500000			
	3.702402	-	0.250000			

Floating Harmonic Oscillator Vibration Suppression Class

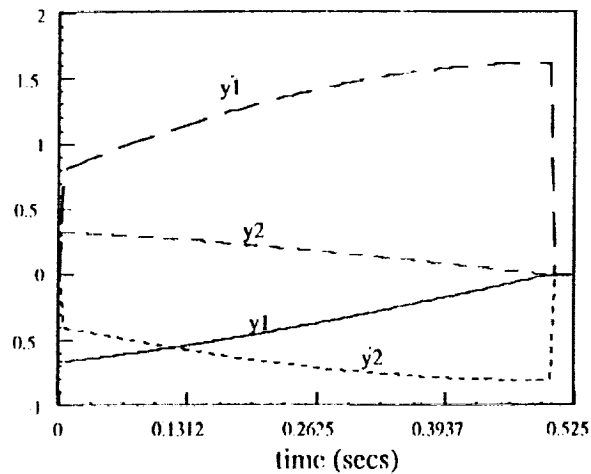


Figure 7 - Vibration Suppression Class, $m_2 = 2m_1$ Case, $T_f = 0.5s$:
Displacement and Velocity of Each Mass versus Time

Floating Harmonic Oscillator Vibration Suppression Class

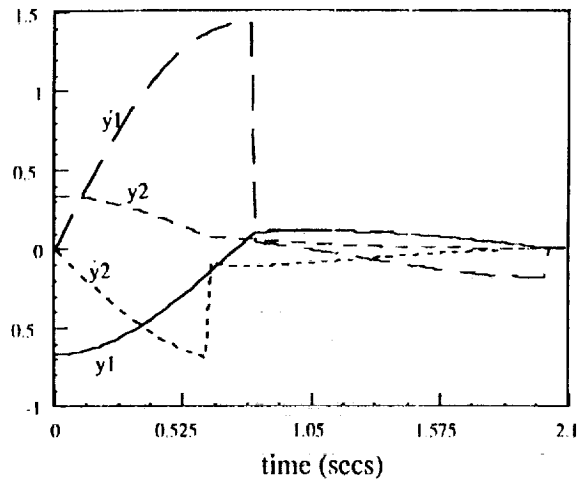


Figure 8 - Vibration Suppression Class, $m_2=2m_1$ Case, $T_f=2.0s$:
Displacement and Velocity of Each Mass versus Time

Floating Harmonic Oscillator Vibration Suppression Class

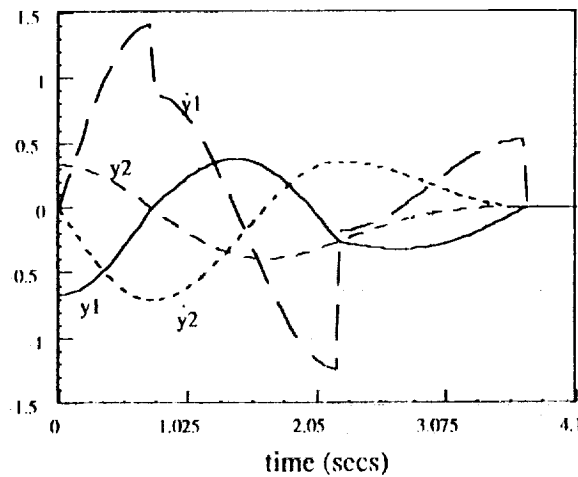


Figure 9 - Vibration Suppression Class, $m_2=2m_1$ Case, $T_f=4.0s$:
Displacement and Velocity of Each Mass versus Time

Initial Conditions: $y_{10} = 1 - \frac{m_2}{m_1 + m_2}$ $y_{20} = 1 + \frac{m_1}{m_1 + m_2}$
 $x_{10} = 1$ $x_{20} = 1$

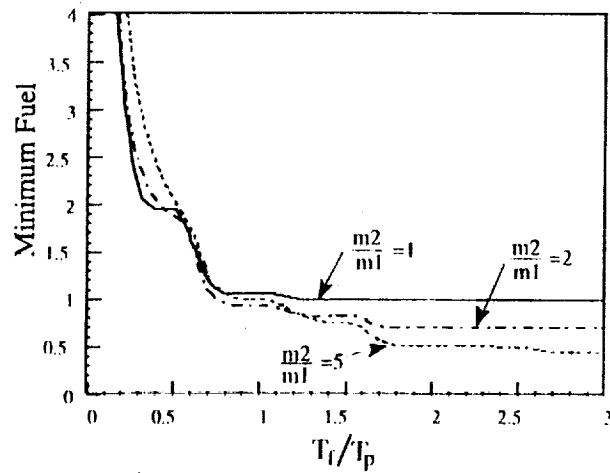


Figure 10 - General Reboost Class:
Minimum Fuel versus Maneuver Time

Table 3 - Control Parameters:
General Reboost Class, $m_2 = 2m_1$ Case

$T_f(\text{secs})$	$u_1(t)$ impulses			$u_2(t)$ impulses		
	$\tau_{1j}(\text{secs})$	$\text{sgn}(g_{1j})$	c_{1j}	$\tau_{2j}(\text{secs})$	$\text{sgn}(g_{2j})$	c_{2j}
0.8	0.000000	-	0.077500	0.000000	-	0.310394
	0.110495	-	0.112258	0.800000	+	0.500151
2.0	0.891020	-	0.164744	0.000000	-	0.337958
	2.000000	+	0.497984			
5.3	0.740480	-	0.377465			
	2.221441	+	0.150000			
	3.702402	-	0.122535			
	5.183363	+	0.350000			

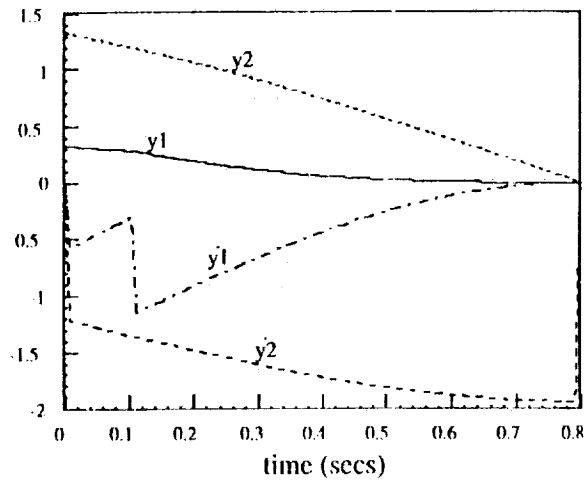


Figure 11 - General Reboost Class, $m_2 = 2m_1$ Case, $T_f = 0.8s$:
Displacement and Velocity of Each Mass versus Time

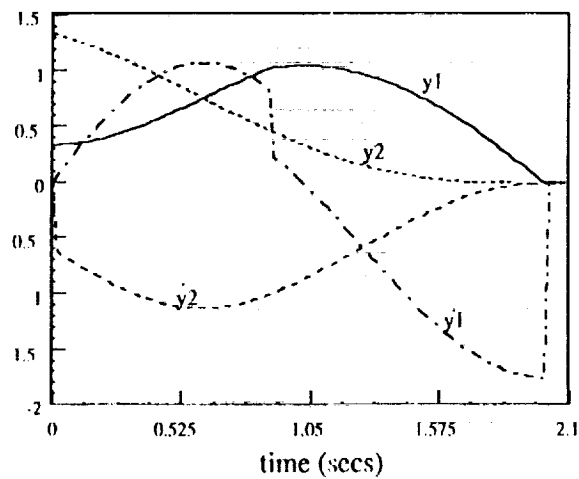


Figure 12 - General Reboost Class, $m_2 = 2m_1$ Case, $T_f = 2.0s$:
Displacement and Velocity of Each Mass versus Time

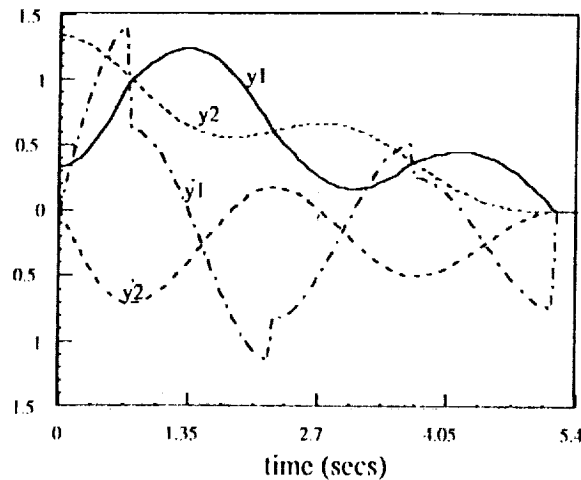


Figure 13 - General Reboost Class, $m_2=2m_1$ Case, $T_f=5.3s$:
Displacement and Velocity of Each Mass versus Time

Concluding Remarks

- Adaptive Grid Bisection can be used to solve some fuel optimal propulsive control problems.
 - "Fuel Optimal Propulsive Reboost of Flexible Spacecraft"
 - "Fuel Optimal Propulsive Reorientation of Axisymmetric Spin-Stabilized Satellites"
 - "An Exact Solution to the Fuel Optimal Propulsive Control of a Tutorial Structure"
- Exact fuel optimal solutions provide a basis for assessing the degree of optimality attained with approximate techniques.
 - Linear Quadratic Regulator
 - Independent Modal Space Control
 - Impulse Damping Control
- Knowledge of exact solutions can be used to improve the optimality of existing approximations.

Ongoing Research in Spacecraft Controls

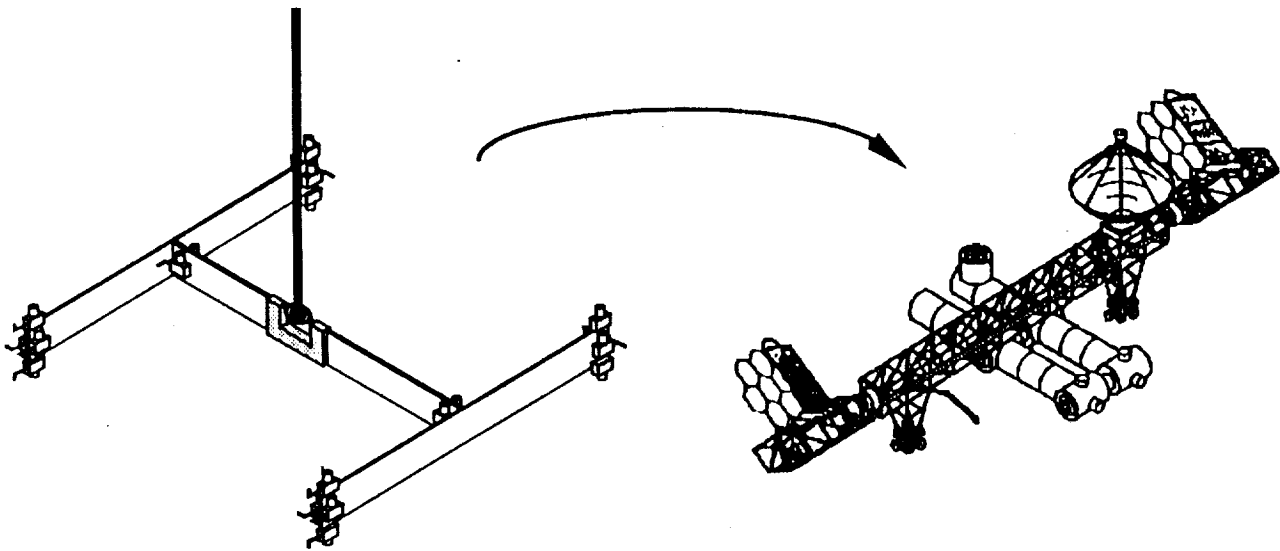
Fuel Optimal Maneuver : Experimental Testbeds

Presented by

John L. Meyer

January 13, 1992

LaRC GNC Technical Committee and Mars Mission Research Center
NASA Langley Research Center
Hampton, Virginia



Objective :

**To Conduct Experiments in Fuel Optimal
Propulsive Maneuver of Flexible Spacecraft
in order to Verify and Extend Recently Developed
Theory and Apply to Various Classes of Spacecraft**

Ongoing Progress in Spacecraft Controls

PRECEDING PAGE BLANK NOT FILMED

Outline

I. Related Experimental Efforts

II. Completed Experiments

- A. Experimental Verification of Impulse Damping Control*
- B. Impulse Damping of the SCOLE Reflector and Mast*
- C. Impulse Damping Control of an Experimental Structure*

III. Experiment Preparations

- A. Reaction Control System*
- B. Rotating Flexible Beam*
- D. IMAGE Testbed*
- C. Aerobrake Configuration*

Ongoing Progress in Spacecraft Controls

Outline

IV. Current and Future Experiments

- A. *Fuel Optimal Control of an Experimental Rotating Flexible Beam*
- B. *Fuel Optimal Aerobrake Maneuver of an Experimental Lunar Orbital Transfer Vehicle*
- C. *Fuel Optimal Propulsive Maneuvers of an Experimental Space Structure Undergoing Translation, Rotation, and Flexible Body Motions*

V. Summary

Ongoing Progress in Spacecraft Controls

Related Experimental Efforts

- 1** Dehghanyar, T. J., Masri, S. F., Miller, R. K., Bekey, G. A., and Caughey, T. K., "An Analytical and Experimental Study into the Stability and Control of Nonlinear Flexible Structures," *Proceedings of the Fourth VPI&SU Symposium on Dynamics and Control of Large Structures*, June 1983.
- 2** Floyd, Michel A., "Single-Step Optimal Control of the RPL Experiment," *Advances in the Astronomical Sciences*, vol. 57, 1985, pp. 323-350.
- 3** Bossi, J. A., and Tsou, J. W., "A Laboratory Experiment in Control/Structure Interaction," *Proceedings of the 1986 American Control Conference*, June 1986, pp. 1034-1038.
- 4** Williams, Jeffrey P., "Slew Maneuvers on the SCOLE Laboratory Facility," *Proceedings of the First NASA/DOD CSI Technology Conference*, November 1986, pp. 851-867.

Ongoing Progress in Spacecraft Controls

Related Experimental Efforts

- 5** Shenhar, J., Sparks, D. Jr., Williams, J. P., and Montgomery, R. C., "Attitude Control System Testing on SCOLE," *Proceedings of the Sixth VPI&SU Symposium on Dynamics and Control of Large Structures*, June 1987, pp. 251-273.
- 6** Meyer, John L., "Experimental Verification of Impulse Damping Control," *Master of Science Thesis*, North Carolina State University, April 1990.
- 7** Redmond, Jim M., Meyer, John L., and Silverberg, Larry M., "Impulse Damping Control of an Experimental Structure," *Journal of Sound and Vibration*, to appear.
- 8** NASA Langley Research Center CSI Program, i.e. Phase 0

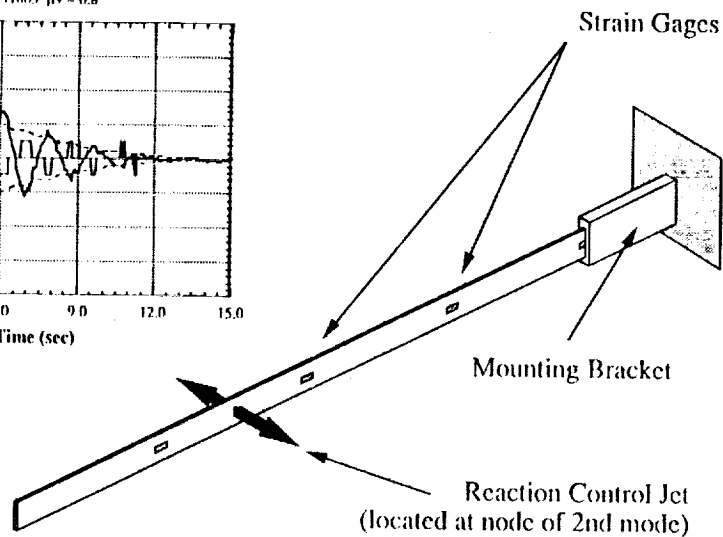
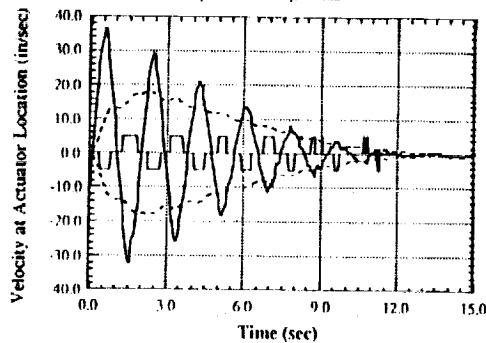
Ongoing Progress in Spacecraft Controls

Completed Experiments

Experimental Verification of Impulse Damping Control

Controlled Response of Mode #1

Window = 2.0 sec, $Y_{db} = 0.20$, $Y_{vdb} = 1.0$
 $\mu d = 1.11805$ $\mu v = 0.8$

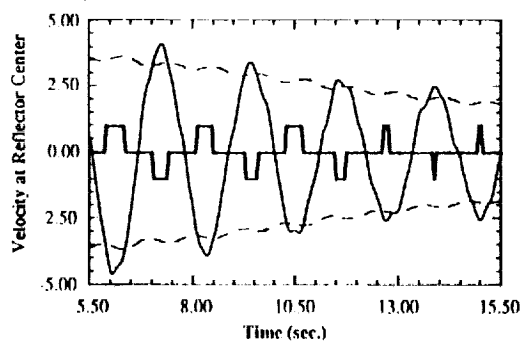


Ongoing Progress in Spacecraft Controls

Completed Experiments

Impulse Damping of the SCOLE Reflector and Mast

SCOLE Reflector Velocity, Running Standard Deviation of Velocity (with a window size of 4.5 seconds), and Thruster Forces



SCOLE Planform



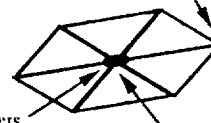
X & Y Accelerometers and Reaction Wheels

SCOLE Reflector and Mast

3 Axis Angular Rate Sensor

X and Y Accelerometers at Reflector Center

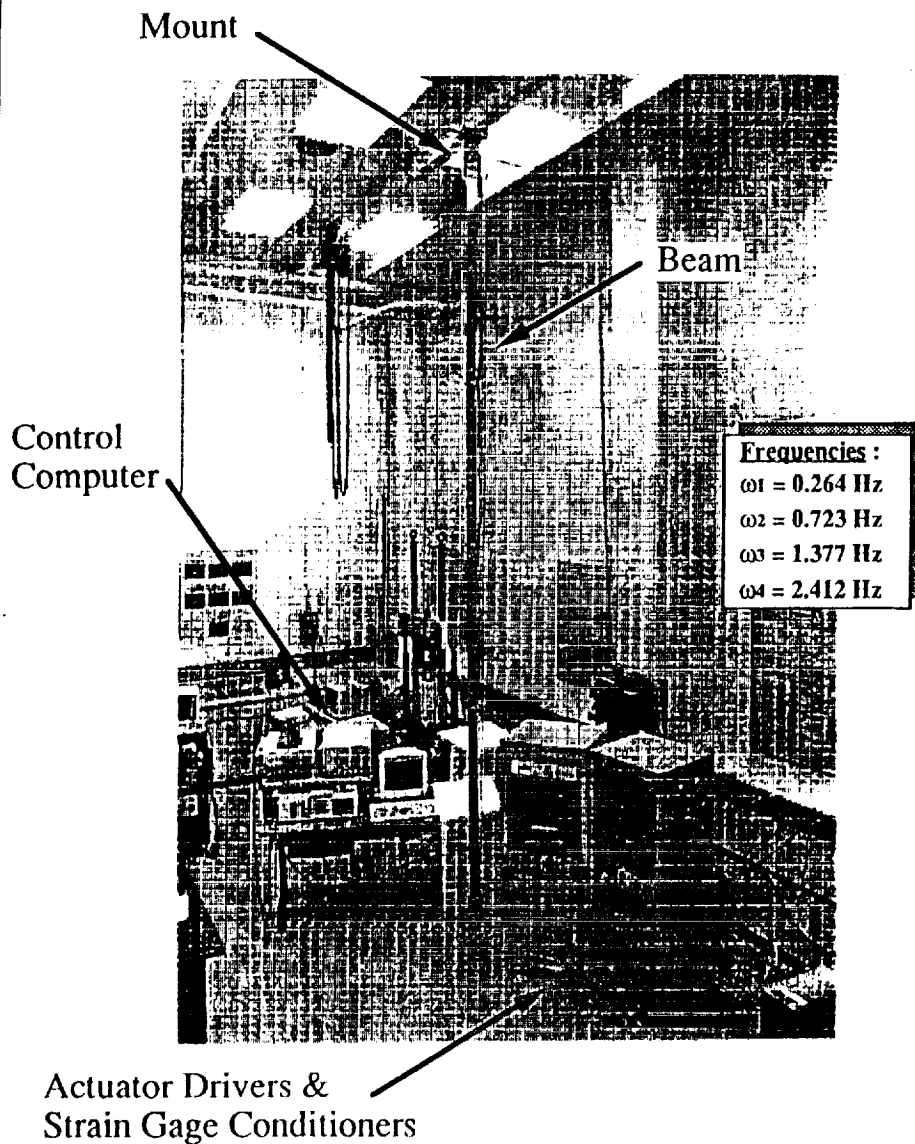
Air Jets at Reflector Center



Ongoing Progress in Spacecraft Controls

Completed Experiments

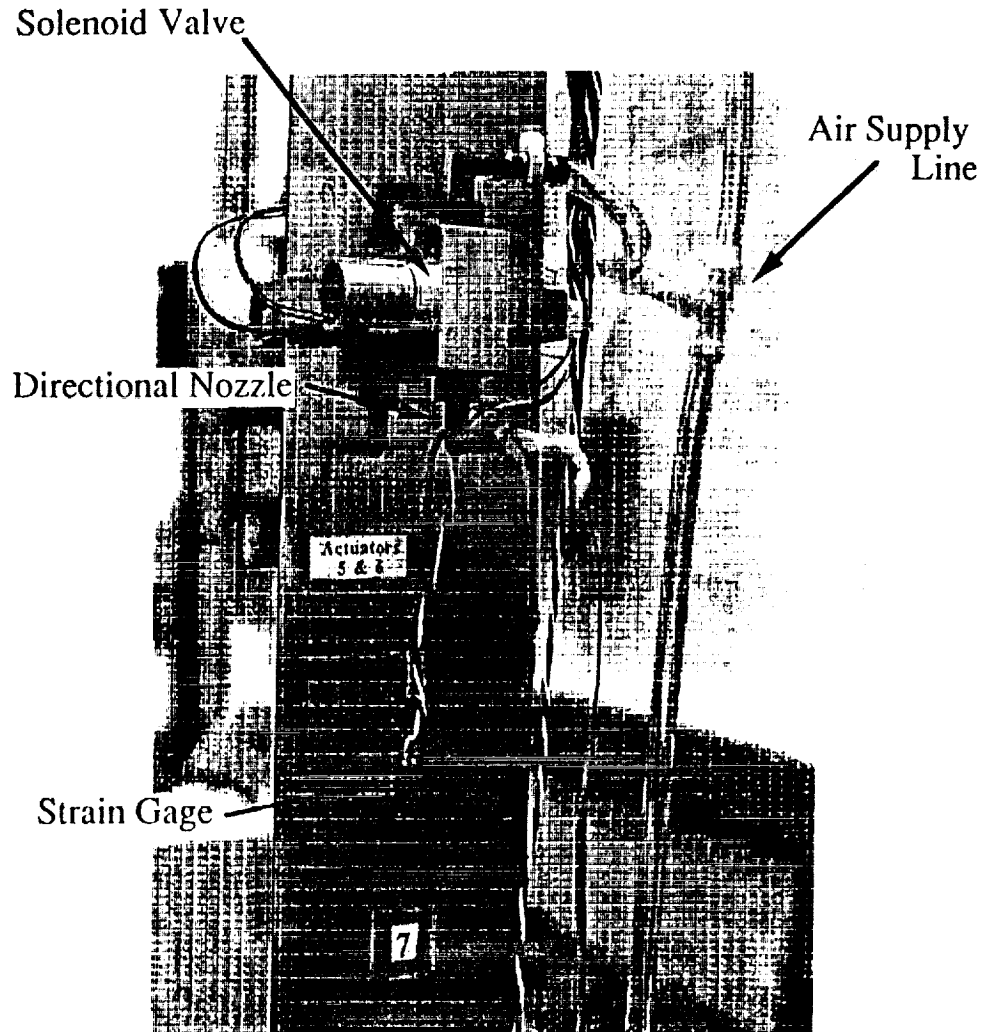
Impulse Damping Control of an Experimental Structure



Ongoing Progress in Spacecraft Controls

Completed Experiments

Impulse Damping Control of an Experimental Structure



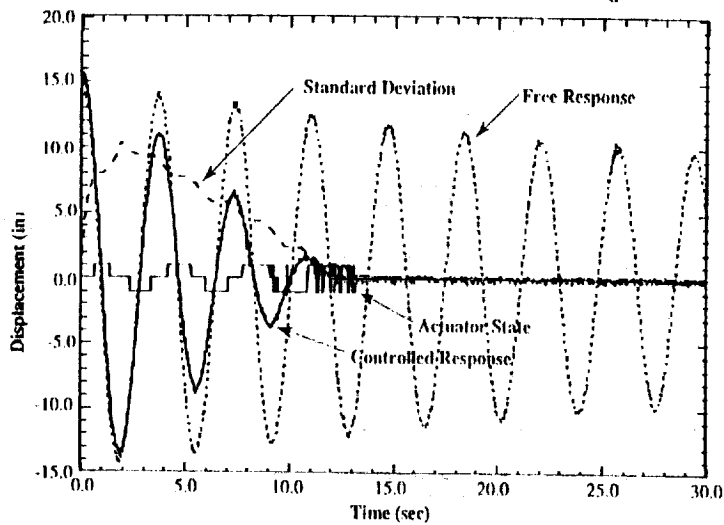
Ongoing Progress in Spacecraft Controls

Completed Experiments

Impulse Damping Control of an Experimental Structure

Control of Vertical Beam Under Mode 1 Excitation

$P_s = 35$ psi, Window = 1.875 sec, Deadband = 0.5 in, $\mu_u = 1.0$



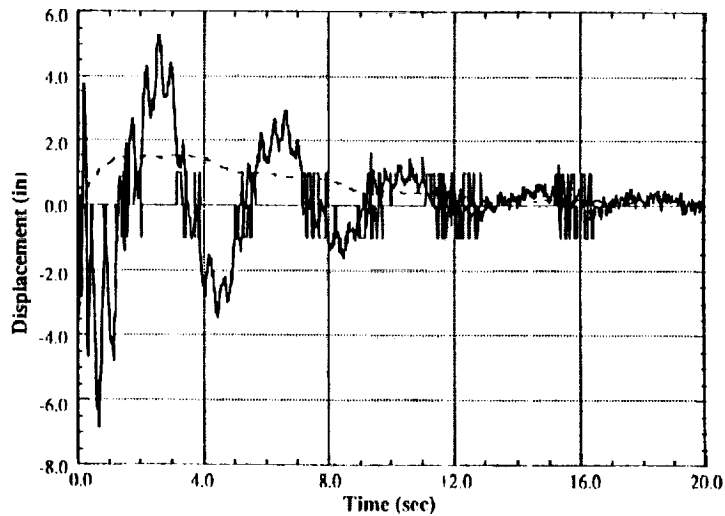
Ongoing Progress in Spacecraft Controls

Completed Experiments

Impulse Damping Control of an Experimental Structure

Control of Vertical Beam Under Multi-Mode Excitation

$P_s = 35$ psi, Window = 1.875 sec, Deadband = 0.35 in, $\mu_u = 0.5$

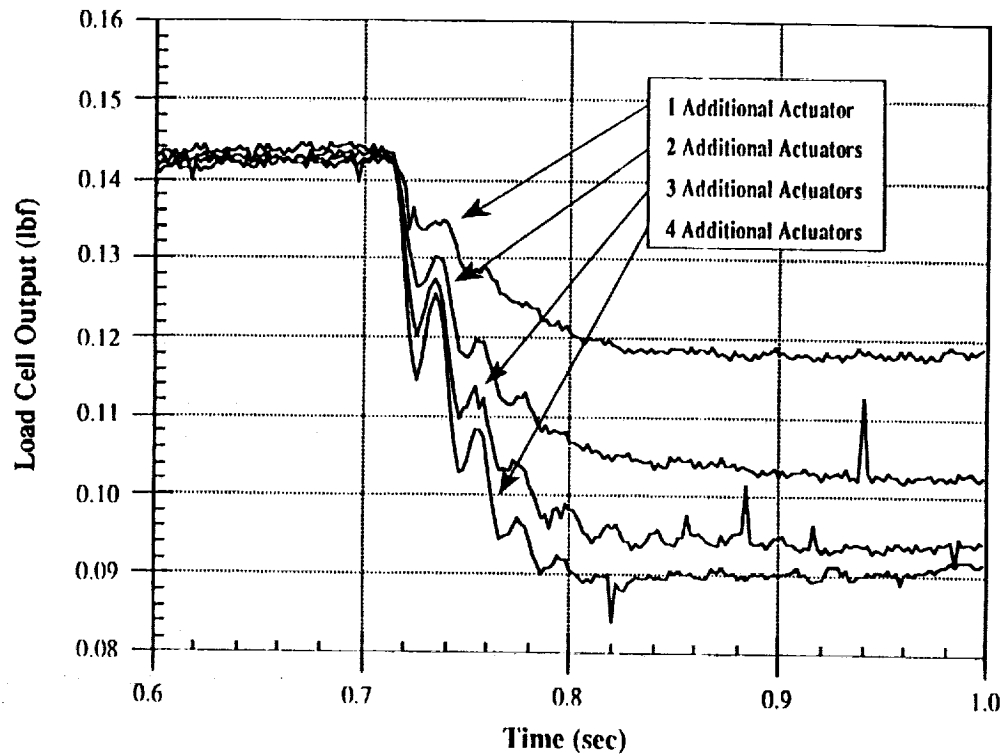


Ongoing Progress in Spacecraft Controls

Experiment Preparations

Reaction Control System

Effect of Additional Actuators on Same Supply
50 psi Supply Pressure



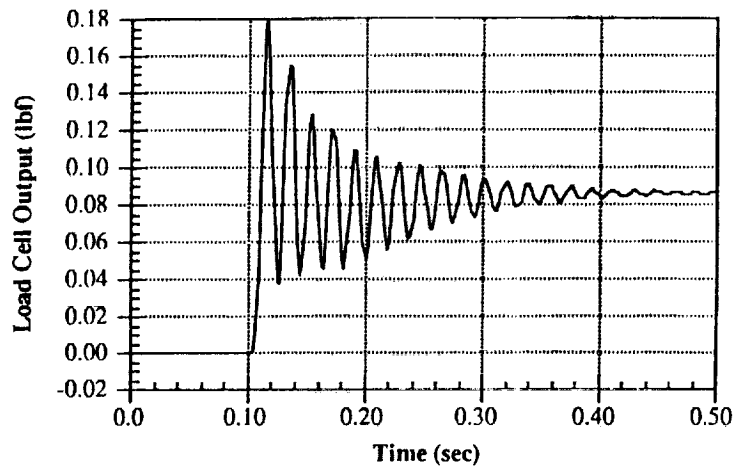
Ongoing Progress in Spacecraft Controls

Experiment Preparations

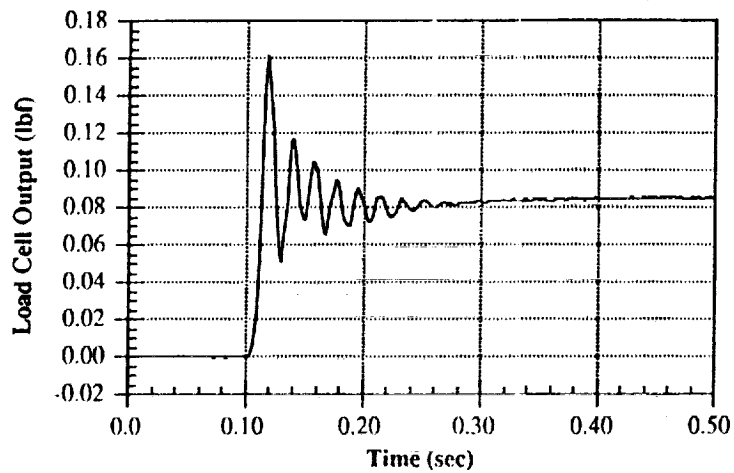
Reaction Control System

Supply Line Length Effects

40 psi Supply Pressure / 12 ft. Supply Line



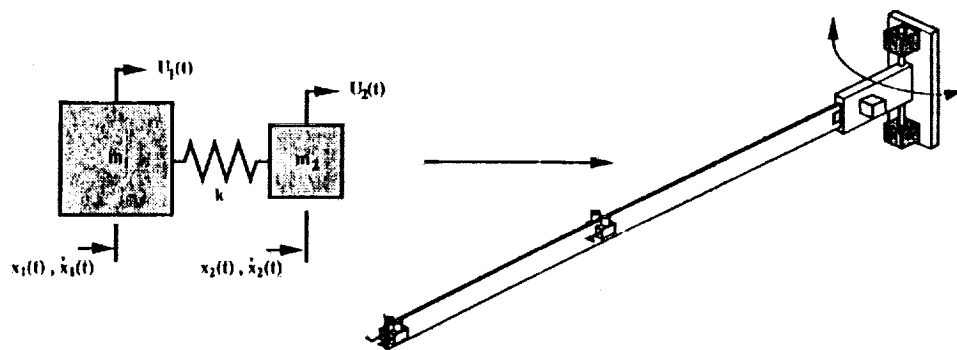
40 psi Supply Pressure / 25 ft. Supply Line



Ongoing Progress in Spacecraft Controls

Experiment Preparations

Rotating Flexible Beam



$$\mathbf{z} = \begin{bmatrix} \theta \\ \dot{\theta} \\ q \\ \dot{q} \end{bmatrix} \quad \mathbf{e}^{-\mathbf{A}T} = \begin{bmatrix} 1 & -T & 0 & 0 \\ 0 & 1 & 0 & 0 \\ 0 & 0 & \cos(\omega T) & -\frac{1}{\omega} \sin(\omega T) \\ 0 & 0 & \omega \sin(\omega T) & \cos(\omega T) \end{bmatrix}$$

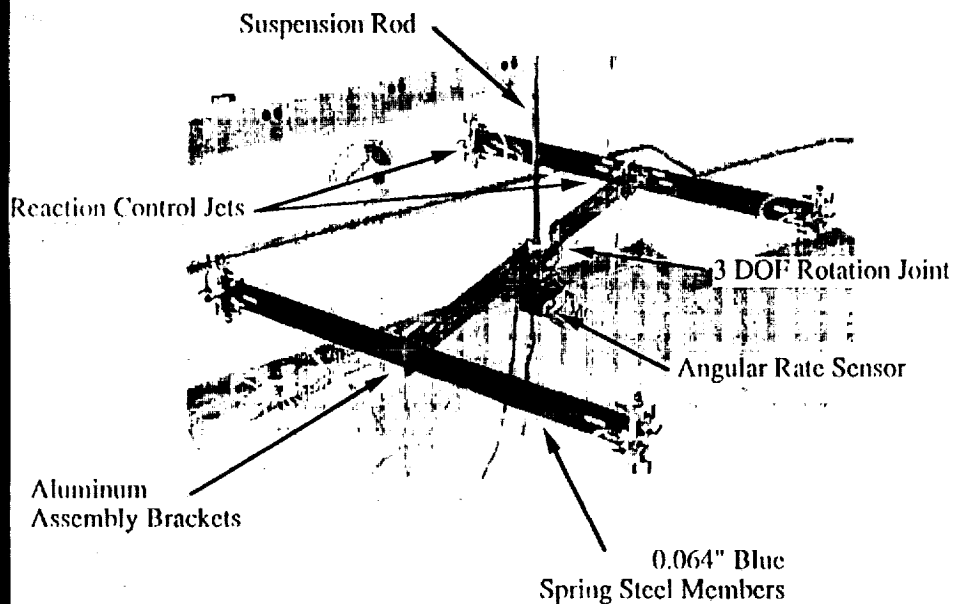
$$g_j(\eta, t) = \eta^T e^{-\mathbf{A}t} \mathbf{b}_j \quad n = 1, 2$$

$$\alpha^* = \min_{\eta \in \Pi} \max_{1 \leq j \leq 2} \sup_{0 \leq t \leq T_f} |g_j(\eta, t)|$$

Ongoing Progress in Spacecraft Controls

Experiment Preparations

IMAGE Testbed

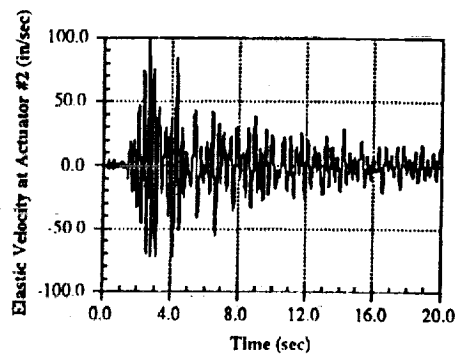
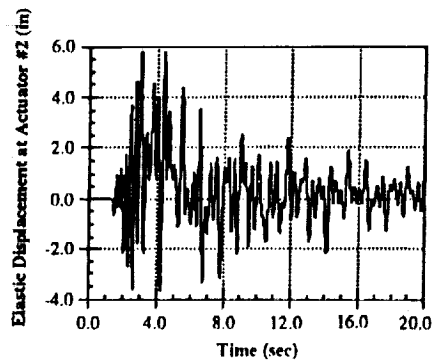


Ongoing Progress in Spacecraft Controls

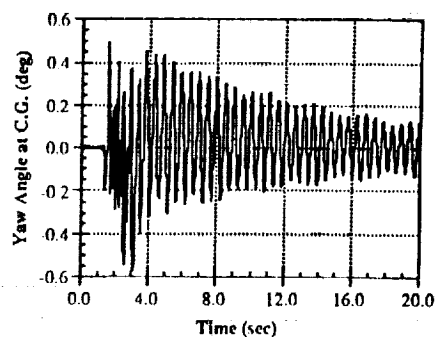
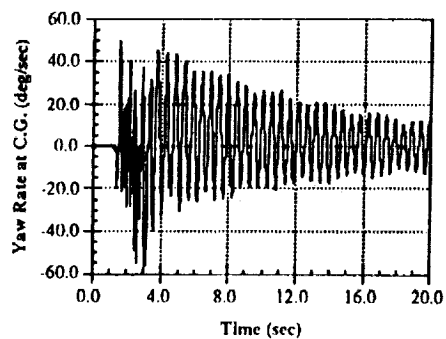
Experiment Preparations

Image Testbed

Free Response of IMAGE Structure to Multi-Mode Excitation



Differentiation Yields



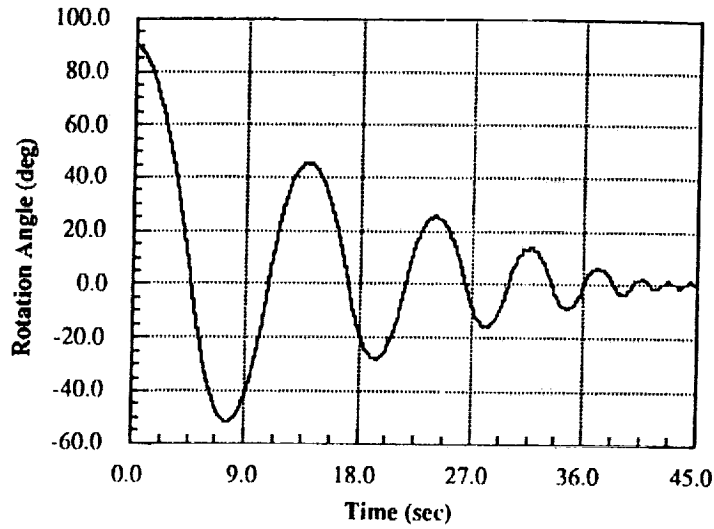
Integration Yields

Ongoing Progress in Spacecraft Controls

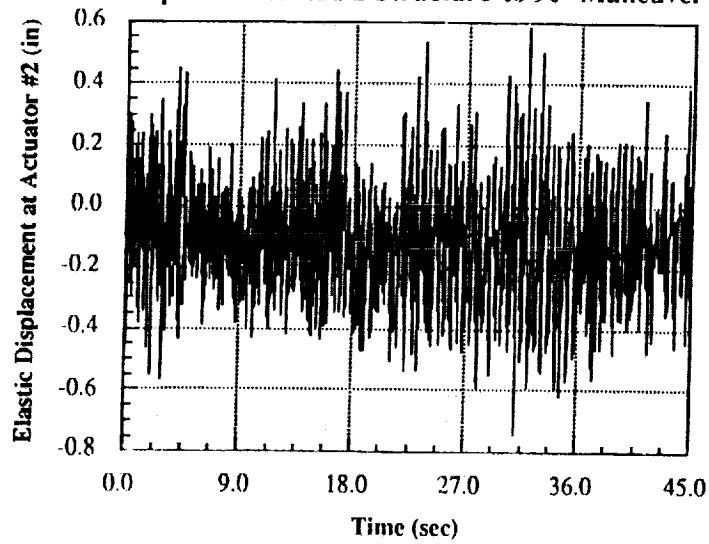
Experiment Preparations

Image Testbed

**90° Rotation Maneuver of IMAGE Structure
(30 psi - 1.0° deadband)**



Response of IMAGE Structure to 90° Maneuver

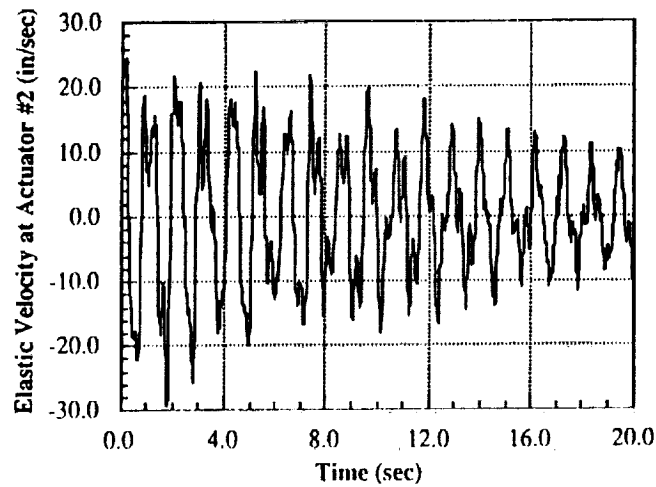
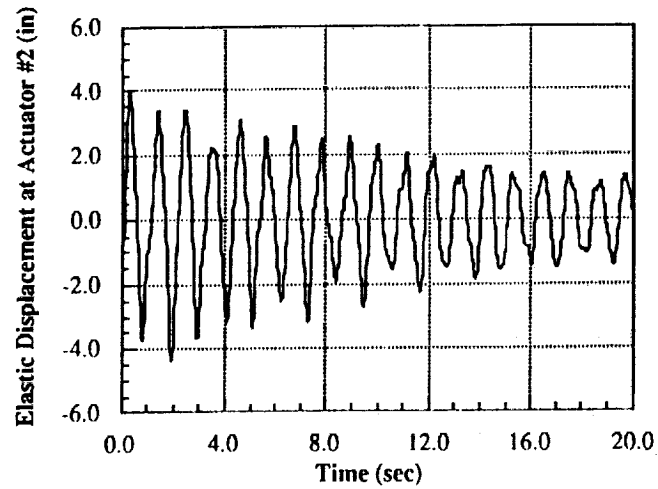


Ongoing Progress in Spacecraft Controls

Experiment Preparations

IMAGE Testbed

Free Response of IMAGE Structure
to 1st Mode Excitation

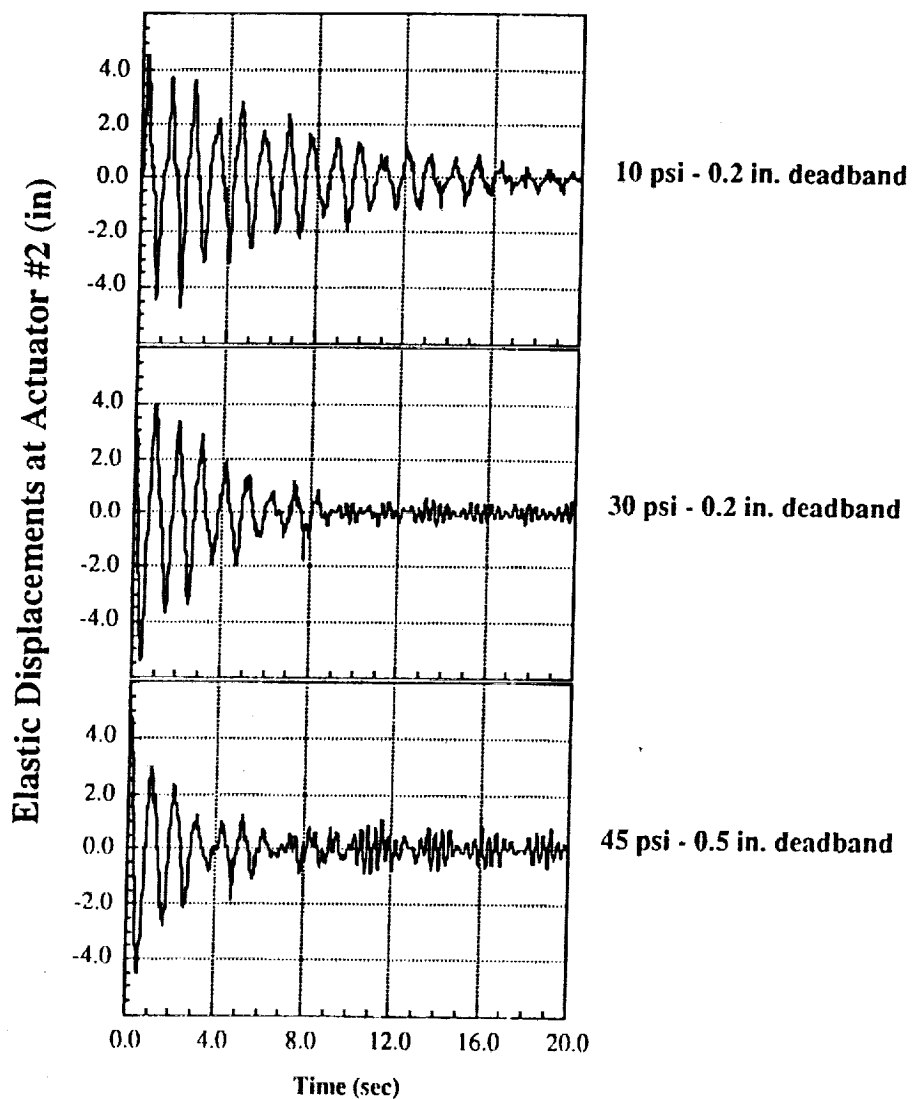


Ongoing Progress in Spacecraft Controls

Experiment Preparations

IMAGE Testbed

Controlled Response of IMAGE Structure



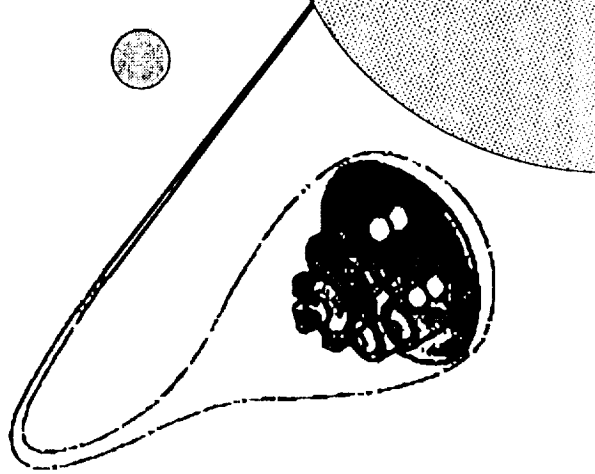
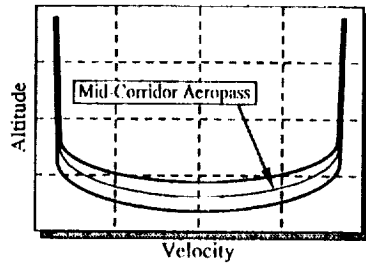
Ongoing Progress in Spacecraft Controls

Experiment Preparations

Aerobrake Configuration

Control Strategies for Lunar Orbital Transfer Vehicle

Pitch Control and Roll Modulation
for
Course Adjustments in Aeropass Corridor



Ongoing Progress in Spacecraft Controls

Current and Future Experiments

Fuel Optimal Control of an Experimental Rotating Flexible Beam

Equation of Motion
$$m(x) \left(x \frac{\partial^2 \Theta(t)}{\partial t^2} + \frac{\partial^2 u(x,t)}{\partial t^2} - u(x,t) \left(\frac{\partial \Theta(t)}{\partial t} \right)^2 \right) = -T u(x,t) + F(x,t)$$

where $T = \frac{\partial^2}{\partial x^2} (EI \frac{\partial^2}{\partial x^2})$

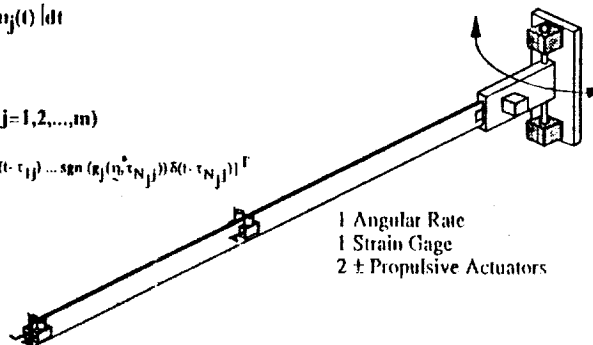
Boundary Conditions
$$u(0,t) = \frac{\partial^2 u(0,t)}{\partial x^2} = \frac{\partial^2 u(L,t)}{\partial x^2} = \frac{\partial^3 u(L,t)}{\partial x^3} = 0$$

Minimize Fuel
$$\text{Fuel} = \sum_{j=1}^m \int_0^T |u_j(t)| dt$$

Control of the Form
$$u_j^*(t) = \frac{\xi_j^T \xi_j}{\alpha^*}, \quad (j=1,2,\dots,m)$$

$$\xi_j = [\text{sgn}(\xi_j(\eta_1^*, \epsilon_{1j})) \delta(t - \tau_{1j}) \dots \text{sgn}(\xi_j(\eta_m^*, \epsilon_{mj})) \delta(t - \tau_{mj})]^T$$

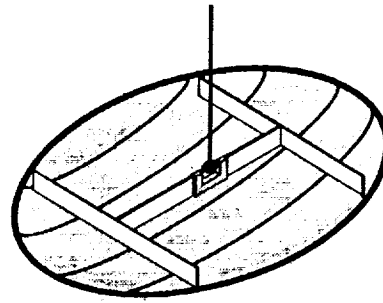
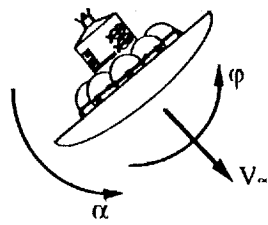
$$\xi_j = [\epsilon_{1j} \ \epsilon_{2j} \ \dots \ \epsilon_{mj}]^T$$



Ongoing Progress in Spacecraft Controls

Current and Future Experiments

Fuel Optimal Aerobrake Maneuver of an Experimental LOTV



Control Form

$$u_j^*(t) = \frac{g_j^T \xi_j}{\alpha^*}, \quad (j=1,2,\dots,m)$$

α = Pitch Angle

$$I_\psi \ddot{\alpha} = - \frac{dC_m}{d\alpha} \frac{1}{2} \rho_\infty V_\infty^2 A_{ref} l_{ref} \alpha = k_p \alpha \quad \omega_\alpha = \frac{1}{2\pi} \sqrt{\frac{k_p}{I_\psi}}$$

ϕ = Roll Angle (rotation about V_∞)

$$I_y \ddot{\phi} = - \frac{dC_l}{d\phi} \frac{1}{2} \rho_\infty V_\infty^2 A_{ref} l_{ref} \phi \quad \frac{dC_l}{d\phi} \equiv 0 \quad \therefore \quad \omega_\phi \equiv 0$$

Ongoing Progress in Spacecraft Controls

Current and Future Experiments

Fuel Optimal Propulsive Maneuvers of an Experimental Space Structure ...

Rigid Body Translation

$$\ddot{0}_x + \frac{g}{L} \sin \theta_x = \frac{M_{0x}}{J_{0x}} \quad X = L \sin \theta_x \approx L \theta_x$$

$$\ddot{0}_y + \frac{g}{L} \sin \theta_y = \frac{M_{0y}}{J_{0y}} \quad Y = L \sin \theta_y \approx L \theta_y$$

Rigid Body Rotation

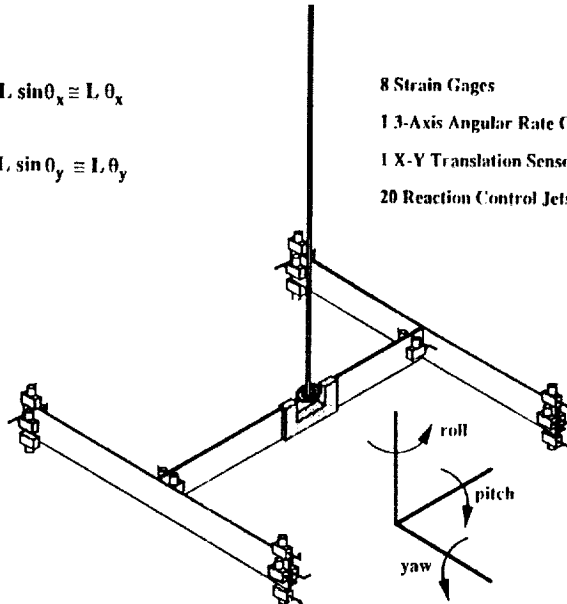
$$I \dot{\Omega} + \Omega \times I \Omega = \dot{h}_c$$

$$\dot{\phi} = [C] \Omega$$

Flexible Body Motion

$$\ddot{q}_r + \omega_r^2 q_r = Q_r, \quad (r = 1, 2, \dots, n)$$

$$u_k = \sum_{r=1}^n \phi_r q_r$$



Ongoing Progress in Spacecraft Controls

Summary



Experimental Verification of Impulse Damping Control



Impulse Damping of the SCOLE Reflector and Mast



Experiment Preparation for RCS, Rotating Flexible Beam, IMAGE, and Aerobrake Configuration



Impulse Damping Control of an Experimental Structure



Fuel Optimal Control of an Experimental Rotating Flexible Beam



Fuel Optimal Aerobrake Maneuver of an Experimental Lunar Orbital Transfer Vehicle



Fuel Optimal Propulsive Maneuvers of an Experimental Space Structure Undergoing Translation, Rotation, and Flexible Body Motions

Ongoing Progress in Spacecraft Controls

N 9 2 - 2 8 7 3 6

**"Initial Investigations of an Adaptive
Discrete-Time Controller for Nonlinear
Time-Varying Robotic Models"**

by

S. S. Giang and Gordon K. F. Lee

Department of Mechanical and Aerospace Engineering

North Carolina State University

Raleigh, North Carolina 27695-7910

PRECEDING PAGE BLANK NOT FILMED

Problem:

Consider a non-linear, time-varying differential equation model of a multi-link rigid robot:

$$D(q(t)) \ddot{q}(t) + C(q(t), \dot{q}(t)) + G(q(t)) + H(\dot{q}(t)) = u(t)$$

$D(\cdot)$: inertial matrix

$C(\cdot)$: centripetal and Coriolis forces

$G(\cdot), H(\cdot)$: parasitic forces (gravity, friction)

$u(t)$: applied torque

$q(t)$: generalized coordinate vector

Objective:

Design a discrete-time controller which forces

$$y(t) = f(q(t), \dot{q}(t))$$

to follow a desired trajectory, when non-linearities may be uncertain.

Note:

$$S(q^{-1}) u(k) = T(q^{-1}) y^*(k + d) - R(q^{-1}) y(k)$$

Let the desired closed-loop poles be

$$P(q^{-1}) \triangleq 1 + p_1 q^{-1} + \dots + p_l q^{-l}$$

Then if the controller parameters $S(q^{-1})$, $R(q^{-1})$ satisfy:

$$\Lambda(q^{-1}) S(q^{-1}) + q^{-d} B(q^{-1}) R(q^{-1}) = P(q^{-1}) ,$$

the tracking requirement will be satisfied with

$$T(q^{-1}) = \frac{P(q^{-1})}{B(1)}$$

and

$$B(1) = \sum_{i=0}^m b_i$$

Because $\Lambda(q^{-1})$ and $B(q^{-1})$ may be unknown, some identification method is employed. Here we use the recursive least-squares method,

Transforming the discrete-time model into parametric form:

$$y(k) = \Phi^T(k-1) \underline{\theta}$$

where $\Phi^T(k-1) = [-y(k-1), \dots, -y(k-n), u(k-1), \dots, u(k-1-m)]$

$$\underline{\theta}^T = [a_1, \dots, a_n, b_0, \dots, b_m],$$

the recursive formula to update the estimate $\hat{\underline{\theta}}(k)$ is:

$$\hat{\underline{\theta}}(k+1) = \hat{\underline{\theta}}(k) + F(k+1) \underline{\Phi}(k) \varepsilon^0(k+1)$$

$$F(k+1) = \frac{1}{\lambda_1} \left[F(k) - \frac{F(k) \underline{\Phi}(k) \underline{\Phi}^T(k) F(k)}{\lambda_1 + \underline{\Phi}^T(k) F(k) \underline{\Phi}(k)} \right]$$

$$\varepsilon^0(k+1) = y(k+1) - \underline{\Phi}^T(k) \hat{\underline{\theta}}^T(k)$$

with forgetting factor $0 < \lambda_1 < 1$.

The closed-loop system is:

$$\left[A(q^{-1}) S(q^{-1}) + q^{-d} B(q^{-1}) R(q^{-1}) \right] y(k) = B(q^{-1}) T(q^{-1}) y^*(k)$$

$$y(k) = \frac{B(q^{-1})}{B(1)} y^*(k)$$

where all parameters are replaced by their estimates.

Issues:

- (1) Since the plant is really time-varying, we should construct a time-varying discrete-time model.**
- (2) Since the plant is really nonlinear, we need to add a correction term in the control law for using a linear model.**
- (3) Since the plant is really continuous-time, we want to add a correction term in the control law for using a discrete-time model.**

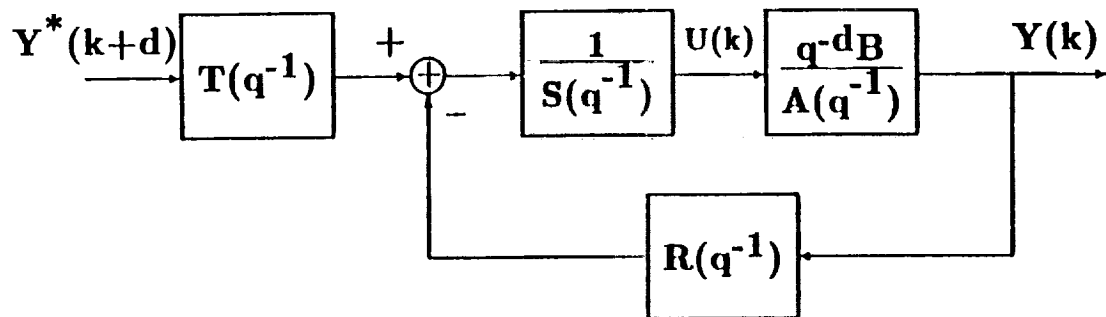


Figure 1: Model-Reference algorithm control structure

Look at one link at a time:

$$A(q^{-1})y(k) = q^d B(q^{-1}) u(k)$$

where q^{-1} is the delay operator, $y(k)$ is the discretized output (assuming a single output per link), d is the system delay and

$$A(q^{-1}) \triangleq a^1 + a_1 q^{-1} + \dots + q_n q^{-n}$$

$$B(q^{-1}) \triangleq b_0 + b_1 q^{-1} + \dots + b_m q^{-m}.$$

It is desired to track a trajectory $y^*(t)$ which, when discretized, is denoted by $y^*(k + d)$. Further, any disturbance due to non-zero initial conditions should be eliminated.

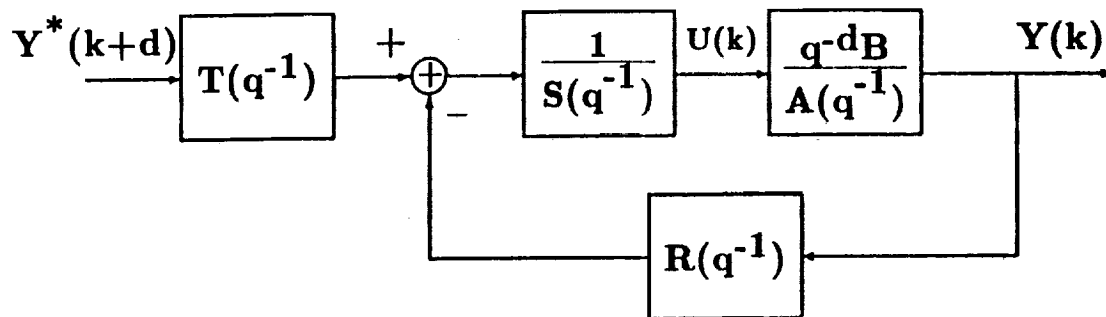


Figure 1: Model-Reference algorithm control structure

Note:

$$S(q^{-1}) u(k) = T(q^{-1}) y^*(k + d) - R(q^{-1}) y(k)$$

Let the desired closed-loop poles be

$$P(q^{-1}) \triangleq 1 + p_1 q^{-1} + \dots + p_l q^{-l}$$

Then if the controller parameters $S(q^{-1})$, $R(q^{-1})$ satisfy:

$$A(q^{-1}) S(q^{-1}) + q^{-d} B(q^{-1}) R(q^{-1}) = P(q^{-1}) ,$$

the tracking requirement will be satisfied with

$$T(q^{-1}) = \frac{P(q^{-1})}{B(1)}$$

and

$$B(1) = \sum_{i=0}^m b_i$$

Because $A(q^{-1})$ and $B(q^{-1})$ may be unknown, some identification method is employed. Here we use the recursive least-squares method,

Transforming the discrete-time model into parametric form:

$$y(k) = \Phi^T(k-1) \underline{\theta}$$

where $\Phi^T(k-1) = [-y(k-1), \dots, -y(k-n), u(k-1), \dots, u(k-1-m)]$

$$\underline{\theta}^T = [a_1, \dots, a_n, b_0, \dots, b_m],$$

the recursive formula to update the estimate $\hat{\underline{\theta}}(k)$ is:

$$\hat{\underline{\theta}}(k+1) = \hat{\underline{\theta}}(k) + F(k+1) \Phi(k) \varepsilon^0(k+1)$$

$$F(k+1) = \frac{1}{\lambda_1} \left[F(k) - \frac{F(k) \Phi(k) \Phi^T(k) F(k)}{\lambda_1 + \Phi^T(k) F(k) \Phi(k)} \right]$$

$$\varepsilon^0(k+1) = y(k+1) - \Phi^T(k) \hat{\underline{\theta}}^T(k)$$

with forgetting factor $0 < \lambda_1 < 1$.

The closed-loop system is:

$$\left[A(q^{-1}) S(q^{-1}) + q^{-d} B(q^{-1}) R(q^{-1}) \right] y(k) = B(q^{-1}) T(q^{-1}) y^*(k)$$

$$y(k) = \frac{B(q^{-1})}{B(1)} y^*(k)$$

where all parameters are replaced by their estimates.

Issues:

- (1) Since the plant is really time-varying, we should construct a time-varying discrete-time model.
- (2) Since the plant is really nonlinear, we need to add a correction term in the control law for using a linear model.
- (3) Since the plant is really continuous-time, we want to add a correction term in the control law for using a discrete-time model.

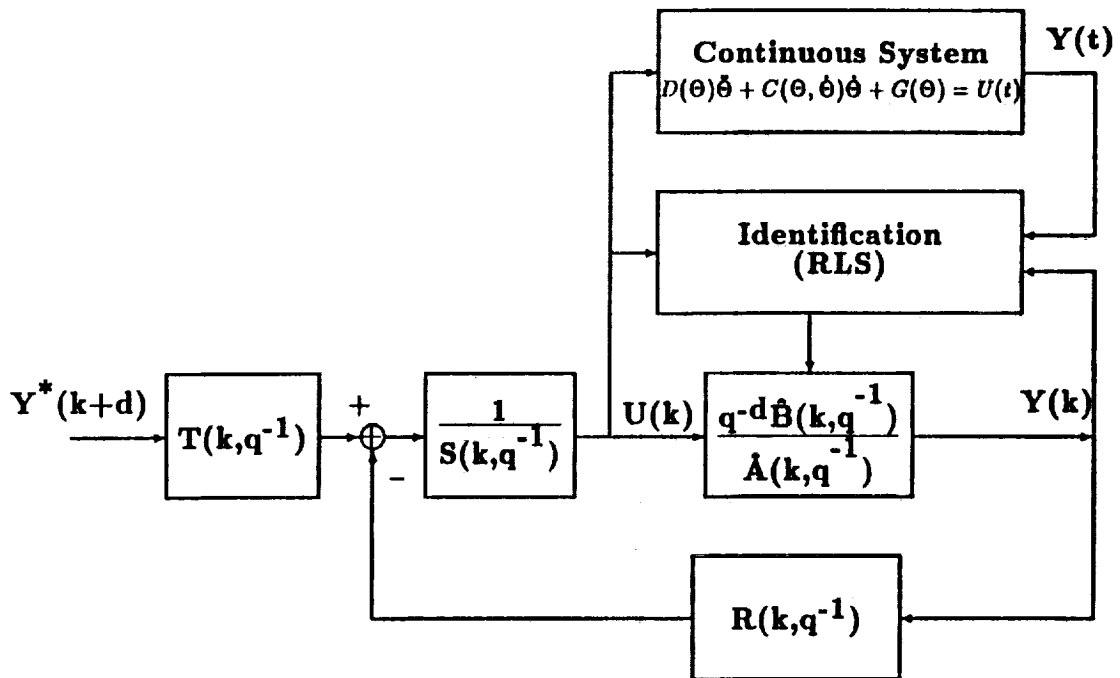


Figure 2: Self-Tuning adaptive control

Adaptive Algorithm:

Assume the continuous-time plant is described by:

$$A(k, q^{-1}) y(k) = q^{-d} B(k, q^{-1}) u(k)$$

Then the algorithm can still be used with the following steps:

1. Use the modified RLS to estimate the parameters of the discrete-time model:

$$y(k) = \Phi^T(k-1) \underline{\theta}(k)$$

where

$$\underline{\theta}^T(k-1) = [a_1(k), \dots, a_n(k), b_0(k), \dots, b_m(k)]$$

and $\Phi^T(k-1)$ is as before.

2. Calculate $\hat{T}(k, q^{-1})$, $\hat{S}(k, q^{-1})$, $\hat{R}(k, q^{-1})$ based upon the estimates $\hat{A}(k, q^{-1})$, $\hat{B}(k, q^{-1})$. The ideal model is:

$$A(k, q^{-1}) S(k, q^{-1}) + q^{-d} B(k, q^{-1}) R(k, q^{-1}) = P(q^{-1})$$

$$T(k, q^{-1}) = \frac{P(q^{-1})}{B(k, 1)}$$

$$B(k, 1) = \sum_{i=0}^m \hat{b}_i(k)$$

Note here the closed-loop poles are still assumed to be selected as constants.

For a robotic manipulator, each link may follow the closed-loop pole

$$P(q^{-1}) = 1 + p_1 q^{-1} + p_2 q^{-2}$$

$$p_1 = -2e^{-\delta w_n h} \cos(\sqrt{1 - \delta^2} w_n h)$$

$$p_2 = e^{-2\delta w_n h}$$

where h is the sampling period, δ is the damping coefficient and w_n is the natural frequency of oscillation, as selected by the designer.

3. Calculate the control law:

$$\hat{S}(k, q^{-1}) u(k) = \hat{T}(k, q^{-1}) y^*(k+1) - \hat{R}(k, q^{-1}) y(k) .$$

4. Repeat step 1 until complete time duration.

Model Parameter	Figure 4	Figure 5	Figure 6	Figure 7
n	2	2	2	2
m	1	1	2	2
λ	0.97	0.97	0.97	0.97
δ	0.9	0.8	0.9	0.8
ω_n	60	30	60	30

Table 1: Simulation Parameters

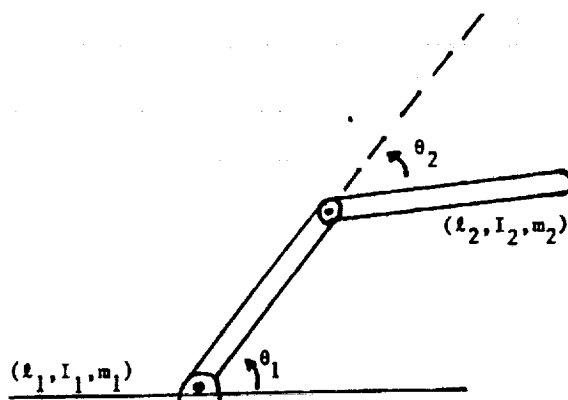


Figure 3: Two-link manipulator example

Robot parameters:

$$d_{11} = a_1 + a_2 \cos \theta_2$$

$$d_{12} = d_{22} = a_3 + 0.5 \times a_2 \cos \theta_2$$

$$d_{22} = a_3$$

$$c_1 = -a_2(\dot{\theta}_1 \dot{\theta}_2 + 0.5\dot{\theta}_1^2) \sin \theta_2$$

$$c_2 = 0.5a_2 \dot{\theta}_1^2 \sin \theta_2$$

$$g_1 = a_4 \cos \theta_1 + a_5 \cos (\theta_1 + \theta_2), h_1 = b_1 \dot{\theta}_1 + b_2 \operatorname{sgn} (\dot{\theta}_1)$$

$$g_2 = a_5 \cos(\theta_1 + \theta_2) \quad h_2 = b_3 \dot{\theta}_2 + b_4 \operatorname{sgn} (\dot{\theta}_2)$$

where $a_1 = m_1 l_1^2 + m_2 l_1^2 + m_2 l_2^2 + I_1 + I_2 = 4.93$

$$a_2 = 2m_2 l_1 l_2 = 0.94$$

$$a_3 = m_2 l_2^2 + I_2 = 0.90$$

$$a_4 = (m_1 l_1 + m_2 l_1)g = 68.65$$

$$a_5 = m_2 l_2 g = 10.64$$

$$b_1 = 6.82$$

$$b_2 = 3.5$$

$$b_3 = 3.91$$

$$b_4 = 3.5$$

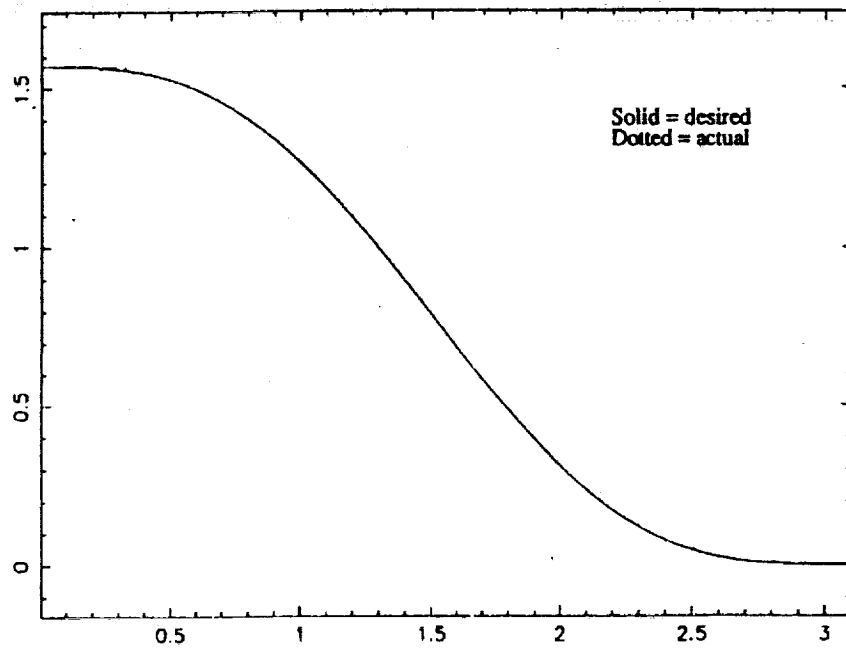


Figure 4a: Trajectory of the 1st link

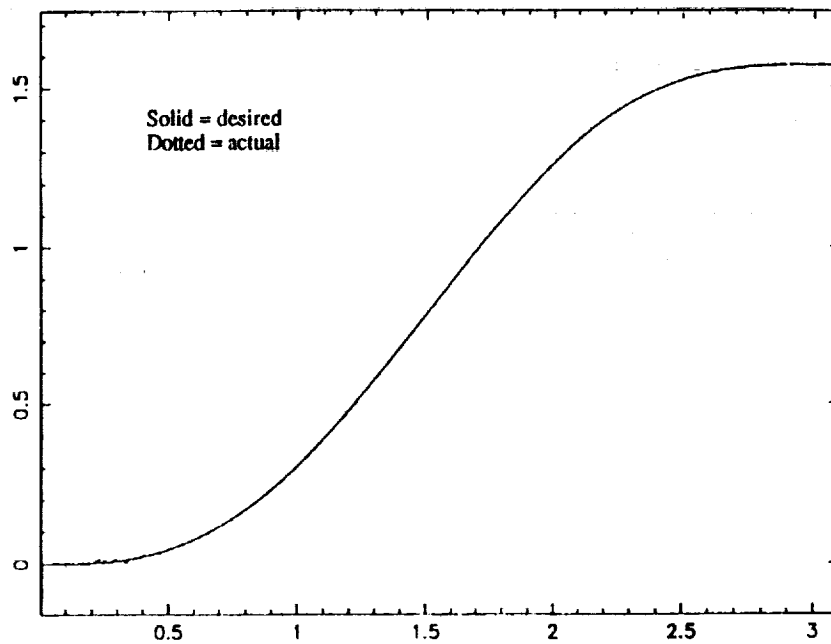


Figure 4b: Trajectory of the 2nd link

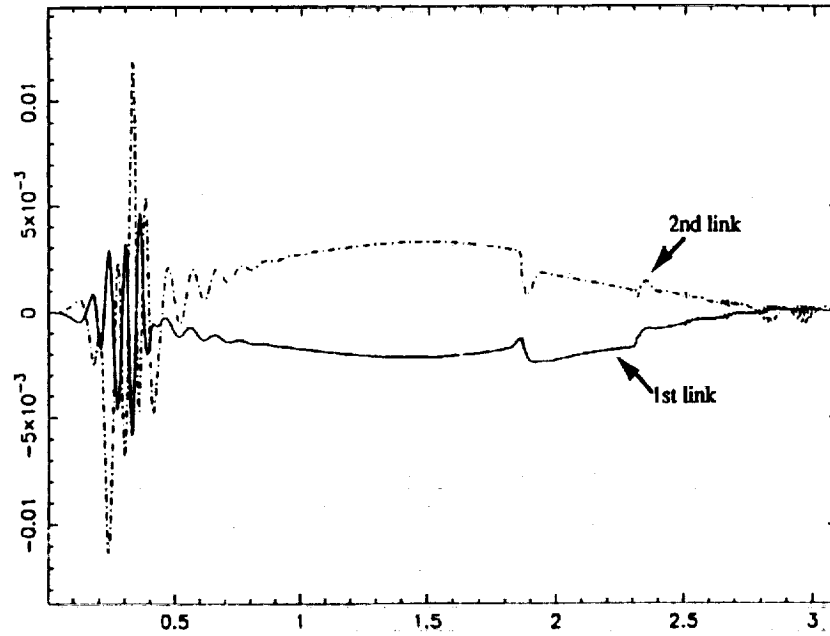


Figure 4c: Tracking error

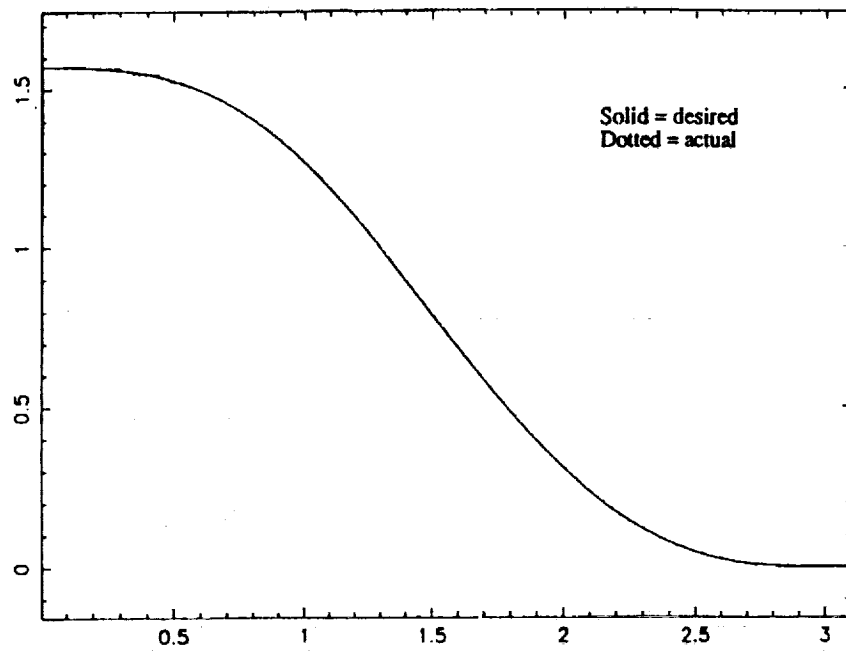


Figure 5a: Trajectory of 1st link

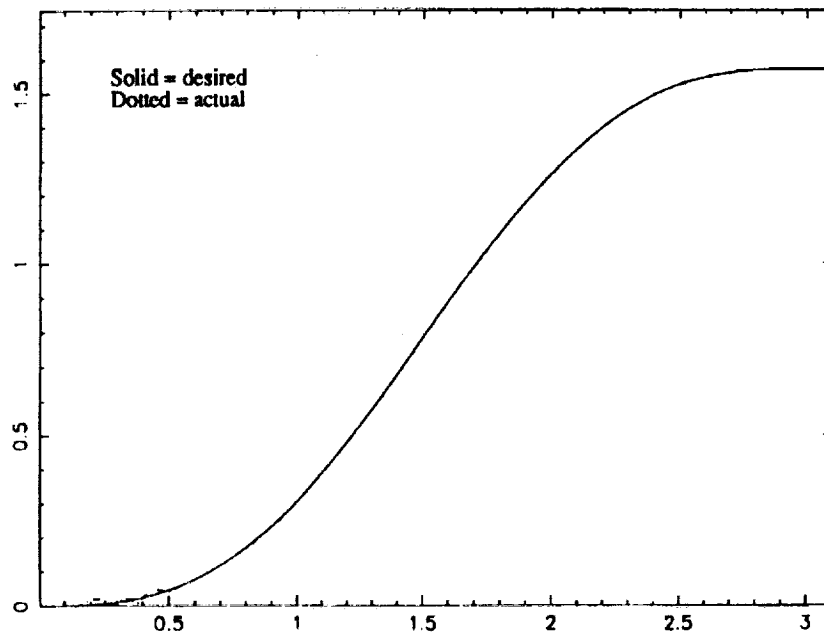


Figure 5b: Trajectory of 2nd link

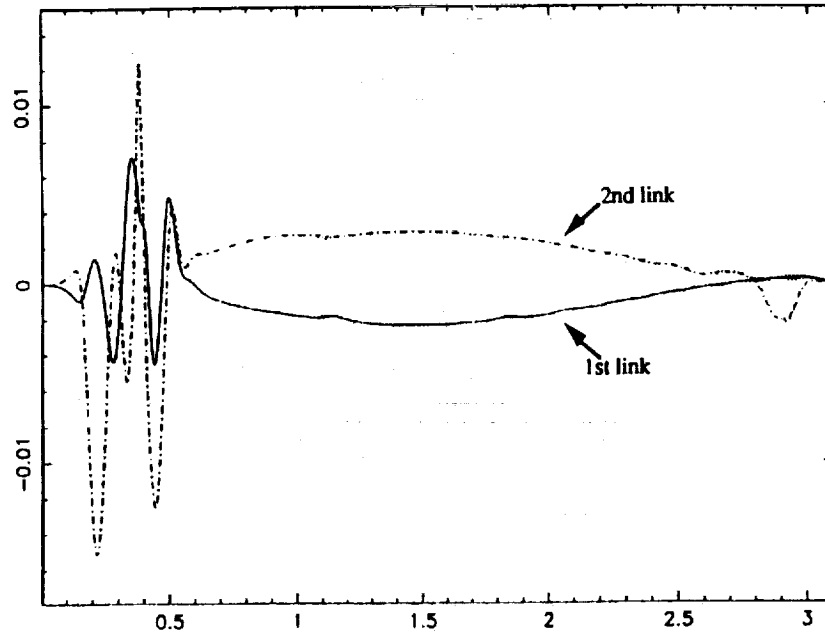


Figure 5c: Tracking error

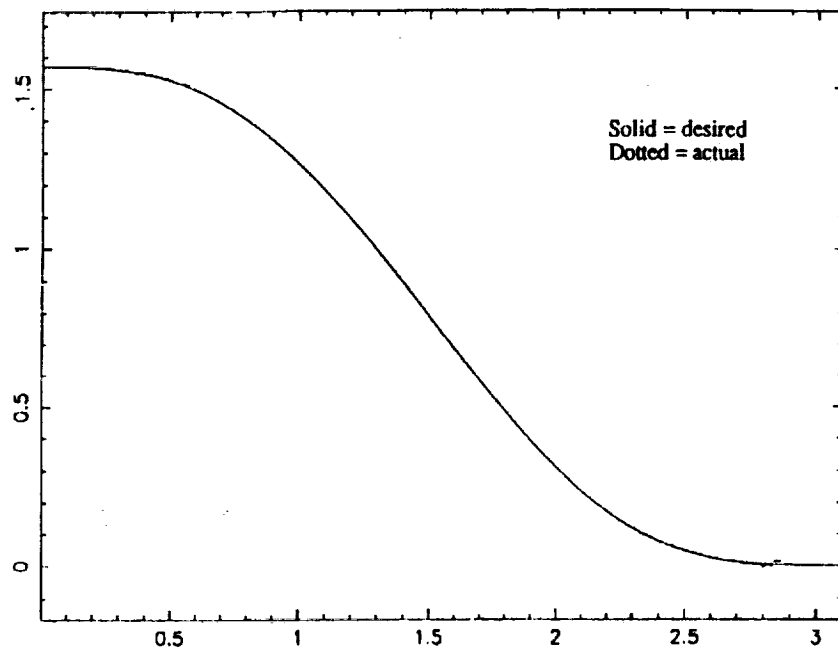


Figure 6a: Trajectory of 1st link

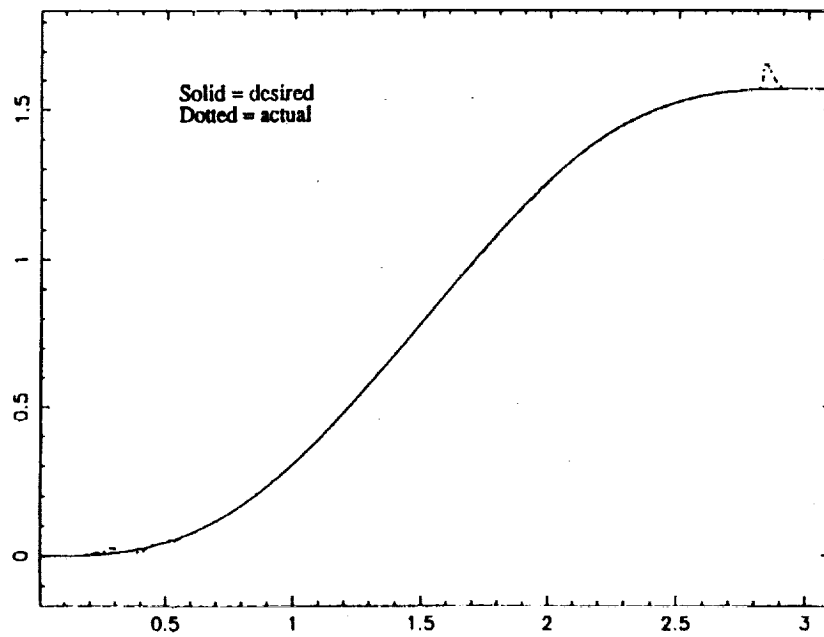


Figure 6b: Trajectory of 2nd link

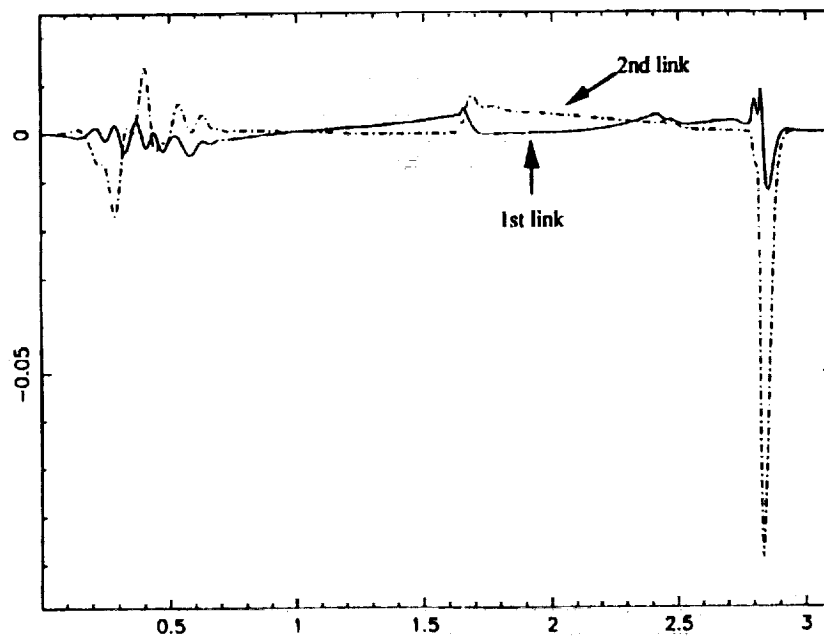


Figure 6c: Tracking error

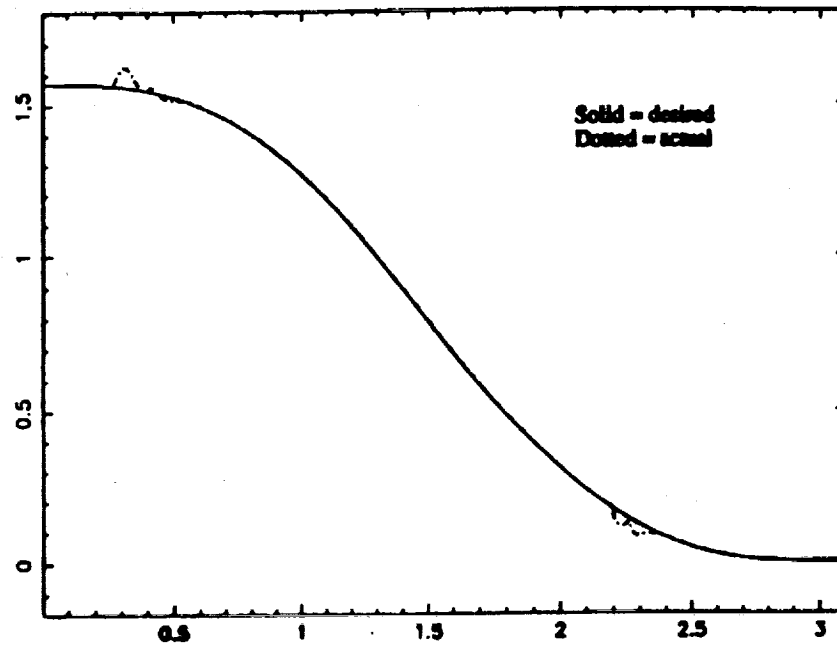


Figure 7a: Trajectory of 1st link

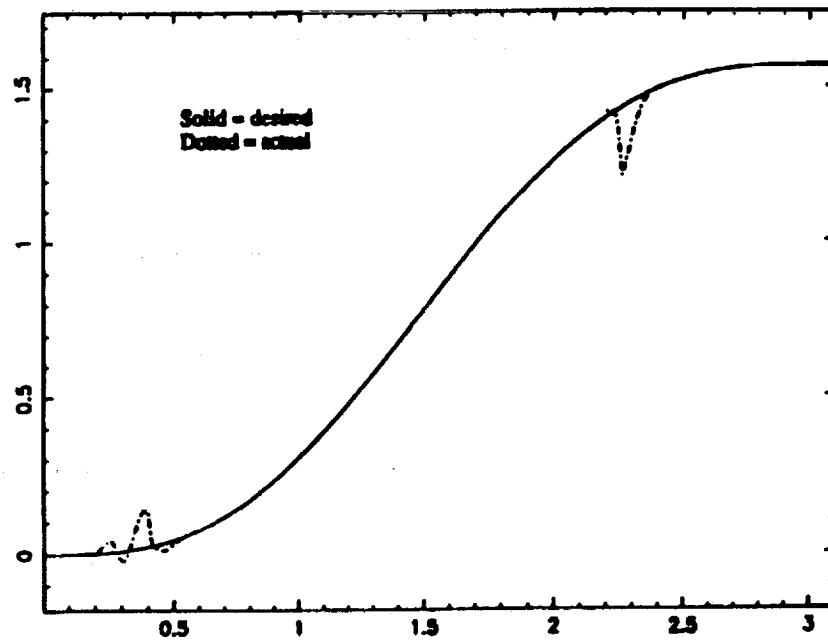


Figure 7b: Trajectory of 2nd link

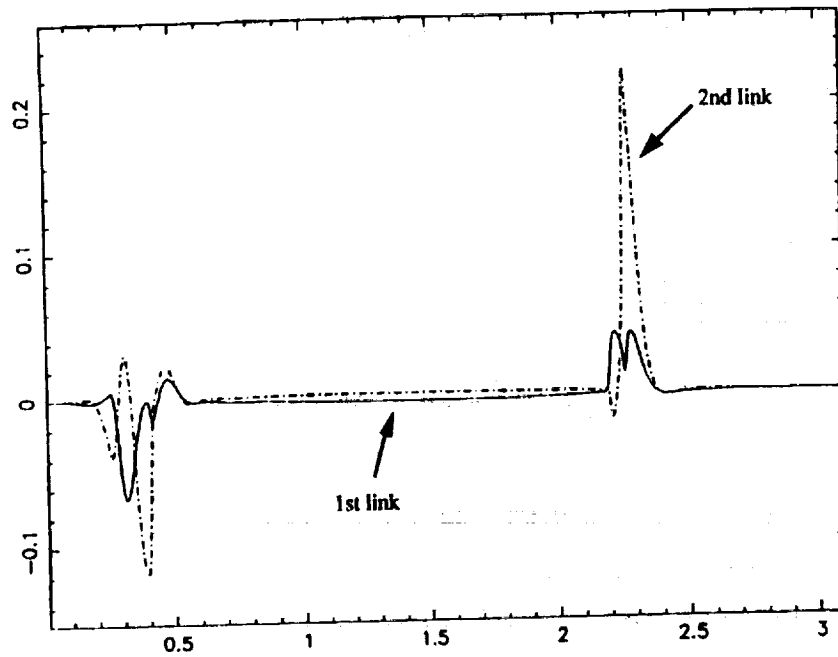


Figure 7c: Tracking error

To include an error term to compensate for going from continuous-time to discrete-time, consider the model:

$$A(k-1, q^{-1}) y(k) = q^{-d} B(k-1, q^{-1}) u(k) + \varepsilon^o(k)$$

or

$$A(k, q^{-1}) y(k) = q^{-d} B(k, q^{-1}) u(k) + \varepsilon(k)$$

where $\varepsilon^o(k)$ and $\varepsilon(k)$ are the *a priori* prediction error and *a posteriori* prediction error, respectively.

$$\varepsilon^o(k) = y(k) - \Phi^T(k-1) \hat{\underline{\theta}}(k-1)$$

$$\varepsilon(k) = y(k) - \Phi^T(k-1) \hat{\underline{\theta}}(k)$$

These errors can be integrated into the closed-loop configuration and the control parameters may be selected to compensate for the errors.

If the pole placement control law is used, the closed-loop system is:

$$\begin{aligned} & [A(k, q^{-1}) S(k-1, q^{-1}) + q^{-d} B(k-1, q^{-1}) R(k-1, q^{-1})] y(k) \\ & = B(k-1, q^{-1}) T(k-1, q^{-1}) y^*(k) + e(k) + \varepsilon^o(k) \end{aligned}$$

where $e(k)$ is added to account for the time-varying discrete-time system.

That is:

$$\begin{aligned}
 e(k) = & \sum_{i=0}^{n-1} \Delta A(k-i, q^{-1}) S^{i+1}(k-1, q^{-1}) y(k-1-i) \\
 & - \sum_{i=0}^{n-1} \Delta B(k-i, q^{-1}) S^{i+1}(k-1, q^{-1}) u(k-2-i) \\
 & + \sum_{i=1}^m B^i(k, q^{-1}) \Delta R(k-i, q^{-1}) y(k-1-i) \\
 & + \sum_{i=1}^m B^i(k, q^{-1}) \Delta S^1(k-i, q^{-1}) u(k-2-i) \\
 & - \sum_{i=1}^m B^i(k, q^{-1}) \Delta T(k-i, q^{-1}) y^*(k-1) + \sum_{i=1}^n S_i(k) \varepsilon^0(k-i)
 \end{aligned}$$

where

$$S^1(k, q^{-1}) = q[S(k, q^{-1}) - S_0(k)]$$

.

$$S^{i+1}(k, q^{-1}) = q[S^i(k, q^{-1}) - S_i(k)]$$

$$B^i(k, q^{-1}) = q[B^{i-1}(k, q^{-1}) - b_{i-1}(k)]$$

$$\Delta A(k, q^{-1}) = A(k, q^{-1}) - A(k-1, q^{-1}).$$

Note $e(k)$ can be calculated at time $k-1$.

We consider the control law as

$$S(k-1, q^{-1}) u(k-1) = T(k-1, q^{-1}) y^*(k) - R(k-1, q^{-1}) y(k-1) + \phi(k-1)$$

The closed-loop system is:

$$\begin{aligned} P(q^{-1}) y(k) &= B(k-1, q^{-1}) T(k-1, q^{-1}) y^*(k) + e(k) \\ &\quad + \varepsilon^{\circ}(k) + B(k-1, q^{-1}) \phi(k-1) \end{aligned}$$

In the ideal case, $B(k-1, q^{-1})$ is stable and $\varepsilon^{\circ}(k)$ is given. We can calculate the correction input term $\phi(k-1)$ as:

$$\phi(k-1) = \frac{[P(q^{-1}) - B(k-1, q^{-1}) T(k-1, q^{-1})] y^*(k) - e(k) - \varepsilon^{\circ}(k)}{B(k-1, q^{-1})}$$

to cancel out $e(k)$ and $\varepsilon^{\circ}(k)$. But, in the actual situation,

$B(k-1, q^{-1})$ may be unstable and $\varepsilon^{\circ}(k)$ is not given. We use

$\varepsilon^{\circ}(k-1)$ instead of $\varepsilon^{\circ}(k)$ to calculate $\phi(k-1)$ as:

$$\phi(k-1) = \frac{[P(q^{-1}) - B(k-1, q^{-1}) T(k-1, q^{-1})] y^*(k) - e(k) - \varepsilon^{\circ}(k-1)}{B(k-1, 1)}$$

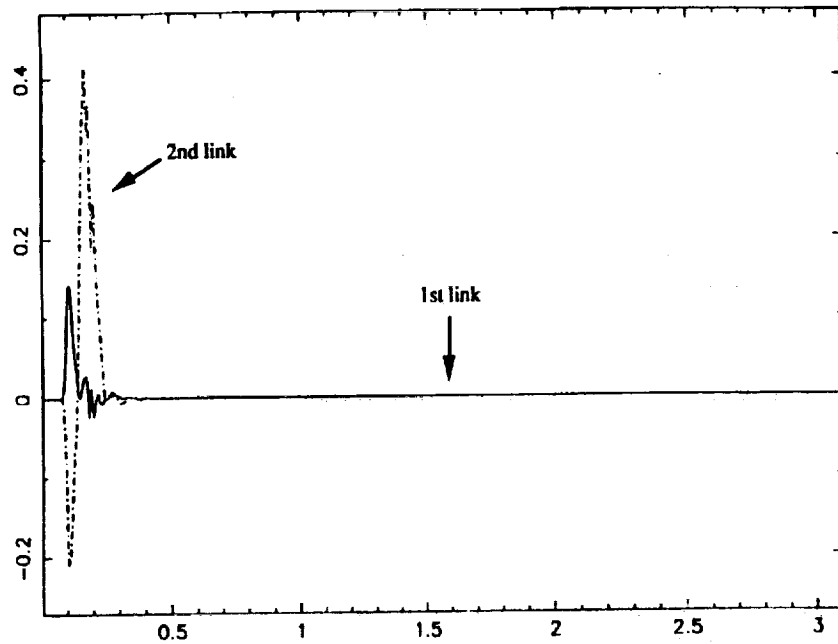


Figure 8: Tracking error (including correction input)

Conclusions:

- Developed an adaptive control methodology which addresses three types of errors:
 - errors due to model linearization
 - errors due to controlling a time-varying plant
 - errors due to discretization
- Further work is needed to
 - determine stability range of model parameters (δ , ω_n)
 - include prediction error term
 - determine efficient methods for tuning correction error term to improve transient characteristics
 - look at implementation on several robotic experimental testbeds

N92-28737

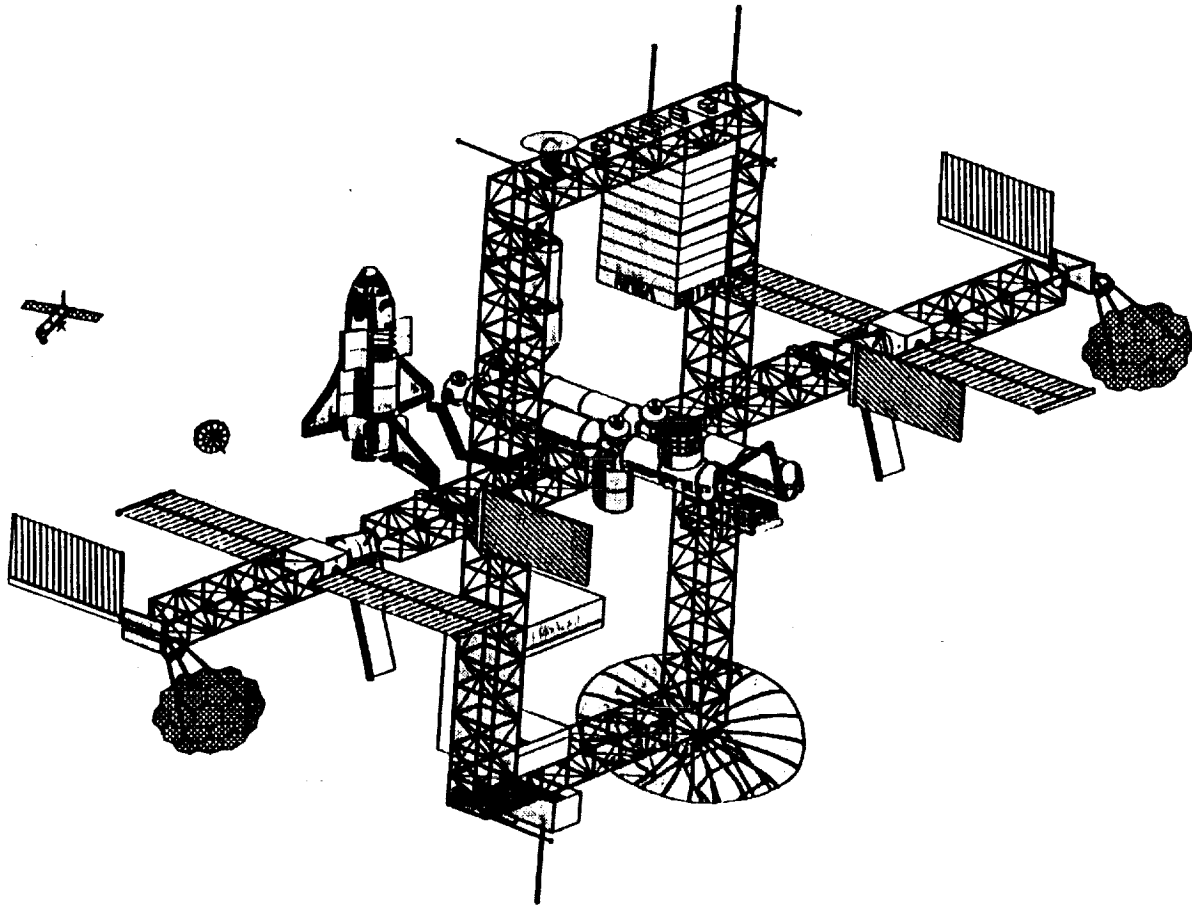
**IDENTIFICATION OF LINEAR SYSTEM MODELS
AND STATE ESTIMATORS FOR CONTROLS**

Dr. Chung-Wen Chen

**Mars Mission Research Center
Dept. of Mechanical & Aerospace Engineering
North Carolina State University**

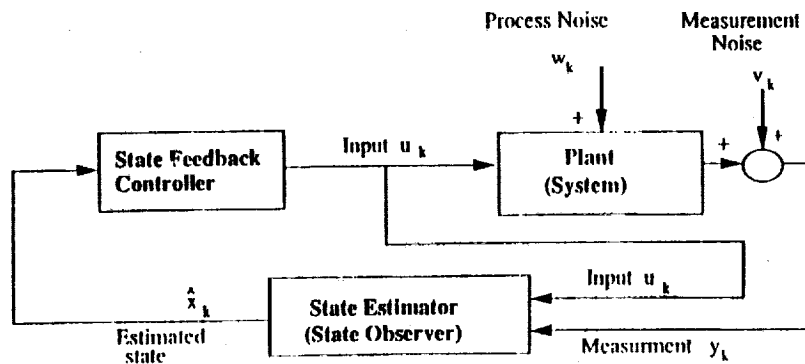
OUTLINE

- Introduction
- State Estimation under Unknown Noises
- State Estimation under Unknown System Model and Unknown Noises
- Examples
- Conclusion



PRECEDING PAGE BLANK NOT FILMED

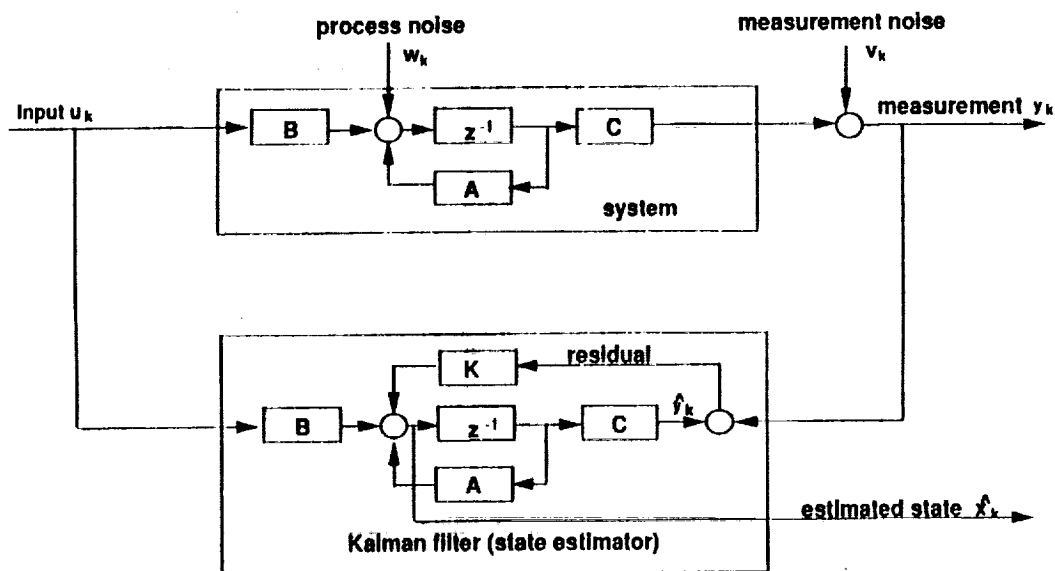
• Linear State Feedback Control System



Reasons for state estimator

- (1) Number of sensors usually are less than number of states interested.
- (2) Interested states are not always directly measurable.
- (3) System is affected by process (input) noise.
- (4) Outputs are corrupted by measurement (output) noise.

• Kalman Filter State Estimation



- Requirements:
- (1) A state-space model of the system
 - (2) The noise statistics (covariances)

- **Some problems in control of flexible space structures**

- (1) Obtaining a model by ground testing might not be possible
- (2) If an analytical model is used, modeling error could cause problem
- (3) Working environment is unknown
- (4) System characteristics might change (reorientation, structural damage, material deterioration, etc.)

- **Techniques in need**

- (1) On-orbits system identification
- (2) Adaptive state estimation
- (3) Adaptive state-space system identification

- **Problem statement**

Given the input/output data of a linear system,

suppose:

- (1) the system model is known but the noise statistics are unknown,
- (2) both the system model and noise statistics are unknown,

how to conduct state estimation for control purposes?

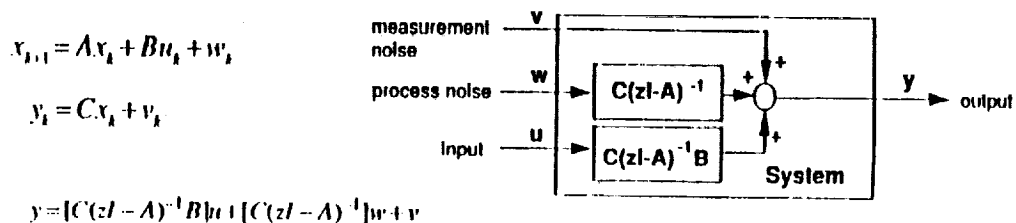
- **State Estimation under Unknown Noises
(Adaptive Kalman Filtering)**

Three approaches:

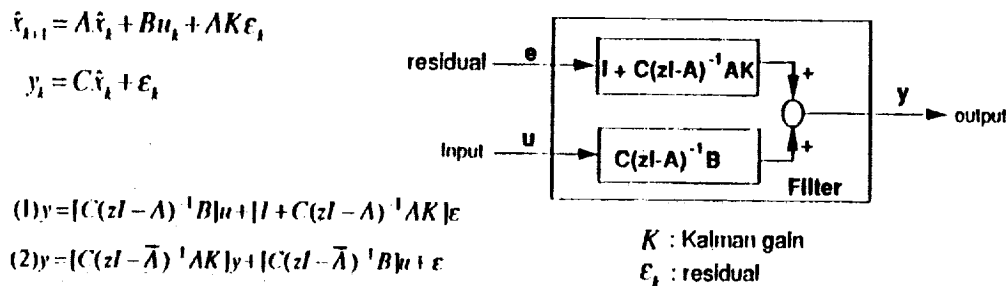
- (1) Estimating noise covariances (Q & R)
- (2) Using weighting least-squares method
- (3) Estimating Kalman filter gain directly

- **Input-output Relationship of a System and of the Kalman Filter**

(1) State-space model of a system

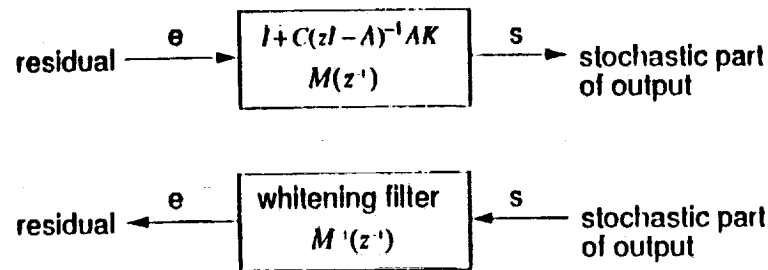


(2) State-space innovation model of the Kalman filter



● Relation between Residual and Stochastic Part of Output

$$s_i = y_i - \sum_{j=1}^i CA^{i-j} B u_{j-1} = \sum_{j=1}^i CA^j K e_{i-j} + \varepsilon_i = \sum_{j=0}^i M_j \varepsilon_{i-j} \quad (\text{MA model})$$



$$\varepsilon_i = \sum_{j=1}^i N_j s_{i-j} \quad (\text{AR model})$$

$$N(z^{-1}) \approx M^-(z^{-1}) \quad \text{or} \quad M(z^{-1}) \approx N^-(z^{-1})$$

$$\begin{aligned} M(z^{-1}) &= I + C(zI - A)^{-1} AK \\ &= I + CAKz^{-1} + CA^2Kz^{-2} + \dots + CA^qKz^{-q} \end{aligned}$$

● Obtaining Kalman Filter Gain

(1) Invert the whitening filter

$$N^-(z^{-1}) \approx M(z^{-1}) = I + CAKz^{-1} + CA^2Kz^{-2} + \dots + CA^qKz^{-q}$$

(2) Form two matrices

$$G = \begin{bmatrix} CAK \\ CA^2K \\ \vdots \\ CA^qK \end{bmatrix} \quad H = \begin{bmatrix} CA \\ CA^2 \\ \vdots \\ CA^q \end{bmatrix}$$

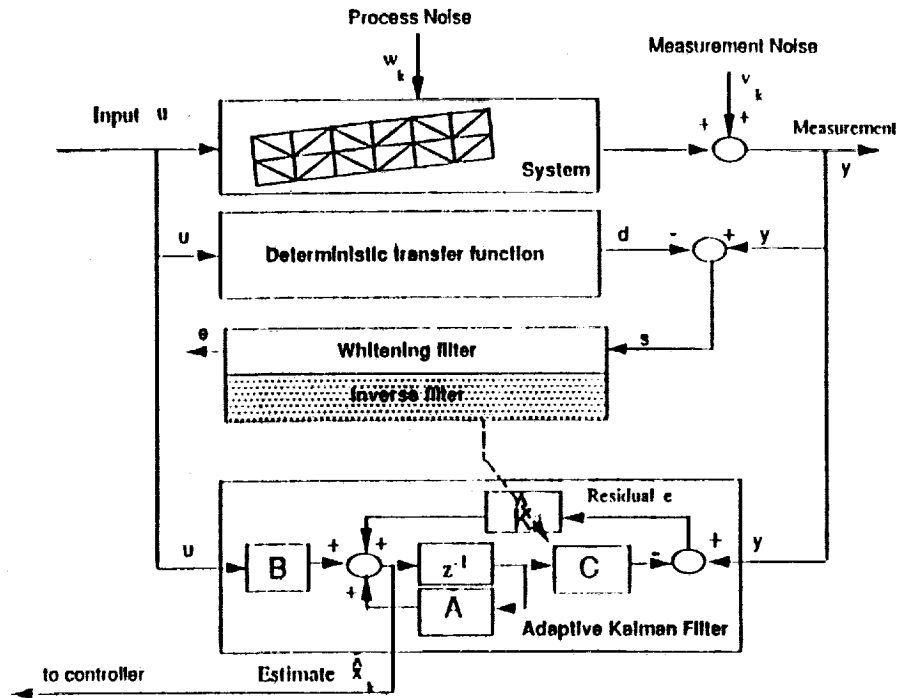
(3) Find the least-squares solution of K

$$\hat{K} = HG \quad \text{where} \quad H^+ = (H^T H)^{-1} H^T$$

(4) Perform state estimation

$$\begin{aligned} \hat{x}_i &= A\hat{x}_{i-1} + Bu_{i-1} \\ \hat{x}_i &= \hat{x}_i + K(y_i - C\hat{x}_i) \end{aligned}$$

- **Inverse Filter Method for Adaptive State Estimation**



State Estimation under Unknown System Model and Unknown Noises

- system Identification
- Kalman filter Identification

State Estimation under Unknown System Model and Unknown Noises

Two approaches:

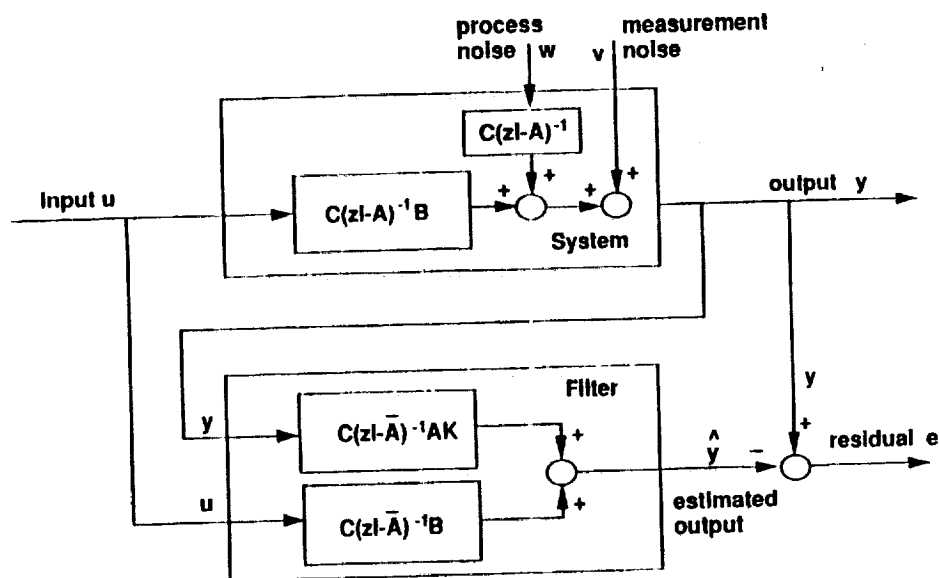
- (1) Identifying a system model first, then the filter gain.
- (2) Identifying a system model and the filter gain at the same time.

System Identification:

- (1) Obtaining system mathematical models from input-output data.
- (2) Frequency-domain and time-domain
- (3) Model types: transfer function, difference equation, state-space equation, impulse response, etc.

For control purposes, time-domain state-space system identification methods are preferred.

• Input-output Relationship for a System and for the Kalman Filter



$$\text{system: } y = [C(zI - A)^{-1}B]u + [C(zI - A)^{-1}]w + v$$

$$\text{filter: } (2)y = [C(zI - \bar{A})^{-1}AK]y + [C(zI - \bar{A})^{-1}B]u + \underline{\epsilon}$$

- **Markov Parameters and Eigensystem Realization Algorithm (ERA)**

(1) System Markov parameters (impulse response)

$$y_k = CBu_{k-1} + CABu_{k-2} + \dots + CA^{j-1}Bu_{k-j} + CA^jKu_{k-j} + CA^2K\epsilon_{k-2} + \dots + CA^jK\epsilon_{k-j} + \epsilon_k$$

$$\begin{bmatrix} CB & CAB & \dots & CA^{j-1}B \\ CA^jK & CA^2K & \dots & CA^jK \end{bmatrix}$$

(2) Filter Markov parameters

$$y_k = CAKy_{k-1} + C\bar{A}AKy_{k-2} + \dots + C\bar{A}^{q-1}AKy_{k-q} + CBu_{k-1} + C\bar{A}Bu_{k-2} + \dots + C\bar{A}^{q-1}Bu_{k-q} + \epsilon_k$$

$$\begin{bmatrix} CAK & C\bar{A}AK & \dots & C\bar{A}^{q-1}AK \\ CB & C\bar{A}B & \dots & C\bar{A}^{q-1}B \end{bmatrix} \quad \bar{A} = A(I_n - KC)$$

(3) ERA (a system identification method)

$$\begin{bmatrix} CB & CAB & \dots & CA^{j-1}B \end{bmatrix} \xrightarrow{\text{ERA}} [A', B', C']$$

- **Relationship between Filter Markov Parameters and System Markov Parameters**

$$\text{ARX model: } y_k = \sum_{i=1}^q C\bar{A}^{i-1}AKy_{k-i} + \sum_{i=1}^q C\bar{A}^{i-1}Bu_{k-i} + \epsilon_k = \sum_{i=1}^q M_i y_{k-i} + \sum_{i=1}^q N_i u_{k-i} + \epsilon_k$$

(1) Markov parameters for stochastic input

$$CAK = M_1$$

⋮

$$CA^qK = M_q + \sum_{i=1}^{q-1} M_{q-i} CA^iK$$

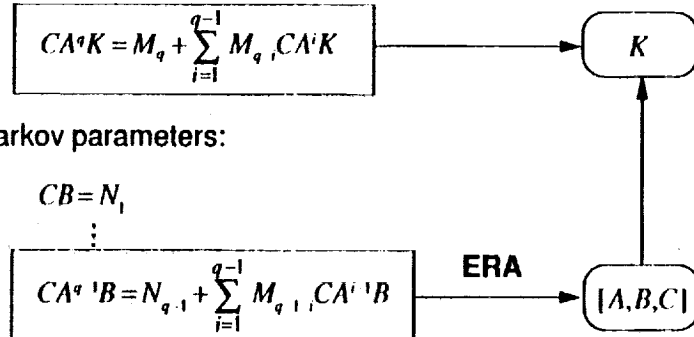
(2) System Markov parameters:

$$CB = N_1$$

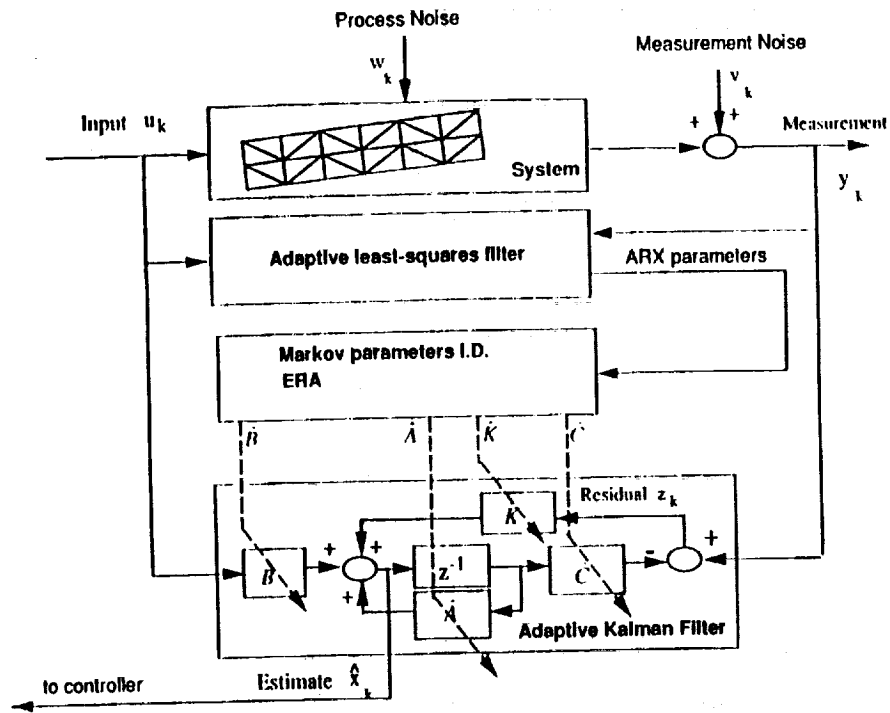
⋮

$$CA^{q-1}B = N_{q-1} + \sum_{i=1}^{q-1} M_{q-i-1} CA^{i-1}B$$

ERA



● Integrated Adaptive System Identification and State Estimation



Examples

- Mini-Mast
- Ten-bay structure

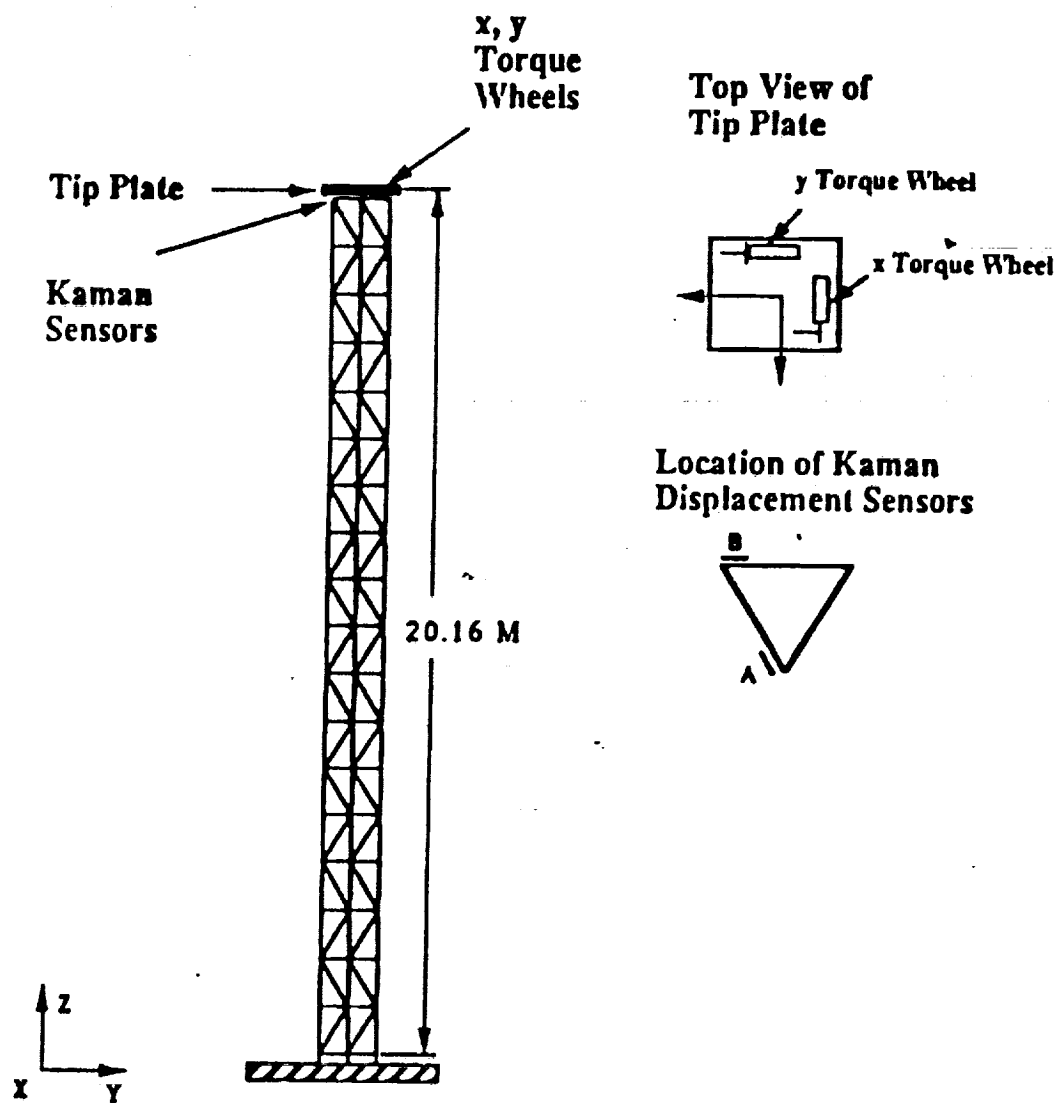


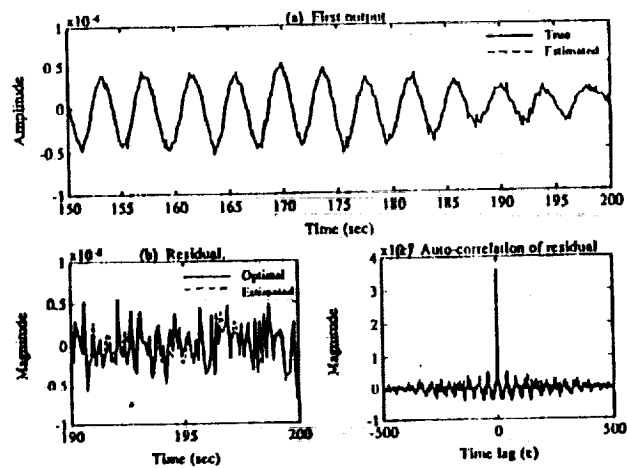
Fig. 6.4 Mini-Mast structure.

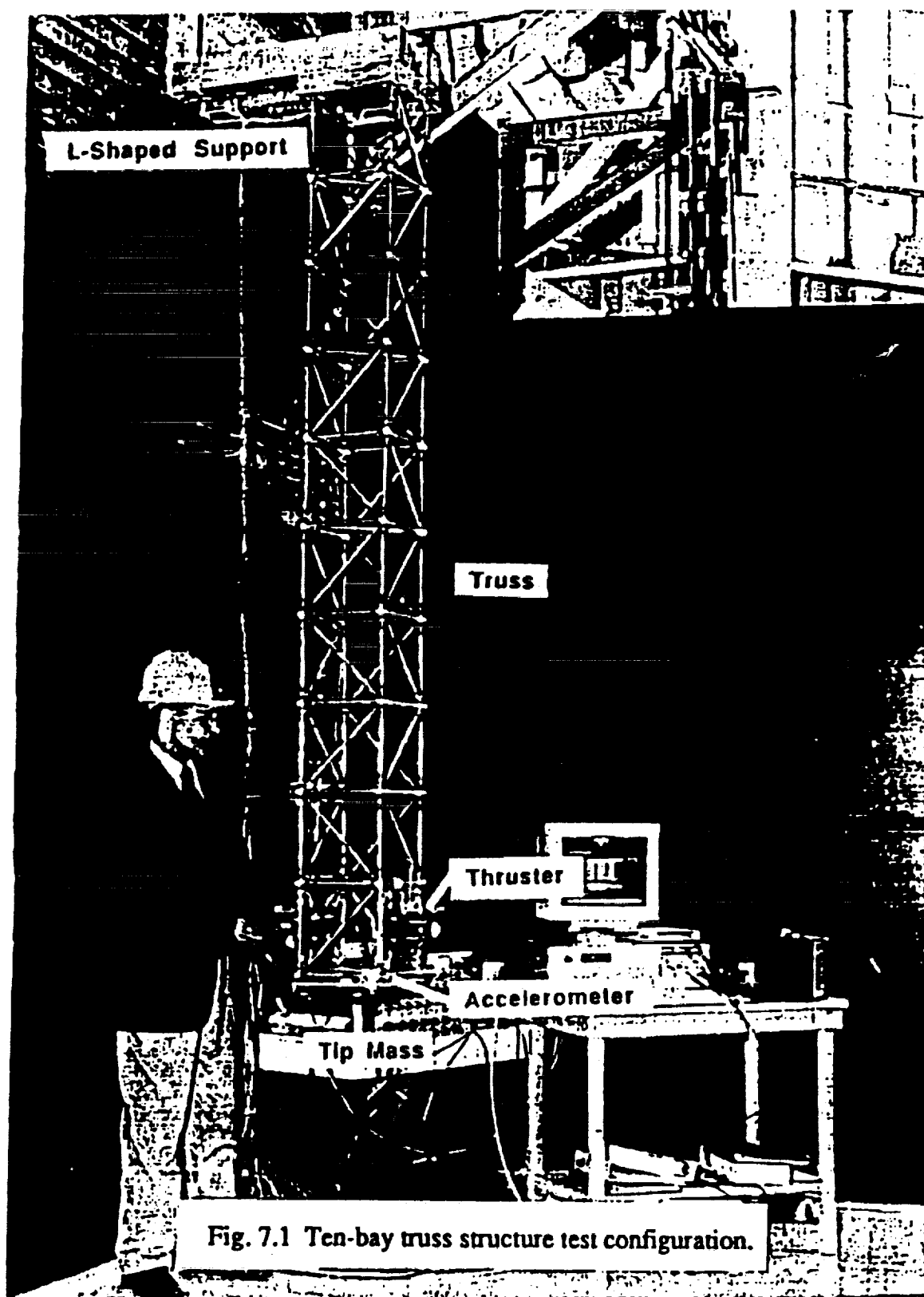
- The identified modal parameters of the Mini-Mast

# of data processed	Mode 1		Mode 2		Mode 3		Mode 4		Mode 5	
	Freq. (rad/sec)	Damp (%)	Freq. (rad/sec)	Damp (%)	Freq. (rad/sec)	Damp (%)	Freq. (rad/sec)	Damp (%)	Freq. (rad/sec)	Damp (%)
1,000	4.9863	2.81	5.0891	1.11	27.0820	1.11	37.5743	3.04	38.6144	1.13
2,000	5.0213	1.91	5.0609	1.94	27.4867	0.87	38.1814	1.45	38.7352	1.22
3,000	5.0246	1.97	5.0610	1.83	27.4548	1.01	38.2935	1.26	38.7079	1.15
4,000	5.0366	1.92	5.0459	1.60	27.5389	0.95	38.2625	1.27	38.7368	1.12
5,000	5.0263	1.97	5.0405	1.50	27.4746	1.13	38.3041	1.20	38.7314	1.09
0 ^a	5.0318	1.80	5.0356	1.80	27.4201	1.20	38.3511	1.00	38.6823	1.00

^a True values

- Output and residual comparisons (1000 data)



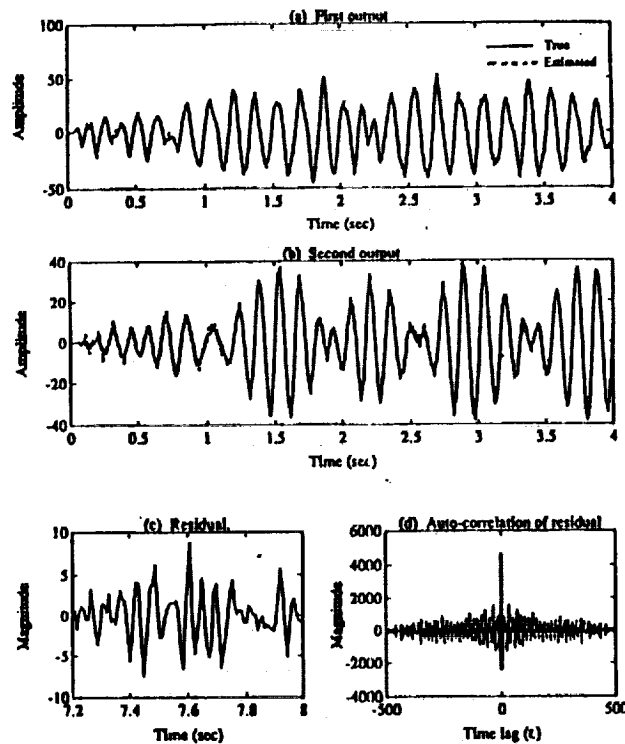


- Identification of a ten-bay structure

The identified modal parameters

Mode	Frequency (Hz)	Damping (%)
1	5.9	0.27
2	7.3	2.87
3	48.5	0.40

- Output and residual comparisons (3750 data)



Conclusions

- (1) Viewing the input-output relationship of a system through the Kalman filter provides helpful insights.
- (2) If the system state-space model is known, the Kalman filter gain can be obtained by whitening the stochastic part of the output.
- (3) A system state-space model and the corresponding Kalman filter can be identified at the same time from the parameters of an ARX (a difference equation) model.
- (4) For a stochastic system, a complete state-space realization is $[A, B, C, K]$, where the Kalman filter gain characterizes stochastic property of the system.

**Fuzzy Logic Controller for
Manipulator Systems:
Preliminary Results**

Presented by
R. J. Stanley II
H. Roberts

**North Carolina State University
Mars Mission Research Center**

Project Members:
D. Gerber
H. Roberts
R. J. Stanley II
J. C. Windsor

Project Advisor:
Dr. G. Lee

Mars Mission Research Center, N.C.S.U.

OUTLINE:

- 1) MOTIVATION
- 2) FUZZY CONTROL
- 3) RESULTS AND COMPARISONS
- 4) FUTURE ACTIVITIES

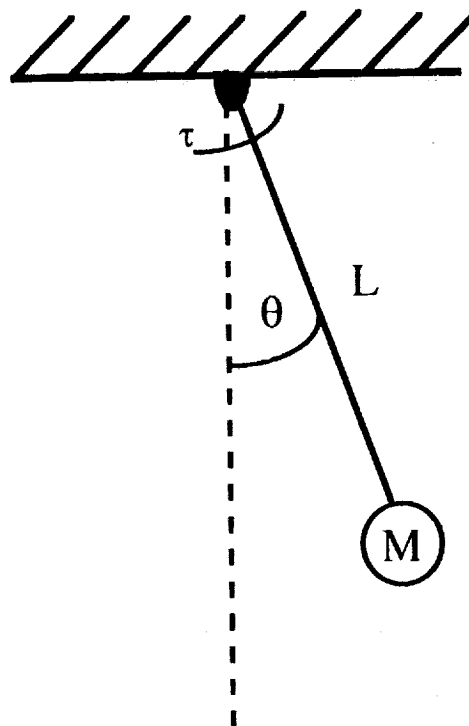


Figure 1.1

$$\sum M = I \ddot{\theta}$$

$$I \ddot{\theta} = -m \cdot g \cdot L \cdot \sin(\theta) + \tau$$

τ = Torque applied by motor

$$I = \text{Inertia} = m \cdot L^2$$

$$\tau = -K_p(\theta - \theta_d) - K_d(\dot{\theta} - \dot{\theta}_d) - K_i \int_0^t (\theta - \theta_d) ds$$

θ_d = desired position

$\dot{\theta}_d$ = desired velocity

$$\ddot{\theta} + \omega_n^2 = -K_p \theta - K_d \dot{\theta} - K_i \int_0^t \theta \cdot ds$$

$$\omega_n^2 = \frac{g}{L}$$

$$y = \int_0^t \theta \, ds$$

Mars Mission Research Center, N.C.S.U.

$$(s + \gamma) \cdot (s^2 + 2\alpha s + \alpha^2 + \beta^2)$$

α = Vibration decay rate

β = Closed-loop frequency of oscillation

γ = Steady-state error decay rate

$$K_p = [(\alpha^2 + \beta^2 + 2\alpha\gamma - \omega_n^2)] \cdot I$$

$$K_i = [(\alpha^2 + \beta^2)\gamma] \cdot I$$

$$K_d = (2\alpha + \gamma) \cdot I$$

Mars Mission Research Center, N.C.S.U.

Philosophy:

"The fuzzy algorithm is based on intuition and experience, and can be regarded as a set of heuristic decision rules or 'rules of thumb'."

Mars Mission Research Center, N.C.S.U.

Quantized Variables (Coarse Control)

Quantized level	v	e	\dot{e}
-5	-90	-100	-1000
-4	-75	-80	-800
-3	-60	-60	-600
-2	-45	-40	-400
-1	-30	-20	-200
0	0	0	0
1	15	20	200
2	30	40	400
3	45	60	600
4	60	80	800
5	75	100	1000

Mars Mission Research Center, N.C.S.U.

Membership Matrix Table

Linguistic Sets	Quantized Levels									
	-4	-3	-2	-1	0	1	2	3	4	
LP	0	0	0	0	0	0	0	0.6	1	
SP	0	0	0	0	0	0.6	1	0.6	1	
ZE	0	0	0	0.6	1	0.6	0	0	1	
SN	0	0.6	1	0.6	0	0	0	0	1	
LN	1	0.6	0	0	0	0	0	0	1	

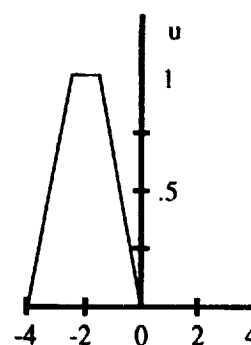
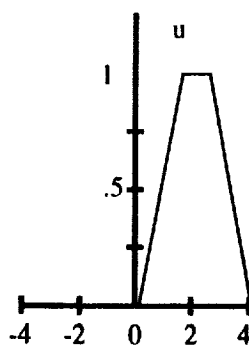
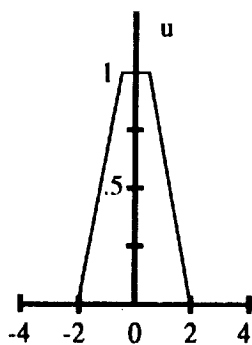
Mars Mission Research Center, N.C.S.U.

Graphical Representation of linguistic Rule 1

Error (e)

Error change (è)

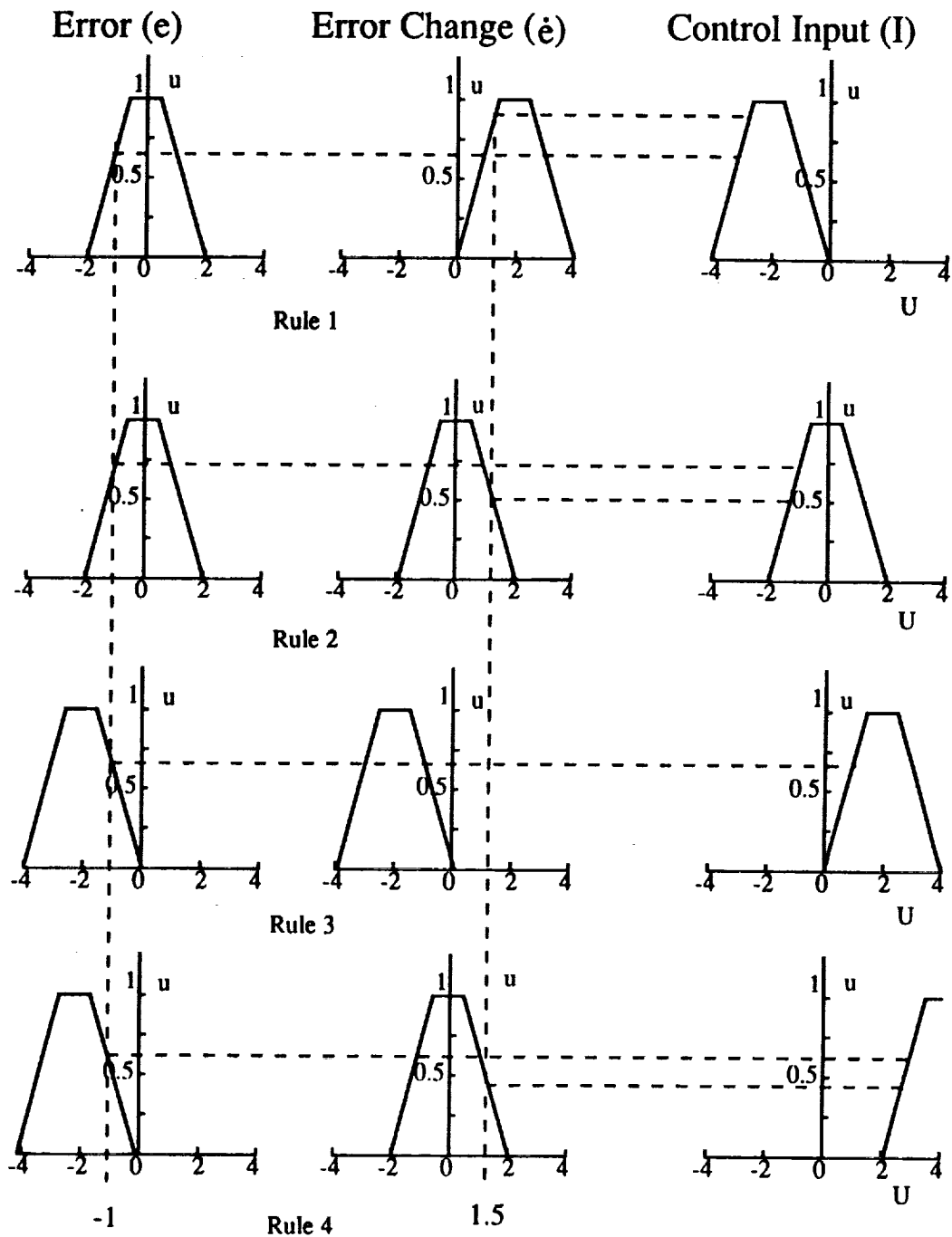
Control input (I)



Universe of discourse (U)

(If error is ZE and error change is SP then control input is SN)

Mars Mission Research Center, N.C.S.U.



Mars Mission Research Center, N.C.S.U.

Center of Gravity

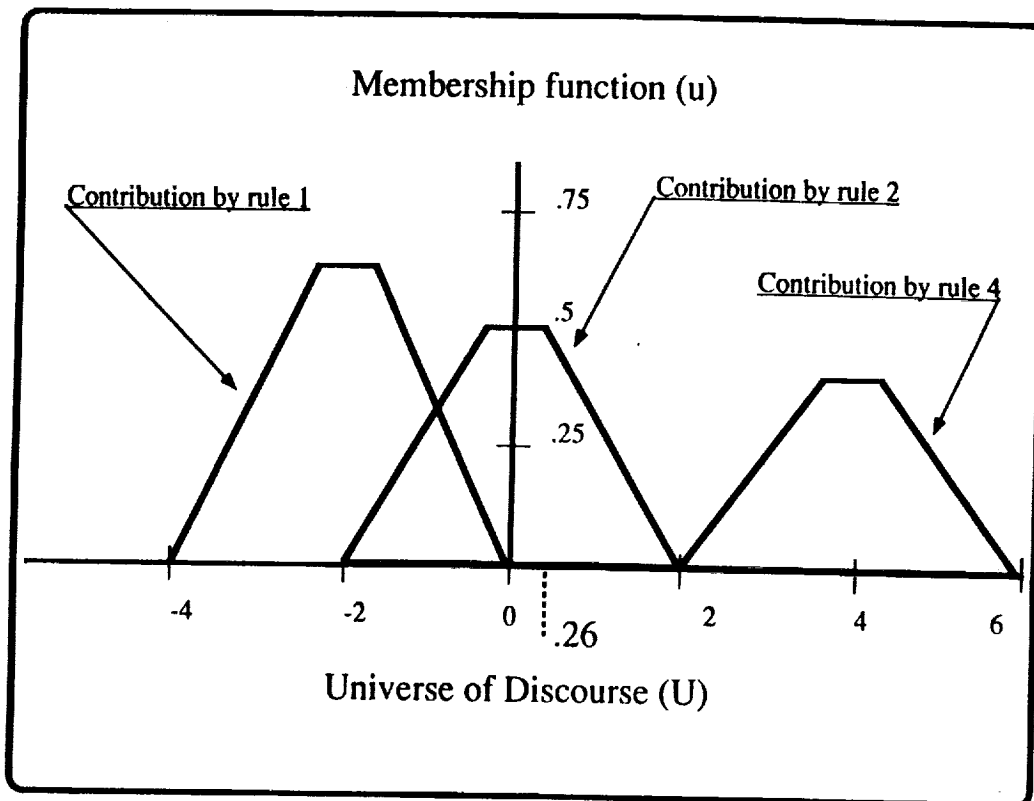
$$I = \sum_1^n \frac{(u_n \times U_n)}{\sum_1^n u_n}$$

$u \equiv$ The membership function

$U \equiv$ The universe of discourse

$n \equiv$ The number of contributions

Mars Mission Research Center, N.C.S.U.



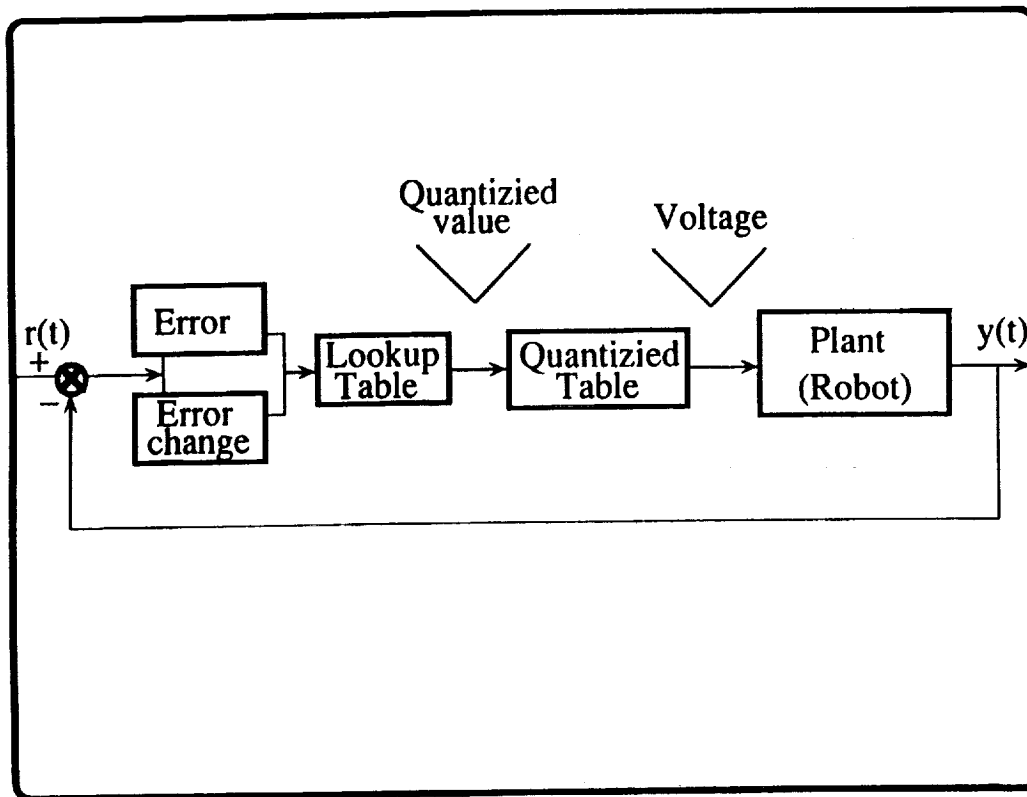
Mars Mission Research Center, N.C.S.U.

Sample Lookup Table

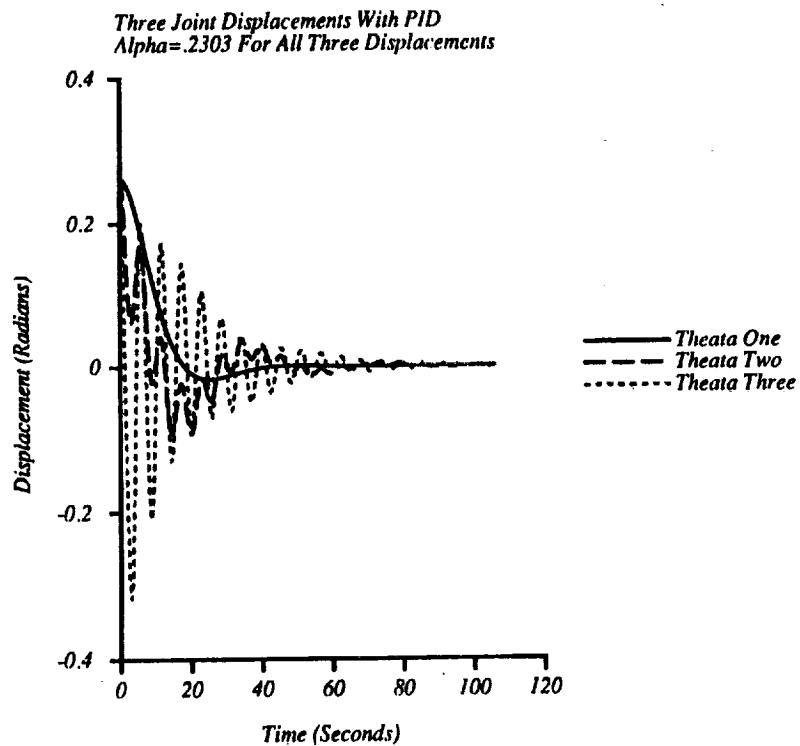
Error Change

Error	-4	-3	-2	-1	0	1	2	3	4
-4	5	4	4	3	3	2	1	1	-1
-3	5	4	3	2	2	1	0	0	-2
-2	4	3	3	2	1	1	0	-1	-3
-1	4	3	2	1	1	0	-1	-2	-3
0	3	3	2	1	0	-1	-2	-3	-4
1	3	2	1	0	-1	-1	-2	-3	-4
2	3	1	0	0	-1	-2	-3	-3	-4
3	2	0	0	-1	-2	-2	-3	-4	-5
4	1	-1	-1	-1	-2	-3	-4	-4	-5

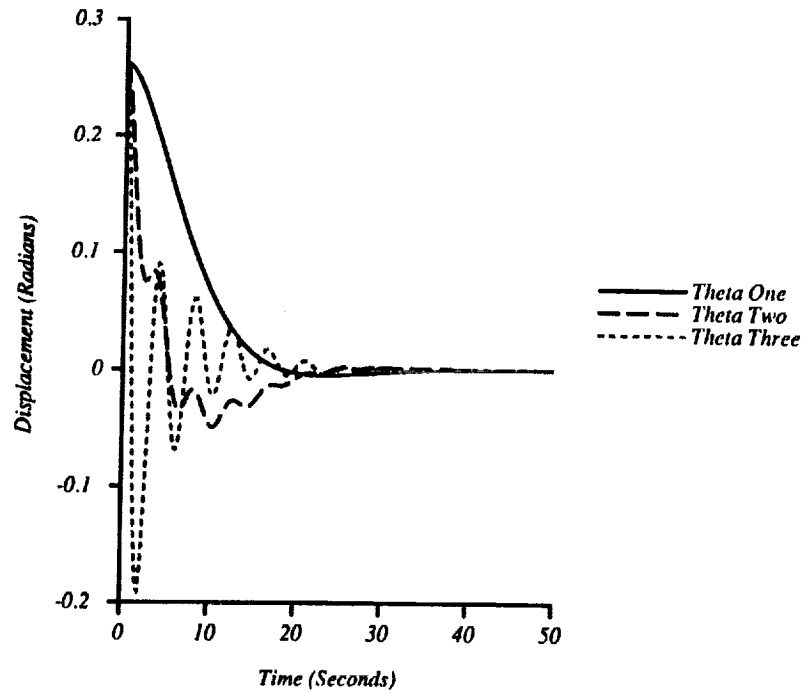
Mars Mission Research Center, N.C.S.U.



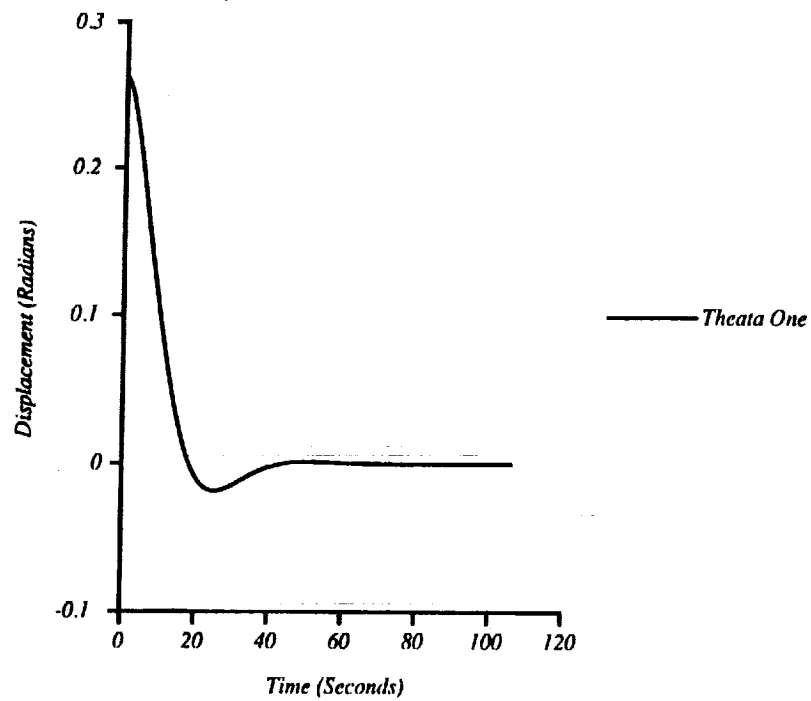
Mars Mission Research Center, N.C.S.U.



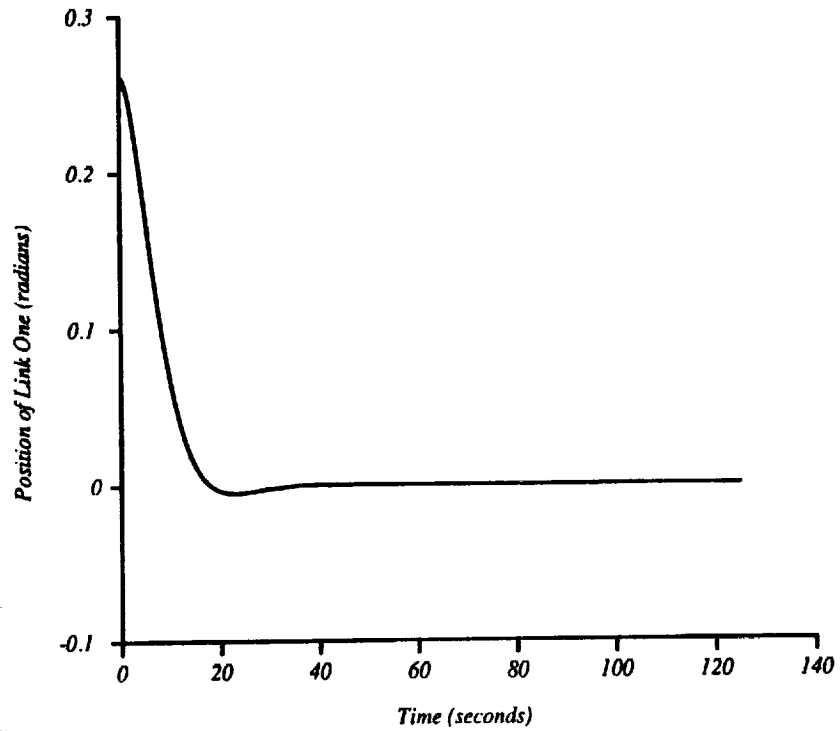
Three Joint Displacement With
Fuzzy Logic Control



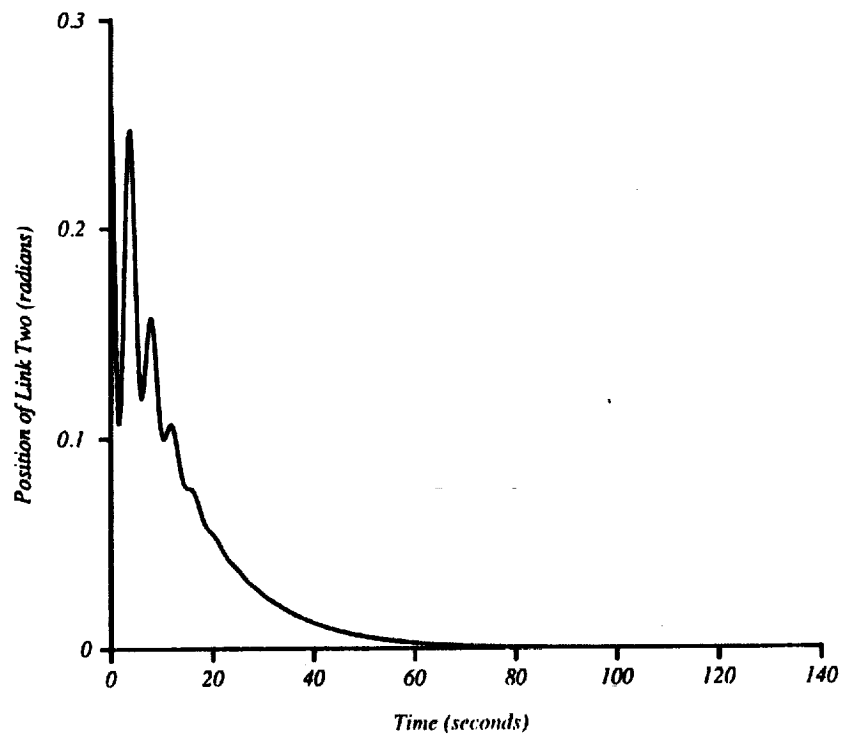
Joint Displacement With PID
Alpha=.2303 For Link One



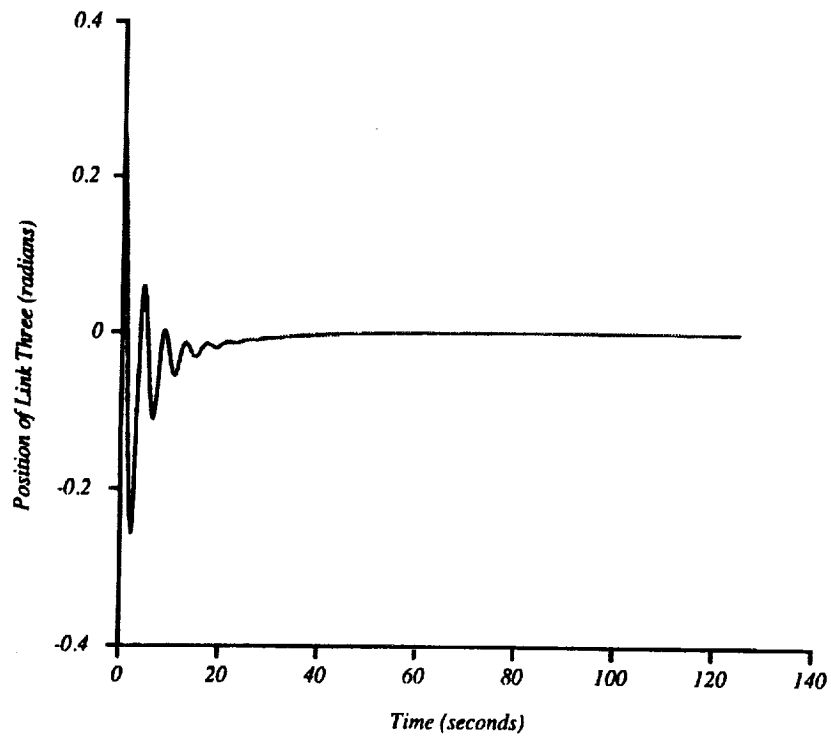
*Position of Link One vs. Time
With Fuzzy Logic Control*



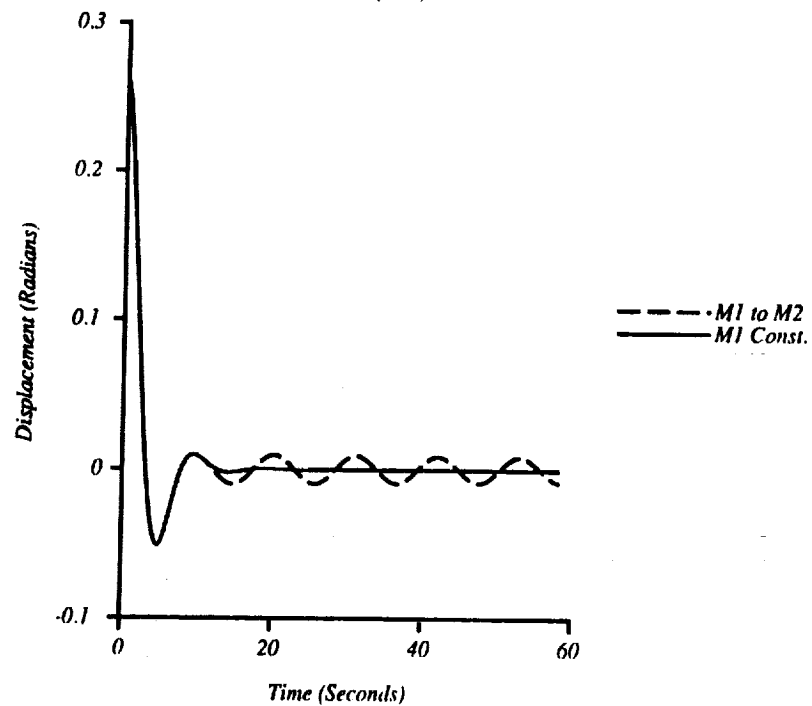
*Position of Link Two vs. Time
With Fuzzy Logic Control*



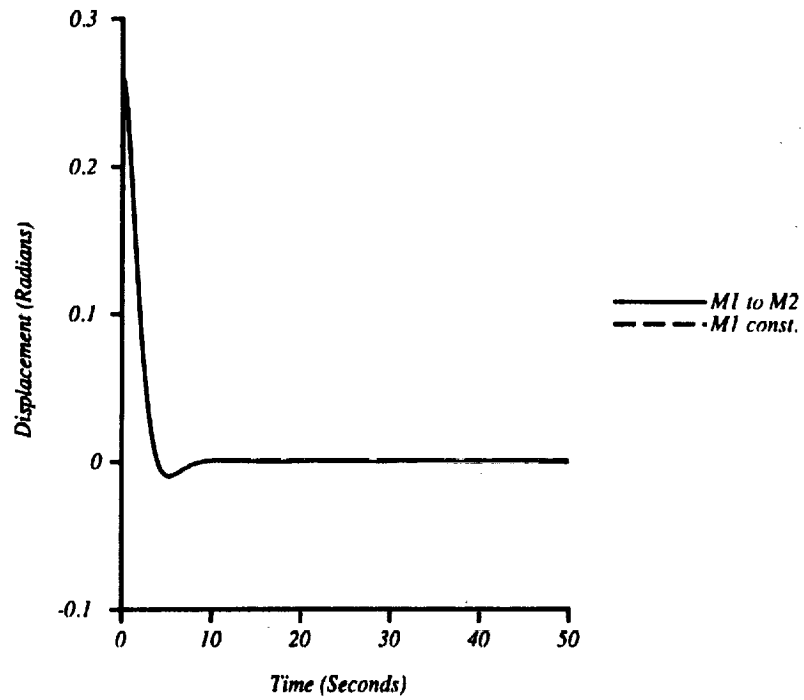
*Position of Link Three vs. Time
With Fuzzy Logic Control*



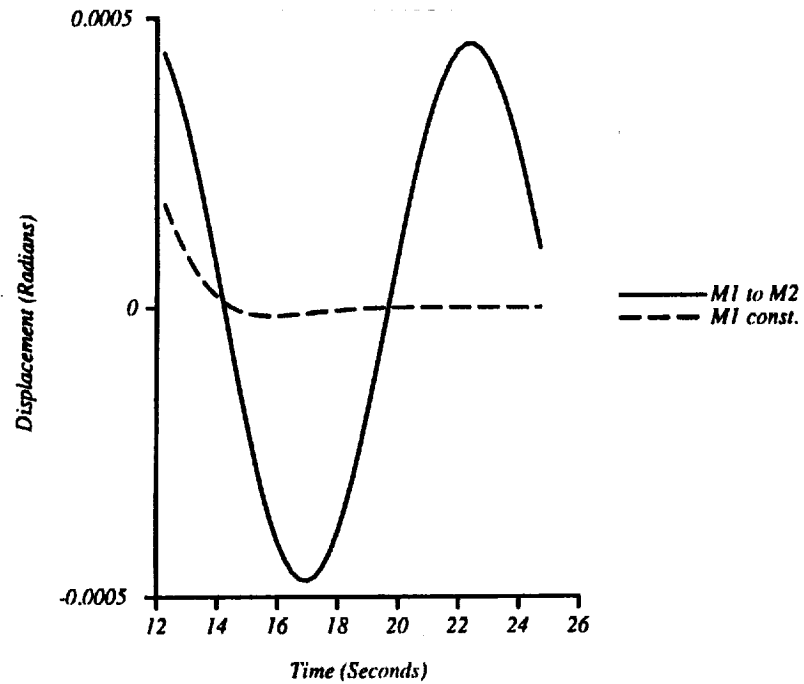
*Joint Displacement With and Without
Parameter Variation (PID)*



Joint Displacement With and Without
Parameter Variation (Fuzzy Controller)



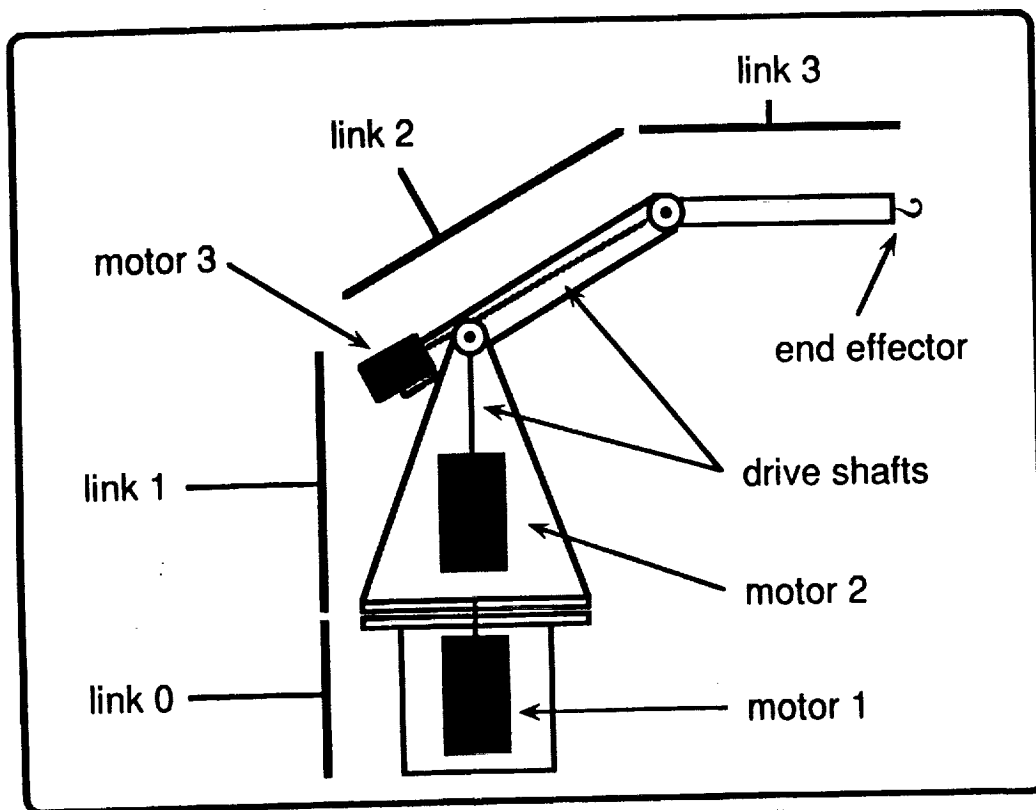
Joint Displacement With and Without
Parameter Variation (Fuzzy Controller)



Future Activities:

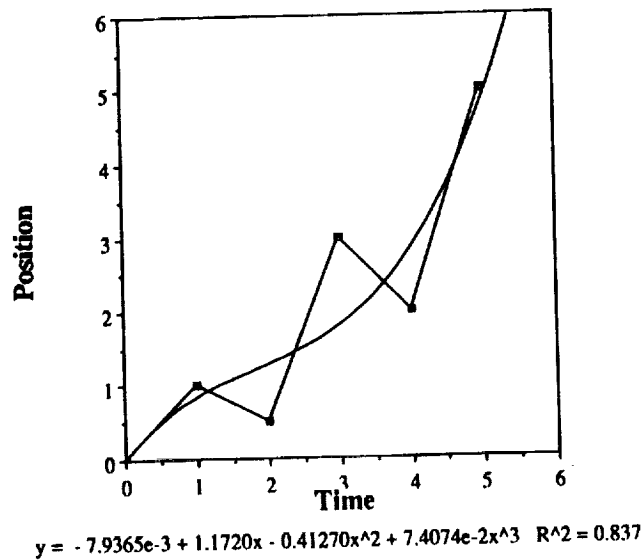
- **Coordinated Robotic Testbed**
 - NASA missions for on orbit assembly.
- **Issues:**
 - Flexibility in links/joints (R.M.S., .A.P.S.)
 - Adaptability to varying inertia
 - Mobility of manipulator system
 - Master / Slave
 - Controller
 - a) Tracking
 - b) Vibration compensation

Mars Mission Research Center, N.C.S.U.

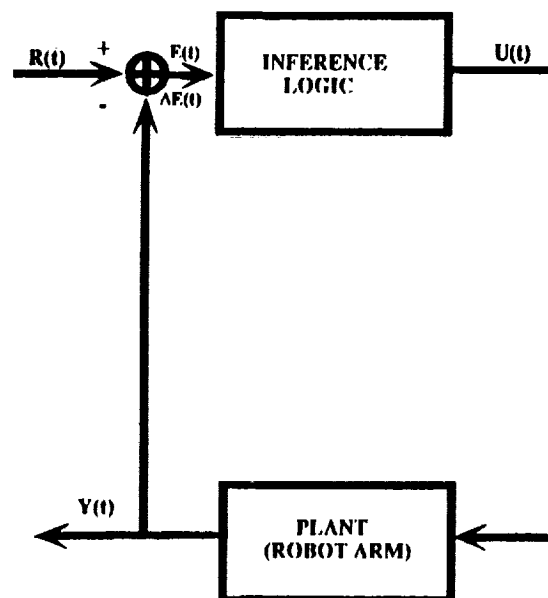
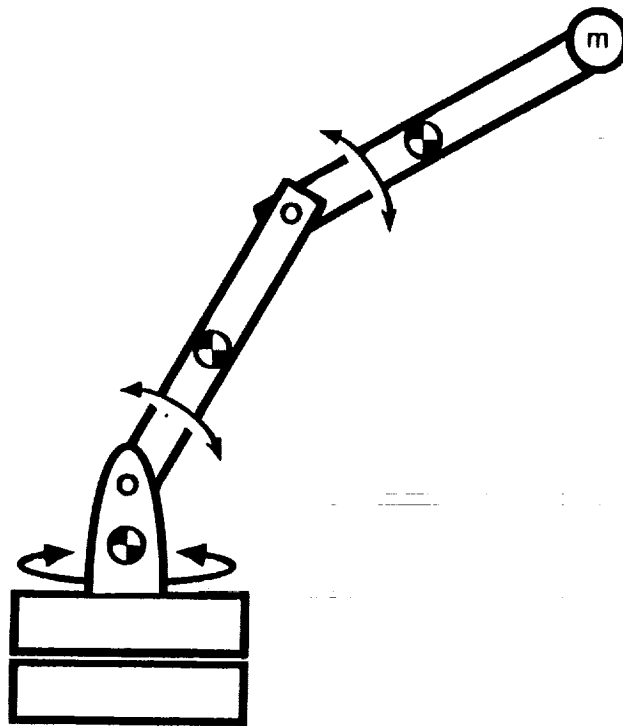


Mars Mission Research Center, N.C.S.U.

Recursive Least Squares Approximation to a Third Order Polynomial



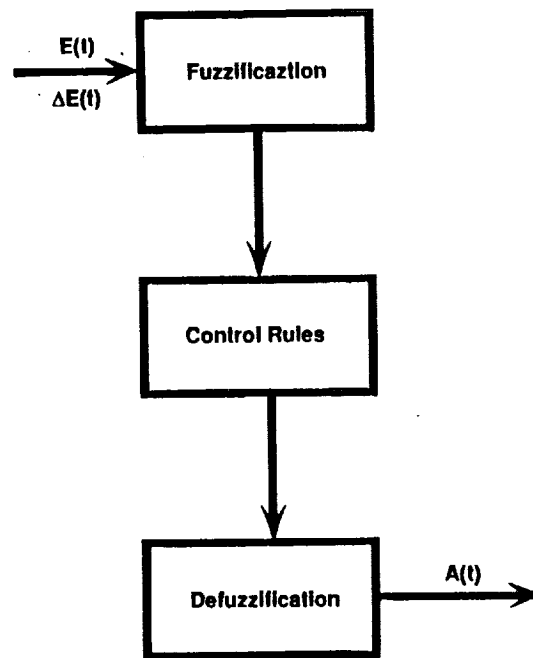
Mars Mission Research Center, N.C.S.U.



$$E(t) := Y(t) - R(t)$$

$R(t)$:= Reference Position

$U(t)$:= Control Command



The Universe Of Discourse Of The Functions

The Error, $E(t)$, ranges from -1000 to 1000

The Error change, $\Delta E(t)$, ranges from -100 to 100

The Gain, $A(t)$, ranges from 0.2 to 0.707

The following rules were implemented.

- (1) If $E(t)$ is LP and $\Delta E(t)$ is any, then $A(t)$ is LP
- (2) If $E(t)$ is MP and $\Delta E(t)$ is LP, then $A(t)$ is LP
- (3) If $E(t)$ is SP and $\Delta E(t)$ is MP, then $A(t)$ is MP
- (4) If $E(t)$ is ZE and $\Delta E(t)$ is any, then $A(t)$ is SP
- (5) If $E(t)$ is SN and $\Delta E(t)$ is MN, then $A(t)$ is MP
- (6) If $E(t)$ is MN and $\Delta E(t)$ is LN, then $A(t)$ is LP
- (7) If $E(t)$ is LN and $\Delta E(t)$ is any, then $A(t)$ is LP

Defining the Fuzzy subsets.

For -1000 to -875 E(t) is -1000

For -875 to -675 E(t) is -750

For -675 to -475 E(t) is -500

For -475 to -275 E(t) is - 250

For -275 to 275 E(t) is 0

Mars Mission Research Center, N.C.S.U.

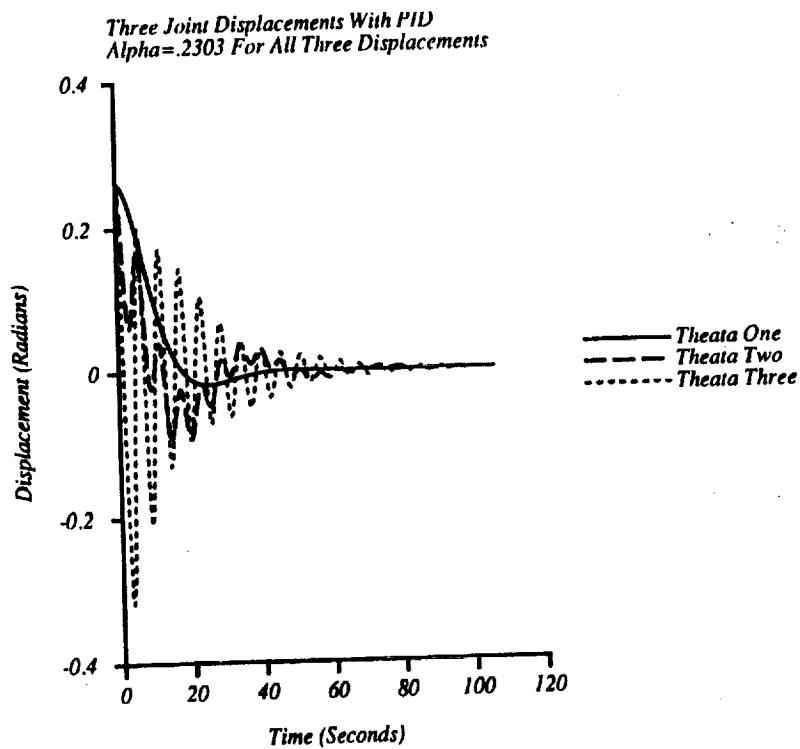
QUANTIZED VARIABLES

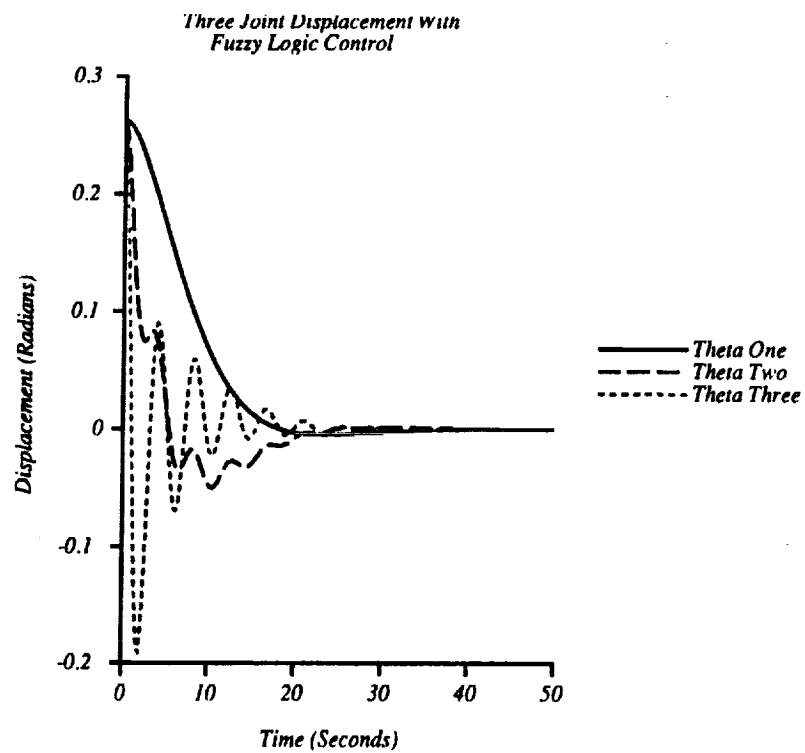
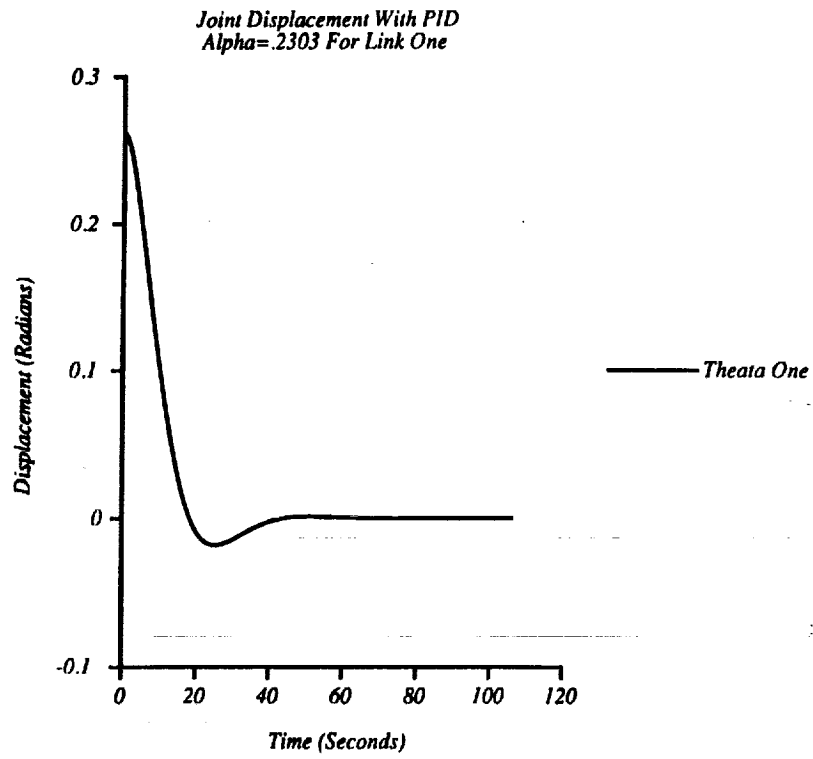
<u>A(t)</u>	<u>E(t)</u>	<u>AE(t)</u>	<u>LEVELS</u>
0.707	-1000	-100	-4
0.625	-750	-75	-3
0.505	-500	-50	-2
0.415	-250	-25	-1
0.230	0	0	0
0.415	250	25	1
0.505	500	50	2
0.625	750	75	3
0.707	1000	100	4

COARSE LOOK-UP TABLE

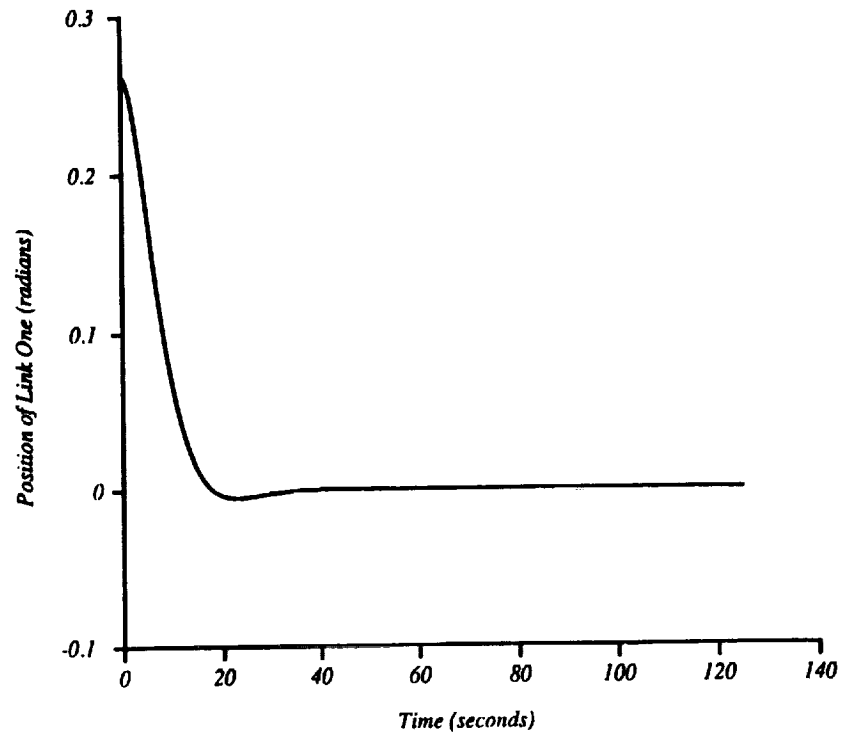
Error, E									Error Change, ΔE
1000	750	500	250	0	-250	-500	-750	-1000	
0.707	0.707	0.707	0.625	0.625	0.625	0.707	0.707	0.707	-100
0.707	0.707	0.625	0.625	0.625	0.625	0.625	0.707	0.707	-75
0.707	0.707	0.625	0.625	0.415	0.625	0.625	0.707	0.707	-50
0.707	0.625	0.625	0.415	0.415	0.415	0.625	0.625	0.707	-25
0.625	0.625	0.415	0.415	0.415	0.415	0.415	0.625	0.625	0
0.707	0.625	0.625	0.415	0.415	0.415	0.625	0.625	0.707	25
0.707	0.707	0.625	0.625	0.415	0.625	0.625	0.707	0.707	50
0.707	0.707	0.625	0.625	0.625	0.625	0.625	0.707	0.707	75
0.707	0.707	0.707	0.625	0.625	0.625	0.707	0.707	0.707	100

Mars Mission Research Center, N.C.S.U.

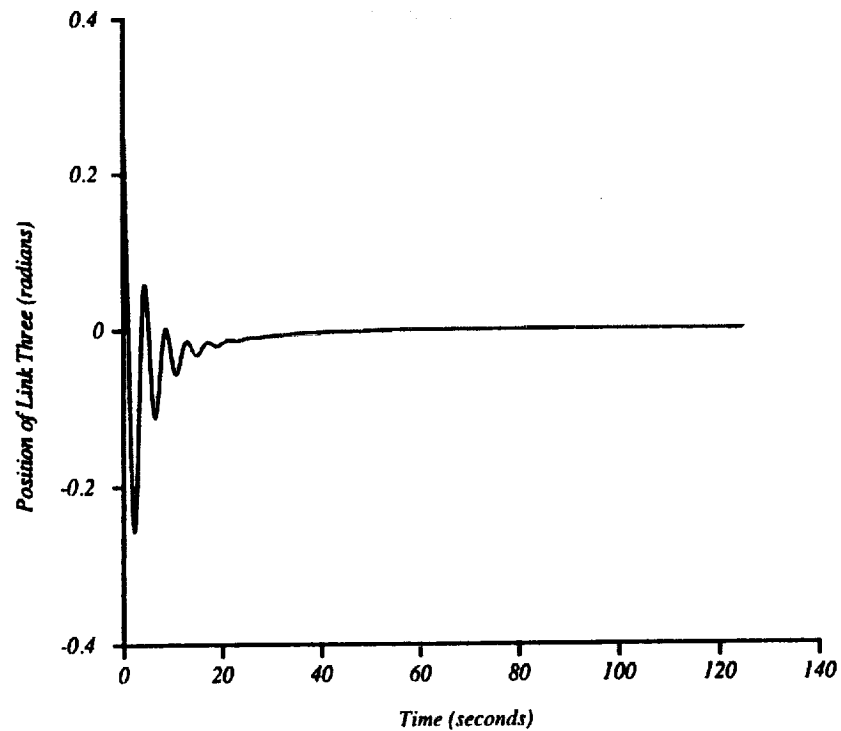




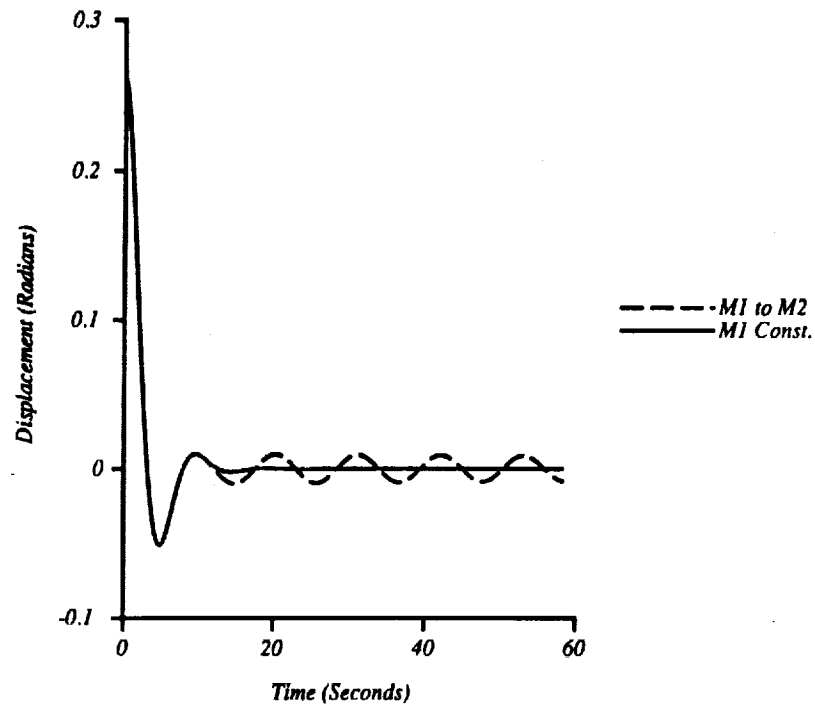
*Position of Link One vs. Time
With Fuzzy Logic Control*



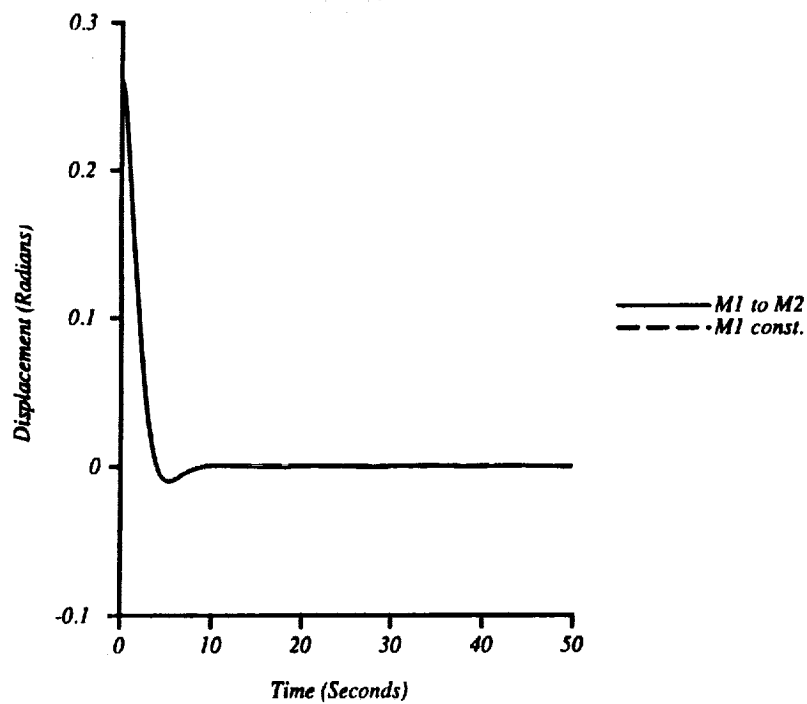
*Position of Link Three vs. Time
With Fuzzy Logic Control*

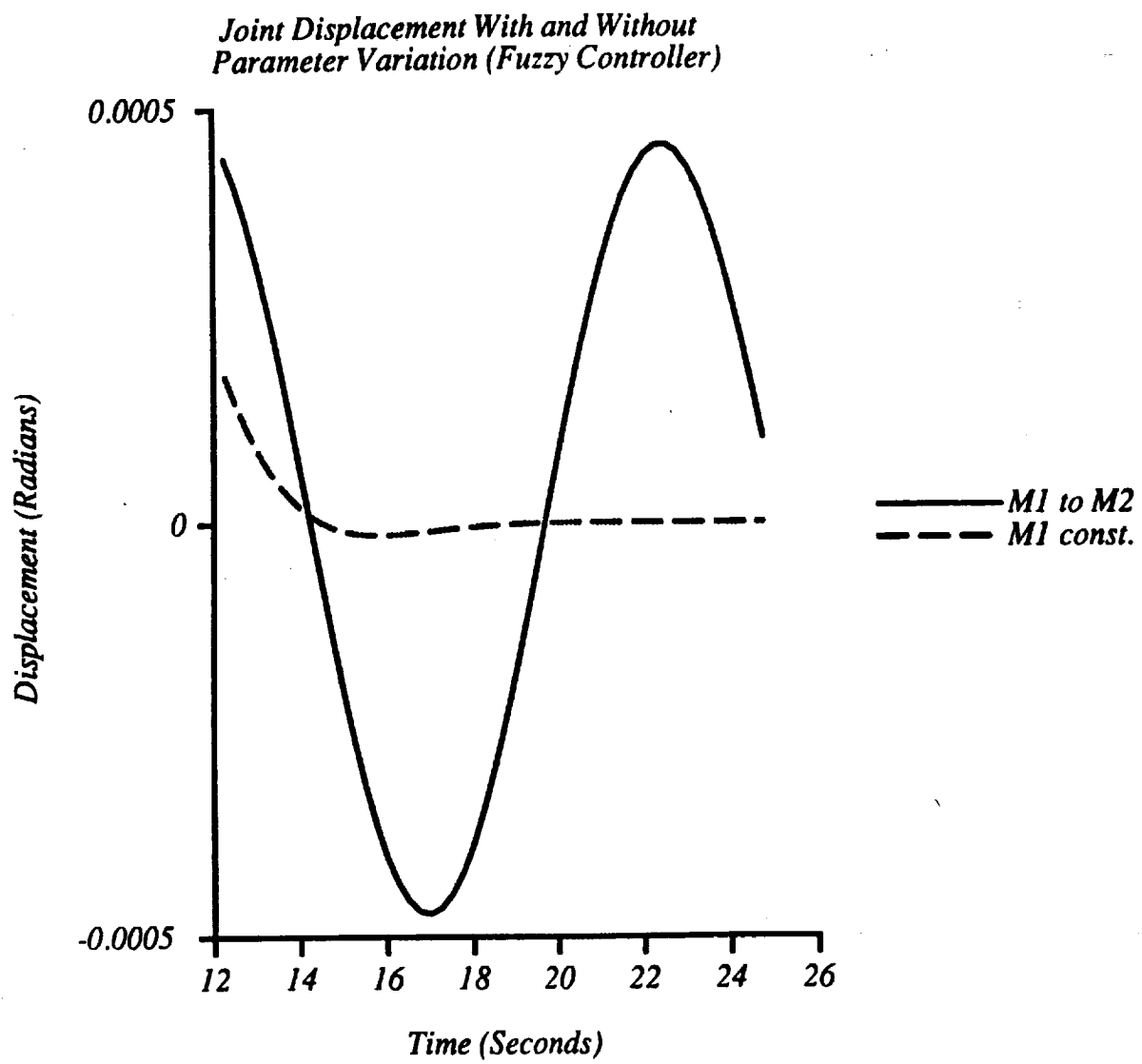


Joint Displacement With and Without
Parameter Variation (PID)



Joint Displacement With and Without
Parameter Variation (Fuzzy Controller)





Future Activities:

- The number of rules
- Overlapping of subsets
- Matrix membership (shape)
- Calibration Techniques
- Predictor (time delays)

Mars Mission Research Center, N.C.S.U.

Editor's Summary of the Panel Discussion

The Panel was moderated by the Editor, Dr. Dave Ghosh, and consisted of six members, three from NASA Langley Research Center and three from the Mars Mission Research Center. The members from NASA Langley were:

Dr. Raymond C. Montgomery
Mr. Jerry R. Newsom
Mr. Lawrence W. Taylor

and the members from the Mars Mission Research Center were:

Dr. Lawrence Silverberg
Dr. Ethelbert Chukwu
Dr. Gordon K. F. Lee

Each panel member was given an opportunity to express his views concerning research needs and opportunities related to control systems technology for accomplishing a manned Mars mission. After this the floor was opened for discussion. This section of the proceedings is the editors independent interpretation of the comments made during the course of the panel discussions.

It was felt that though theoretical development is essential, especially in the initial phases of a new control problem, experiments must be carried out in conjunction to establish a thorough understanding of problems and refinement of theories. In short, experimental activity is an essential element of research. In this regard Langley testbeds should be developed and made available to test new ideas emanating from the MMRC. It was recognized that in an university environment faculty tend to work independently and isolate themselves from practical problems. It was also recognized that 'design' is an important part of engineering curricula and there should be a balance between research and design. In view of this, MMRC is trying to integrate faculty from different areas to work in a design framework. It was also felt that research plans for Mars Mission should reflect its long term nature and should not pander to groups looking for quick results.

Several suggestions were made for inclusion in the university research activity. Students should work on simple and fundamental problems. Computationally exact solutions, now available, should be used to revisit old problems and to throw light on new problems. On-orbit

assembly issues involving human and robots especially in the presence of time delay, should be explored. Also, human operator models should be developed and used in control system synthesis, analysis, and design.

REPORT DOCUMENTATION PAGE			Form Approved OMB No. 0704-0188	
Public reporting burden for this collection of information is estimated to average 1 hour per response, including the time for reviewing instructions, searching existing data sources, gathering and maintaining the data needed, and completing and reviewing the collection of information. Send comments regarding this burden estimate or any other aspect of this collection of information, including suggestions for reducing this burden, to Washington Headquarters Services, Directorate for Information Operations and Reports, 1215 Jefferson Davis Highway, Suite 1204, Arlington, VA 22202-4302, and to the Office of Management and Budget, Paperwork Reduction Project (0704-0188), Washington, DC 20503.				
1. AGENCY USE ONLY (Leave blank)		2. REPORT DATE July 1992		3. REPORT TYPE AND DATES COVERED Conference Publication
4. TITLE AND SUBTITLE Ongoing Progress in Spacecraft Controls			5. FUNDING NUMBERS WU 506-59-61-01	
6. AUTHOR(S) D. Ghosh, Editor				
7. PERFORMING ORGANIZATION NAME(S) AND ADDRESS(ES) NASA Langley Research Center Hampton, VA 23685-5225			8. PERFORMING ORGANIZATION REPORT NUMBER	
9. SPONSORING / MONITORING AGENCY NAME(S) AND ADDRESS(ES) National Aeronautics and Space Administration Washington, DC 20546-0001			10. SPONSORING / MONITORING AGENCY REPORT NUMBER NASA CP-10099	
11. SUPPLEMENTARY NOTES D. Ghosh: Lockheed Engineering & Sciences Company, Hampton, Virginia				
12a. DISTRIBUTION / AVAILABILITY STATEMENT Unclassified-Unlimited Subject Category 18			12b. DISTRIBUTION CODE	
13. ABSTRACT (Maximum 200 words) This publication is a collection of papers presented at the Mars Mission Research Center workshop on Ongoing Progress in Spacecraft Controls held at the NASA Langley Research Center, Hampton, Virginia, on January 13, 1992. It was jointly sponsored by the NASA Langley Research Center Guidance, Navigation, and Control Technical Committee and the Mars Mission Research Center. The technical program addressed additional Mars mission control problems that currently exist in robotic missions in addition to human missions. Topics include control system design in the presence of large time delays, fuel-optimal propulsive control, and adaptive control to handle a variety of unknown conditions.				
14. SUBJECT TERMS Large Flexible Spacecraft Control, Structural Dynamics			15. NUMBER OF PAGES 155	
			16. PRICE CODE A08	
17. SECURITY CLASSIFICATION OF REPORT Unclassified	18. SECURITY CLASSIFICATION OF THIS PAGE Unclassified	19. SECURITY CLASSIFICATION OF ABSTRACT	20. LIMITATION OF ABSTRACT	